DESIGN OF A POLARIZATION AGILE RECONFIGURABLE ANTENNA IN S BAND

A Project report submitted in partial fulfilment of the requirements for the award of the degree of

BACHELOR OF TECHNOLOGY

IN

ELECTRONICS AND COMMUNICATION ENGINEERING

Submitted by

K. Yasaswini (319126512092)

M. Dhanush Karthik (319126512096)

G. Bhavana Sai Sree (319126512082)

Ch. Sandeep Reddy (319126512077)

Under the guidance of

Mrs. B. Deepa, Mtech, (Ph.D)

(Assistant professor)

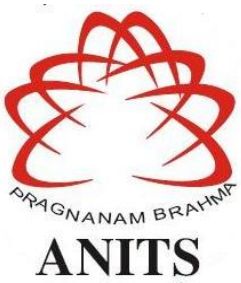

DEPARTMENT OF ELECTRONICS AND COMMUNICATION ENGINEERING

ANIL NEERUKONDA INSTITUTE OF TECHNOLOGY AND SCIENCES
(UGC AUTONOMOUS)
(*Permanently Affiliated to AU, Approved by AICTE and Accredited by NBA & NAAC)*
Sangivalasa, Bheemili mandal, Visakhapatnam dist.(A.P)

2022-2023

DEPARTMENT OF ELECTRONICS AND COMMUNICATION ENGINEERING

ANIL NEERUKONDA INSTITUTE OF TECHNOLOGY AND SCIENCES

(UGC AUTONOMOUS)

(Permanently Affiliated to AU, Approved by AICTE and Accredited by NBA & NAAC)

Sangivalasa, Bheemili mandal, Visakhapatnam dist. (A.P)

ANITS

CERTIFICATE

This is to certify that the project report entitled **"DESIGN OF A POLARIZATION AGILE RECONFIGURABLE ANTENNA IN S BAND"** submitted by **K. Yasaswini (319126512092), M. Dhanush Karthik (319126512096), G. Bhavana Sai Sree (319126512082)** and **Ch. Sandeep Reddy (319126512077)** in partial fulfilment of the requirements for the award of the degree of **Bachelor of Technology** in **Electronics & Communication Engineering** of Anil Neerukonda Institute of technology and Sciences (A), Visakhapatnam is a record of bona fide work carried out under my guidance and supervision.

Project Guide

Mrs. B. Deepa

Assistant Professor

Department of E.C.E

ANITS

Assistant Professor
Department of E.C.E.
Anil Neerukonda
Institute of Technology & Sciences
Sangivalasa, Visakhapatnam-531 162

Head of Department

Dr. B. Jagadeesh

Professor & HOD

Department of E.C.E

ANITS

Head of the Department
Department of E C E
Anil Neerukonda Institute of Technology & Sciences
Sangivalasa - 531 162

ACKNOWLEDGEMENT

We would like to express our deep gratitude to our project guide **Mrs. B. Deepa,** Assistant Professor, Department of Electronics and Communication Engineering, ANITS, for his guidance with unsurpassed knowledge and immense encouragement. We are grateful to **Dr. B. Jagadeesh**, Head of the Department, Electronics and Communication Engineering, for providing us with the required facilities for the completion of the project work.

We are very much thankful to the **Principal and Management, ANITS, Sangivalasa,** for their encouragement and cooperation to carry out this work.

We express our thanks to all **teaching faculty** of Department of ECE, whose suggestions during reviews helped us in accomplishment of our project. We would like to thank **all non-teaching staff** of the Department of ECE, ANITS for providing great assistance in accomplishment of our project.

We would like to thank our parents, friends, and classmates for their encouragement throughout our project period. At last, but not the least, we thank everyone for supporting us directly or indirectly in completing this project successfully.

PROJECT STUDENTS

K. Yasaswini (319126512092)

M. Dhanush Karthik (319126512096)

G. Bhavana Sai Sree (319126512082)

Ch. Sandeep Reddy (319126512077)

ABSTRACT

An S-band polarization-configurable antenna is suggested. The antenna is small in size and has an excellent axial ratio and frequency response. It consists of a driven patch and a parasitic patch that comprises a two element array. The reconfiguration for the right-hand, left-hand, and linear polarizations is managed by two PIN diode switches. The reflection coefficient $|S_{11}|$ was well preserved and reconfigurable polarizations were made possible by varying the states of the two PIN diode switches which are efficient as they are fast at switching, which is a significant advantage of this design. The separation-reconfigurable antenna that has been proposed has been modelled using the HFSS program. Left hand circular polarization is achieved when the diode 1 is switched off and diode 2 is switched on, and the antenna resonates between 2.20 GHz and 2.8650 GHz with a gain of 6.66 dB in this condition. When the diode 1 is switched on and diode 2 is switched off, the antenna achieves right hand circular polarization, and it resonates between 2.20 GHz and 2.8510 GHz with a gain of around 6.20 dB. If both the diodes are switched on, then the antenna achieves linear polarization with a gain of 5.55 dB and resonates in the frequency ranges 2.1480-2.3750 and 2.5260-2.7850. The recommended microstrip antenna was created on a FR-4 substrate with a relative dielectric constant of 4.4 and a loss tangent of 0.02. The proposed antenna has dimensions of 200 mm by 150 mm.

CONTENTS

LIST OF FIGURES

LIST OF TABLES

CHAPTER 1:
Introduction

1.1 History Of Antennas

The first radio antennas were created by Heinrich Hertz, a professor at the Technical Institute in Karlsruhe, Germany. Heinrich Hertz's end-loaded half-wave dipole transmitting antenna and resonant half-wave receiving loop operated at $\lambda = 8$ m in 1886.

Sir Jagadish Chandra Bose is widely recognized as the inventor of wireless telecommunication. He was born on November 30, 1858, in the Bengal Presidency of British India. In November 1895, Bose conducted a public demonstration at Calcutta's Town Hall, where he remotely rang a bell and detonated gunpowder using an electromagnetic wave that passed through walls, which he had sent across a distance of 75 feet. Bose is often referred to as the father of wireless telecommunication for his pioneering work in the field. One of Bose's key contributions to the field was the invention of the Mercury Coherer, a radio wave receiver that was later used by Guglielmo Marconi to build an operational two-way radio. Bose demonstrated the science behind capturing radio waves before Marconi did. Despite Marconi being celebrated for his invention, Bose remained relatively unknown to many people, as he never patented his work.

Figure 1.1 illustrates the microwave apparatus that was designed and used by Sir Jagadish Chandra Bose. The spark gap transmitter, located on the right side of the figure, utilized a spark gap radiator consisting of three small metal balls, each measuring 3 mm in diameter. The high voltage from an induction coil was used to excite the radiator and generate microwaves at a frequency of 60 GHz. The transmitter was enclosed inside a metal box to prevent sparks from the coil's interrupter from interfering with the receiver. The microwaves were emitted from a waveguide, which is a metal tube that guides and contains the microwaves. On the left side of the figure is the

receiver, which utilized a galena point contact crystal rectifier inside the horn antenna to detect the waves. A galvanometer was used to measure the detected waves. The galvanometer and battery shown in the figure are modern replacements for the original equipment used by Bose.

Figure 1.1 Microwave Apparatus - Jagadish Chandra Bose Museum

Heinrich Hertz, the father of radio and a pioneer in the field, made a significant innovation in radio technology, but it remained a laboratory curiosity until Guglielmo Marconi, a 20-year-old from Bologna, Italy, added tuning circuits, larger antennas, and ground systems for longer wavelengths. By doing so, he was able to transmit signals over long distances. In December 1901, Marconi astonished everyone by receiving signals in St. Johns, Newfoundland, from a transmitting station he had built in Poldhu, Cornwall, England.

In 1905, Marconi used a square conical antenna near Poldhu, England, to transmit signals over the Atlantic at wavelengths of thousands of meters. The development of radar during World War II made centimeter wavelengths common, and the entire radio spectrum became available for widespread use. Today, thousands of communication satellites covered with antennas orbit the planet in low, medium, and geostationary orbits. The geostationary satellites create an orbital ring around the planet, similar to the rings around Saturn. A GPS receiver can provide latitude, longitude, and elevation

information with centimeter accuracy regardless of the time of day, weather conditions, or location on the planet.

The Very Large Array (VLA), located near Socorro, New Mexico, is a collection of 27 steerable parabolic dish antennas, each measuring 25 meters in diameter. It is used to observe radio sources located billions of light-years away. Our probes, equipped with arrays of antennae, have travelled to planets inside and outside the solar system, taking and returning images in response to our commands. Radio telescope antennas that operate at millimeter to kilometer wavelengths pick up signals from objects that have been traveling for over 10 billion years, providing valuable information about the universe's origins.

1.2 Concept Of Antennas

Antennas are crucial components in communication systems that rely on the transmission and reception of electromagnetic waves, such as mobile phone networks, TV, and radio. They function as devices that can convert electrical energy into electromagnetic waves and vice versa. The primary objective of antenna engineering and design is to achieve the highest possible efficiency in radiating or receiving electromagnetic waves. Radiation efficiency, which is the ratio of the radiated power to the power supplied to the antenna, is a crucial factor in antenna design. A well-designed antenna should have low losses and high radiation efficiency. In addition, antennas are designed with specific radiation patterns to meet the needs of various applications, such as directional or omni-directional patterns.

Several factors influence the performance of an antenna, such as its operating frequency, size, construction material, and the shape and orientation of its elements. In modern antenna design, computer simulations and optimization techniques are commonly utilized to achieve the desired level of performance.

Wireless communication systems heavily rely on antennas, making the development of new and innovative antenna designs a crucial field of research. As the demand for high-

speed data transfer continues to increase, there is a pressing need for efficient and effective antennas. The antenna plays a critical role in harnessing the electromagnetic spectrum, which is one of humanity's most valuable natural resources. Choosing an appropriate antenna for a specific application requires considering several essential characteristics such as power gain, directivity, polarization, and radiation patterns.

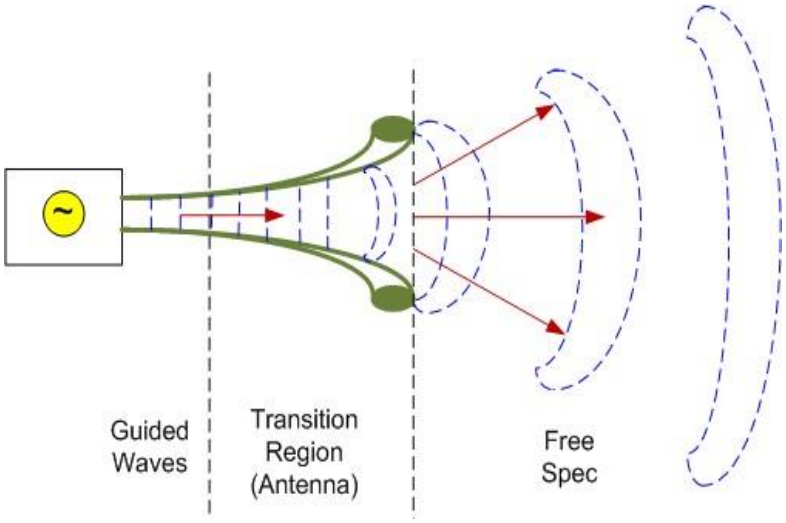

Figure 1.2 Simple Antenna

1.2.1 Working Of Antenna

An antenna is an essential component of an RF system that enables the transmission and reception of signals wirelessly. It operates by converting electrical signals into electromagnetic waves, which follow the principles of Maxwell's equations. The concept of wireless energy transfer was first proposed by Nikola Tesla, who noticed radiation being emitted from an energized electric coil. While his experiments were significant, they lacked mathematical proof, which was provided by James Clerk Maxwell. Maxwell proposed a mathematical relationship between the electric and magnetic fields surrounding an energized coil. When an analog feed is provided to the strip of an antenna, the metal patch is energized and emits a magnetic flux according to Maxwell's equations. The ground is used to terminate the electrical circuit, and the radiation emitted from the patch emerges at the ground, creating a magnetic field between the two layers of the antenna. The substrate material is used to control the flux

merging into the ground, and the amount of radiation depends on the dielectric material and its thickness. The magnetic field emitted creates an electric field perpendicular to it, which, in turn, creates another magnetic field, and the cycle continues, resulting in the propagation of electromagnetic waves in the medium.

1.3 Microstrip Patch Antenna

Traditional antennas are known for their high gain and radiation efficiency, but they also come with limitations such as large size and high-power requirements. In the current era of technological advancement, there is a need for compact and efficient devices that operate quickly and consume minimal power. Microstrip antennas are a viable solution, as they are compact, have high gain, and offer a wide bandwidth. By adjusting factors such as the size and shape of the antenna, the type of feeding, and the grounding technique, a patch antenna can be customized to meet any required bandwidth.

1.3.1 Advantages and Disadvantages

A microstrip antenna is a type of antenna that consists of a thin metallic patch mounted on a grounded substrate. It is widely used in various wireless communication systems due to its compact size, low profile, and ease of integration with other electronic components. Here are some advantages and disadvantages of a microstrip antenna:
Advantages:

1. Compact size: Microstrip antennas have a low profile and small footprint, which makes them ideal for use in devices with limited space, such as mobile phones, laptops, and wearables.
2. Low cost: Microstrip antennas are relatively inexpensive to manufacture and require fewer components than other types of antennas, making them a cost-effective option for many applications.
3. Easy integration: Microstrip antennas can be easily integrated with other electronic components, such as amplifiers, filters, and switches, which simplifies the design and reduces the overall size of the system.

4. Wide bandwidth: Microstrip antennas can be designed to operate over a wide range of frequencies, providing good performance over a broad frequency band.
5. Low interference: Microstrip antennas radiate most of their energy in a narrow beam, which reduces interference with nearby electronic devices and improves signal quality.

Disadvantages:

1. Low efficiency: Microstrip antennas typically have lower radiation efficiency than other types of antennas, which can result in weaker signals and reduced range.
2. Narrow bandwidth: The bandwidth of a microstrip antenna can be limited by the size of the patch and the substrate thickness, which can reduce its flexibility and performance.
3. Sensitivity to environmental factors: Microstrip antennas can be affected by nearby objects, such as buildings, trees, and other electronic devices, which can cause interference and reduce signal quality.
4. Polarization limitations: Microstrip antennas are typically designed to radiate in a single polarization, which can limit their performance in environments with multiple polarization signals.
5. Low power handling capability: Microstrip antennas may have limited power handling capability, which can cause damage or performance degradation at high power levels.

The Q factor (also known as quality factor) of an antenna is a measure of its ability to store and radiate energy efficiently and is defined as the ratio of the energy stored in the antenna to the energy lost per cycle. Antennas with high Q factors can radiate energy more efficiently but have a narrower bandwidth. The bandwidth of an antenna is the range of frequencies over which it can efficiently radiate or receive energy and is typically defined as the frequency range between the two points where the antenna's power gain is half of its maximum value. There is an inverse relationship between the Q factor and the bandwidth of an antenna, meaning that a high Q factor corresponds to

a narrower bandwidth, while a low Q factor corresponds to a wider bandwidth. This relationship can be seen in the equation for the bandwidth of an antenna.

$$BW = \frac{f_0}{Q} \qquad 1.1$$

where BW is the bandwidth, f0 is the resonant frequency of the antenna, and Q is the Q factor. As the Q factor increases, the bandwidth decreases, and as the Q factor decreases, the bandwidth increases.

Microstrip patch antennas have a high Q factor, which represents the losses associated with the antenna. A large Q factor results in a narrow bandwidth and low efficiency. To decrease the Q factor, the thickness of the dielectric substrate can be increased. However, as the thickness increases, a larger portion of the total power delivered by the source is converted into a surface wave. This surface wave is considered an unwanted power loss because it is scattered at the dielectric bends and ultimately degrades the antenna's characteristics.

1.3.2 Construction of basic microstrip antenna

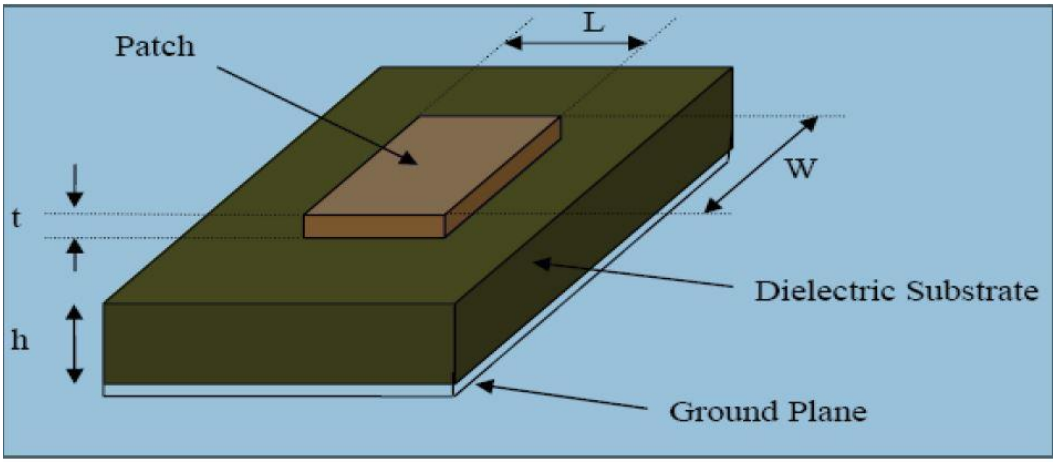

Figure 1.3 Microstrip patch antenna

There are three major parts constructing a microstrip patch antenna. They are:

1. Radiating patch (metal conductor)

2. Substrate (commonly dielectric material)
3. Ground (metal conductor)

Radiating patch is layered above the PCB which is responsible for radiating energy. It is connected to feed of the antenna directly and positive polarity. The shape and size of this patch is very much concerned with the behaviour of antenna. There are several types of patches. Based on the application we are using the antenna the size and shape of the patch are decided.

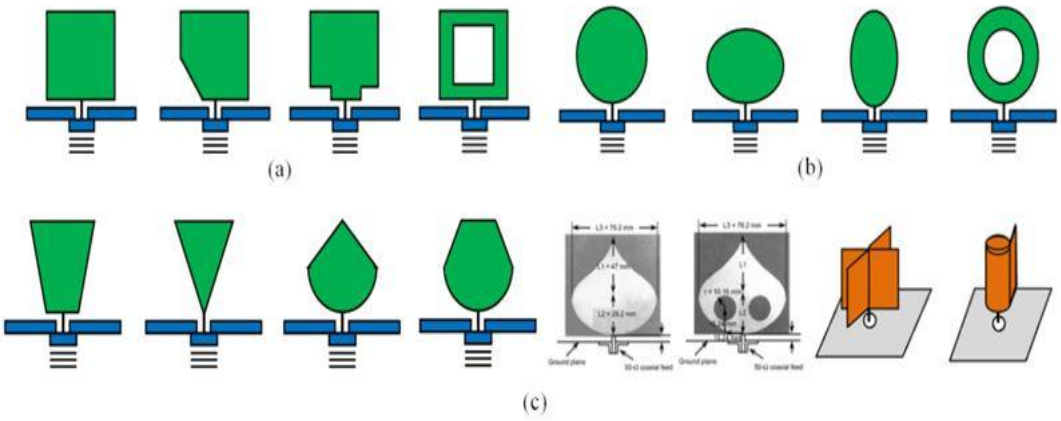

Figure 1.4 Shapes of patches

The frequency of operation of patch is governed by the length of the antenna and its mathematically given by the following expression.

$$f_c \approx \frac{c}{2L\sqrt{\varepsilon_r}} = \frac{1}{2L\sqrt{\varepsilon_0 \varepsilon_r \mu_0}} \qquad 1.2$$

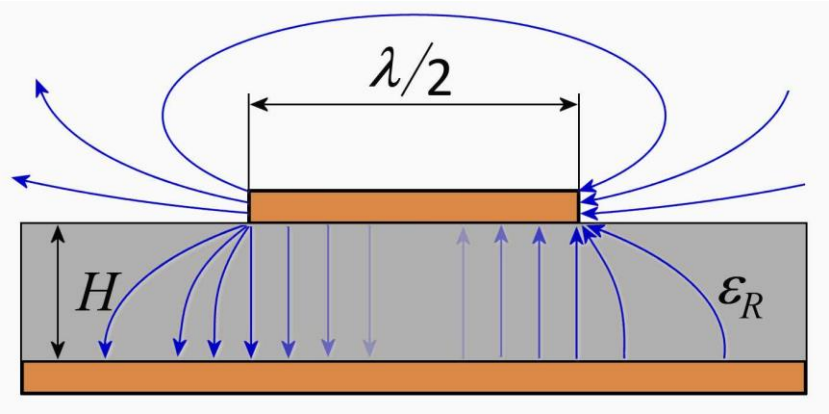

Figure 1.5 Cutaway view of simple patch antenna

The substrate used in a microstrip antenna is a dielectric material with a specific value of dielectric constant (Ɛr). It does not have any electrical activity but allows electromagnetic waves to pass through it. The performance of the antenna depends on the choice of dielectric material as it determines how the electromagnetic energy from the patch is terminated into the ground. The dielectric constant of the substrate material is a measure of its permittivity with respect to electromagnetic waves, and it is essential to use a substrate with suitable dielectric constant and thickness to achieve optimal antenna performance. The dielectric constant of the antenna material affects the resonant frequency of the antenna, which in turn affects the bandwidth. The resonant frequency of an antenna is inversely proportional to the square root of the dielectric constant of the surrounding material, according to the following equation:

$$f_0 = \frac{c}{(2\Pi\sqrt{\varepsilon_r \mu_r})} \qquad 1.3$$

where f0 is the resonant frequency, c is the speed of light, εr is the relative permittivity (dielectric constant) of the surrounding material, and μr is the relative permeability of the surrounding material.

The relationship between the efficiency of an antenna and the dielectric constant can be expressed as follows:

$$\eta = \eta_0\sqrt{(1 - \varepsilon_r)} \qquad 1.4$$

where η is the efficiency of the antenna, η0 is the efficiency of the same antenna without any surrounding material (i.e., in free space), and εr is the relative permittivity (dielectric constant) of the surrounding material. This equation shows that the efficiency of an antenna decreases as the dielectric constant of the surrounding material increases. In other words, the presence of a material with a high dielectric constant reduces the efficiency of the antenna.

Overall, the dielectric constant of the substrate material is a critical parameter in antenna design. It can affect the resonant frequency, antenna size, bandwidth, radiation pattern, and input impedance of the antenna. Antenna designers must carefully choose the substrate material and its dielectric constant to optimize the performance of the antenna for a given application.

Thickness of substrate, and permittivity of the material used for substrate accounts a lot in the performance of antenna, FR_4 is used in our design, having a dielectric constant 4.4. If the thickness of the substrate is too bulky, then the EM waves emerging from the patch will not terminate properly into the ground. If the thickness is too low, there will be unwanted losses for the signals emerging from patch.

Table 1.1 List of few substrates

DIELECTRIC SUBSTRATE	**PERMITIVITY (DIELECTRIC CONSTANT-Ɛr)**
Air	1
FR_4	4.4
FR_5	4.5
Nylon	3.1
Polystyrene	2.5
Rogers_RO3003	3.0
Rogers_RO3006	6.15
Rogers_Duroid5880	2.20
Rogers_Duroid5881	2.17
Silicon Dioxide	3.9

1.4 Feeding Techniques

There are two types of methods to feed microstrip patch antennas: contacting and non-contacting. In the contacting method, a connecting element like a microstrip line is used to directly feed RF power to the radiating patch. On the other hand, the non-contacting method involves power transfer through electromagnetic field coupling between the microstrip line and the radiating patch. There are four widely used feed techniques: microstrip line and coaxial probe, which belong to the contacting schemes, and aperture coupling and proximity coupling, which belong to the non-contacting schemes.

1.4.1 Microstrip feed line

The microstrip line feeding technique utilizes a conductive strip that is connected to the edge of the microstrip patch, as illustrated in figure 2.8. The width of the conductive strip is smaller than the patch. This feeding arrangement has the benefit of allowing the feed to be etched onto the same substrate, creating a planar structure.

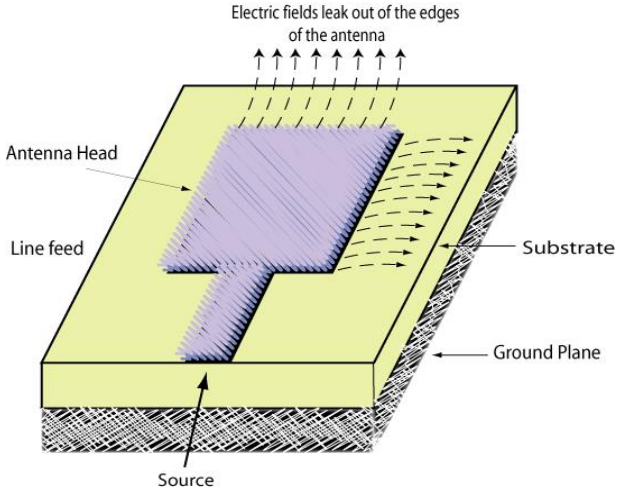

Figure 1.6 Microstrip feed line technique

To achieve a good impedance match in microstrip patch antennas, one effective method is to use an inset cut in the patch. This approach is uncomplicated to implement and does not necessitate any additional matching components. Optimal control of the inset position can result in excellent impedance matching. However, increasing the thickness

of the dielectric substrate can result in greater surface waves and spurious feed radiation, leading to a narrower bandwidth. Furthermore, this technique may cause unintended cross-polarization effects.

1.4.2 Coaxial feed

The coaxial feed or probe feed is a prevalent method for feeding microstrip patch antennas. Figure 2.9 illustrates this technique, which entails extending the inner conductor of the coaxial connector through the dielectric and attaching it to the radiating patch via soldering, while the outer conductor is linked to the ground plane.

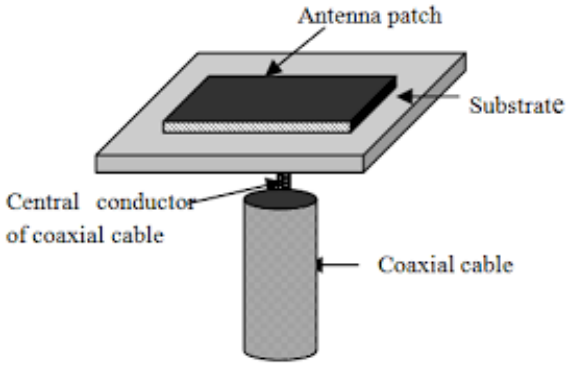

Figure 1.7 Coaxial Feed technique

The coaxial feed or probe feed is a common technique used for feeding microstrip patch antennas, offering the advantage of being able to place the feed at any desired position inside the patch for impedance matching, while also being easy to fabricate with low spurious radiation effects. However, its major disadvantages include narrow bandwidth and difficulty in modelling due to drilling a hole into the substrate, as well as increased probe length leading to inductive input impedance and matching problems for thicker substrates. To address these issues, non-contacting feed techniques have been developed.

1.4.3 Aperture coupled feed

Aperture coupling is a feed technique commonly used in microstrip patch antennas. In this technique, the radiating patch element is etched on the top layer of the antenna substrate, while the microstrip feed line is etched on the bottom layer of the feed substrate. The two substrates can be chosen independently based on their thickness and

dielectric constants to optimize the distinct electrical functions of radiation and circuitry.

The coupling aperture, which determines the amount of coupling from the feed line to the patch, is usually located at the center of the patch, leading to lower cross-polarization due to symmetry. The size, shape, and location of the aperture can be adjusted to control the coupling.

One of the advantages of the aperture coupled feed technique is that spurious radiation is minimized since the ground plane separates the patch and the feed line. Additionally, this technique provides better impedance matching than the other feeding techniques. However, the complexity of the feed network is increased, and the bandwidth may be limited compared to other feed techniques.

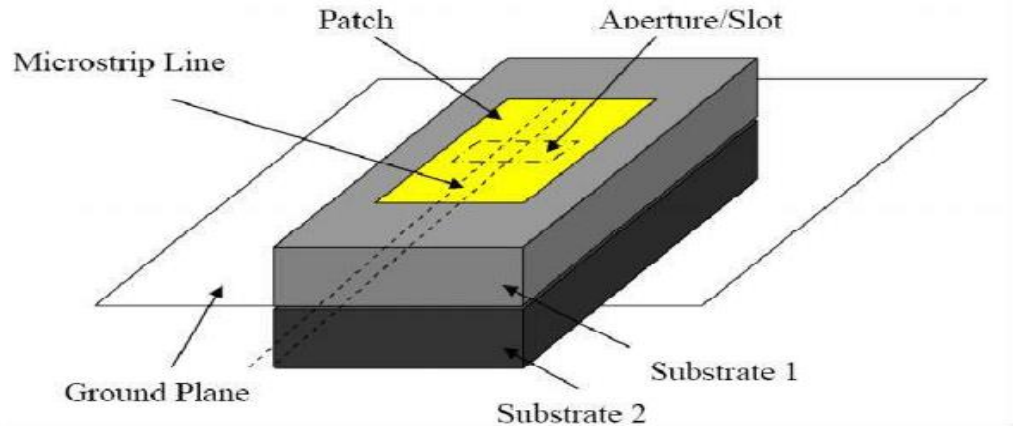

Figure 1.8 Aperture Coupled Feed

1.4.4 Proximity coupled feed

The electromagnetic coupling scheme, also known as the two-layer feed technique, involves using two dielectric substrates to feed the microstrip patch antenna. The feed line is placed between the two substrates while the radiating patch is located on the upper substrate. This technique has several advantages, such as the elimination of spurious feed radiation and a high bandwidth of approximately 13%. This increase in bandwidth is due to the electrical thickness of the microstrip patch antenna. The main

disadvantage of this technique is the difficulty in fabricating it, as proper alignment of the two dielectric layers is required. However, this scheme provides options for optimizing the performance of each individual component by using different dielectric media for the patch and the feed line.

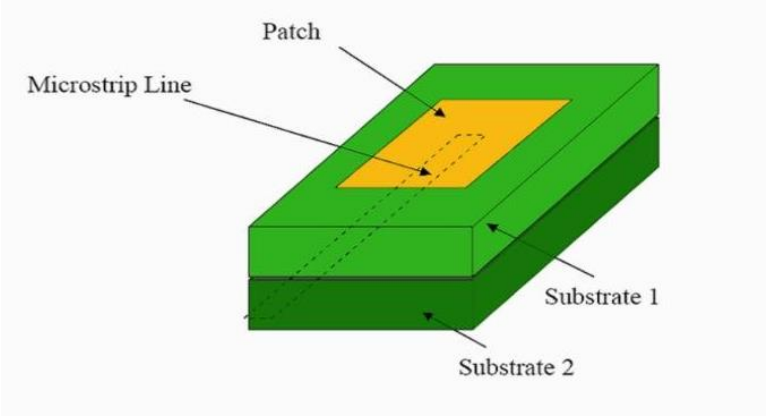

Figure 1.9 Proximity Coupled Feed

One of the main drawbacks of the two-layer feed technique is the complexity of its fabrication process. Proper alignment of the two dielectric layers is necessary, which can be challenging. Additionally, the use of two layers increases the overall thickness of the antenna, which can limit its practicality in certain applications.

1.5 Antenna Parameters

1.5.1 Gain

The gain of an antenna is an important parameter that determines the ability of the antenna to radiate or receive signals in a particular direction. It is defined as the ratio of the radiation intensity in a specific direction to the radiation intensity that would be obtained if the power were radiated isotropically, i.e., uniformly in all directions. Gain is measured in decibels (dB) and is usually reported relative to a reference isotropic radiator (dBi) or a reference dipole antenna (dBd). A higher gain value indicates a more directional radiation pattern, which can be useful in applications where the antenna needs to focus its energy in a specific direction, such as in satellite communications,

radar systems, and point-to-point wireless links. The radiation intensity of a lossless isotropic antenna can be calculated by dividing the power supplied to the antenna by the solid angle of 4π Steradians.

$$Gain = \frac{4\pi \text{ radiation intensity}}{\text{total input(transmitted)power}} \quad 1.5$$

1.5.2 Radiation pattern

An antenna's radiation pattern refers to the mathematical or graphical representation of its radiation properties as a function of spatial coordinates. These radiation properties include power flux density, radiation intensity, field strength, directivity, phase, and polarization. The radiation pattern is typically determined in the far-field region and is represented in terms of directional coordinates. The radiation pattern of an antenna consists of lobes, which are its different parts, classified as major lobe, minor lobe, side lobe, and back lobe. The major lobe is also known as the main beam, and it is the lobe that contains the direction of maximum radiation. Any lobe other than the major lobe is called a minor lobe. A side lobe is a radiation lobe that occurs in any direction other than the intended lobe, usually adjacent to the main lobe and occupying the hemisphere in the direction of the main beam. Finally, a back lobe is a radiation lobe whose axis makes an angle of approximately 180° with respect to the beam of an antenna. The lobes of the radiation pattern are essential to understanding the directional properties of an antenna. The major lobe determines the main radiation direction of the antenna, while the minor lobes provide secondary radiation directions. The presence of side lobes and back lobes can negatively impact the antenna's performance by directing energy in unwanted directions. Therefore, antenna designers aim to minimize the presence of side lobes and back lobes while maximizing the directivity of the main lobe. The design of the antenna's elements, their shape and orientation, and the antenna's size and frequency of operation all play a role in determining the radiation pattern of an antenna.

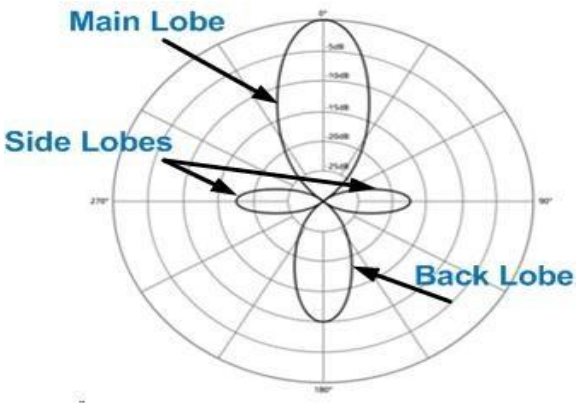

Figure 1.10 Radiation pattern

1.5.3 Directivity

The directivity of an antenna is a measure of how well the antenna focuses its power in a particular direction in three-dimensional space, relative to an isotropic radiator that emits power equally in all directions. It is expressed as the ratio of the radiation intensity in a given direction to the average radiation intensity over all directions.

$$\text{Directivity} = \frac{4\pi U}{P_{rad}} \qquad 1.6$$

Where, U= radiation intensity of the antenna

P_{rad} = Power radiated by the antenna

1.5.4 Bandwidth

The bandwidth of an antenna is the range of frequencies over which it can operate effectively. It is typically defined as the difference between the upper and lower frequencies at which the antenna's performance is within a specified range of its maximum value.

$$\text{ABW} = f_L - f_H \qquad 1.7$$

$$\text{FBW} = 2\frac{f_H - f_L}{f_H + f_L} \qquad 1.8$$

Where, ABW= Absolute bandwidth

FBW= Fractional bandwidth

f_L = Lower cut-off frequency

f_H = Higher cut-off frequency

1.5.5 Polarization

Polarization of an antenna refers to the orientation of the electric field of the electromagnetic wave that it radiates or receives. It is the property of the antenna that determines the direction of the electric field in the radiated or received wave. The polarization of an antenna can be either linear or circular, and it is determined by the orientation of the antenna elements and the direction of the current flow. In general, antennas are designed to have a specific polarization to match the polarization of the transmitting or receiving antenna in a communication system, to ensure efficient transfer of electromagnetic waves.

1.5.6 Radiation efficiency

The radiation efficiency of an antenna refers to how effectively it converts RF power into radiated power. It is defined as the ratio of the radiated power to the total power delivered to the antenna terminals in transmitting mode. The higher the radiation efficiency, the less power is lost as heat and the more power is available for radiation.

$$\eta_e = \frac{P_t}{P_{in}} \tag{1.9}$$

where, η_e = radiation efficiency

P_t = power transmitted by the antenna

P_{in} = power given as input to the antenna

1.5.7 Voltage standing wave ratio

Voltage Standing Wave Ratio (VSWR) is a measure of how efficiently radio-frequency power is transmitted from a power source through a transmission line and into an antenna. It is a dimensionless ratio of the maximum voltage to the minimum voltage along the transmission line and is also sometimes referred to as the voltage reflection coefficient. A low VSWR indicates that the antenna is well-matched to the transmission line and power is efficiently transferred from the source to the antenna. A high VSWR indicates that there is an impedance mismatch between the antenna and the transmission line, which can result in poor signal transmission and potential damage to the equipment. VSWR is typically measured using a network analyzer or a VSWR meter.

$$\text{VSWR} = \frac{v_{max}}{v_{min}} = \frac{1+|\Gamma|}{1-|\Gamma|} \qquad 1.10$$

Where, VSWR = voltage standing wave ratio

v_{max} = maximum voltage on the line

v_{min} = minimum voltage on the line

Γ = reflection coefficient

1.5.8 Q-factor

The Q factor, also known as the quality factor, is a dimensionless parameter that measures an antenna's bandwidth in relation to its center frequency. The Q factor is commonly used to describe the efficiency of an antenna, and there are various formulas that can be applied to calculate the Q factor based on the antenna's specific characteristics and the type of analysis being conducted. If the antenna operates over a band between f_1 and f_2 with center frequency is given by

$$Q = \frac{f_0}{(f_2 - f_1)} \qquad 1.11$$

Where f_0 is the resonant frequency of the antenna, f_1 is the lower frequency limit of the bandwidth and f_2 is the upper frequency limit of the bandwidth.

1.5.9 Axial Ratio

The axial ratio of an antenna is a measure of the polarization purity of the electromagnetic waves it radiates. It is defined as the ratio of the major and minor axes of the polarization ellipse of the radiated wave. The polarization ellipse is a graphical representation of the orientation and magnitude of the electric field vector of the radiated wave as it propagates through space. The axial ratio is a dimensionless quantity that ranges from 0 to 1 dB for perfectly circularly polarized waves to infinity for linearly polarized waves. An antenna with a low axial ratio indicates that it radiates electromagnetic waves with good polarization purity, while a high axial ratio indicates that the waves have poor polarization purity. The axial ratio is an important parameter in applications where polarization is critical, such as satellite communication, radar, and navigation systems.

1.5.10 Return loss

The Return Loss (RL) is a measure of the amount of power reflected by an antenna or transmission line. It indicates the degree of impedance matching between the load and the source and is expressed in decibels (dB). When there is a mismatch in the impedance between the source and load, some of the energy sent by the source is reflected back towards the source. This reflected power adds up with the incident power, leading to the formation of standing waves. A high RL value indicates a good match between the source and load, and therefore a low amount of reflected power. Ideally, the RL value

$$S_{11}(10\text{dB}) = 10\log_{10}\frac{P_i}{P_r} \qquad 1.12$$

should be as low as possible. In the case of a patch antenna, an RL value of less than -10 dB is considered good.

An S11 value below -10 dB indicates that at least 90% of the input power is being delivered to the device and less than 10% is being reflected. This value is considered acceptable for many applications. S11 represents the return loss of the antenna and is an important parameter in antenna testing.

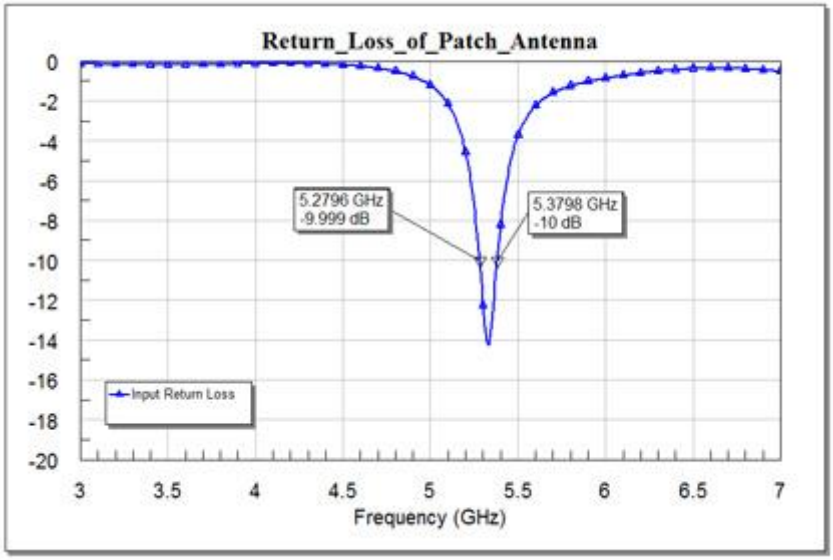

Figure 1.11 Return loss graph of a patch antenna

1.6 Reconfigurable Antenna

1.6.1 Introduction

Reconfigurable antennas are a type of antenna that can change their operating frequency, radiation pattern, polarization, or other characteristics dynamically or statically in response to changing requirements or environmental conditions. The ability to reconfigure the antenna's properties allows for greater flexibility and adaptability in communication systems. Reconfigurable antennas can be designed to operate in multiple frequency bands, which is particularly useful for communication systems that require wide frequency coverage. By adjusting the operating frequency, the antenna can adapt to different communication standards or overcome interference from other sources. Another important feature of reconfigurable antennas is the ability to change

the radiation pattern. This can be achieved by altering the shape, size, or configuration of the antenna elements, or by using additional components such as switches or phase shifters. A reconfigurable antenna with a controllable radiation pattern can be useful in applications such as beamforming, where the antenna can focus the radiation in a particular direction for improved signal strength or interference rejection. Overall, reconfigurable antennas offer a promising approach to enhance the performance and functionality of communication systems, especially in the context of emerging wireless technologies and the increasing demand for high data rates and reliable communication.

1.6.2 Necessity of Reconfigurability

Reconfigurable antennas are becoming increasingly popular in modern wireless communication systems due to their ability to adapt to varying operational conditions. In traditional antenna designs, the antenna properties are fixed and cannot be changed once it is fabricated. However, in modern communication systems, the operating environment can change rapidly, and the antenna may need to adapt to the changes in the environment to ensure optimal performance. This is where reconfigurable antennas come into play.

Reconfigurable antennas are designed to change their properties, such as frequency, radiation pattern, polarization, or impedance, in response to changing operating conditions. This reconfiguration can be achieved through several methods, including the use of switches, varactors, or tunable materials. By reconfiguring the antenna properties, the antenna can adapt to different frequencies, environmental conditions, or communication standards, without the need for physical changes to the antenna structure.

The need for reconfiguration in antennas is driven by the increasing demand for more flexible and adaptable wireless communication systems. With the proliferation of wireless devices and the ever-increasing demand for high-speed data transfer, there is a need for communication systems that can operate in a variety of frequencies and

environments. Reconfigurable antennas can provide flexibility and adaptability, which is crucial for the success of modern wireless communication systems. Furthermore, reconfigurable antennas can also help to improve the efficiency and performance of wireless communication systems. By optimizing the antenna properties for specific operating conditions, reconfigurable antennas can reduce interference, increase data transfer rates, and improve signal quality. This makes reconfigurable antennas a promising technology for future wireless communication systems.

1.6.3 Challenges

Achieving reconfigurability in antennas is a challenging task, as it requires the integration of various components and technologies to achieve the desired performance. Some of the challenges faced in achieving reconfigurability in antennas include:

1. Integration of multiple radiating elements: In order to achieve reconfigurability, antennas often require multiple radiating elements that can be switched on and off or reconfigured to achieve the desired radiation pattern. The integration of these multiple elements can be challenging, as it requires careful design and optimization to ensure that they work together seamlessly.

2. Control and switching mechanisms: The ability to reconfigure an antenna requires precise control and switching mechanisms that can turn on and off individual elements or adjust their properties. These mechanisms can be complex and require precise control to ensure that the antenna functions properly.

3. Bandwidth limitations: Reconfigurability often comes at the cost of reduced bandwidth, as the addition of multiple elements and switching mechanisms can limit the range of frequencies over which the antenna can operate effectively.

4. Power consumption: Reconfigurable antennas often require additional power to operate the switching and control mechanisms, which can reduce overall efficiency and increase power consumption.

5. Size and weight: The integration of multiple elements and control mechanisms can increase the size and weight of the antenna, making it less practical for some applications.

Despite these challenges, the development of reconfigurable antennas has the potential to greatly improve the performance and flexibility of wireless communication systems, making them a focus of ongoing research and development.

1.7 Division Of Reconfigurable Antenna based on Parameters

1.7.1 Reconfigurable Antenna based on Frequency

Frequency reconfigurable antennas are a type of reconfigurable antenna that can adjust their frequency of operation based on the specific requirements of the communication system. These antennas can operate over a range of frequencies and can be dynamically tuned to a specific frequency or band of frequencies. One approach to achieve frequency reconfigurability is to use active tuning techniques, which involve the use of electronic components such as varactors or switches to dynamically tune the antenna's resonant frequency. Another approach is to use passive tuning techniques, such as the use of switchable parasitic elements or metamaterial structures that can be tuned by external stimuli, such as magnetic or electric fields. These approaches can provide significant improvements in frequency agility while minimizing the impact on other performance characteristics. Frequency reconfigurable antennas have a wide range of applications in communication systems, including multi-band systems, cognitive radio, and wireless sensor networks. These antennas enable more efficient use of the available frequency spectrum, by allowing a single antenna to operate over multiple frequency bands, reducing the need for multiple antennas and simplifying system design.

Frequency reconfigurability in antennas can be achieved using various techniques, including:

- Frequency reconfigurability in Tunable capacitor elements: One way to achieve frequency reconfigurability is by incorporating tunable capacitors (such as varactor diodes or MEMS capacitors) into the antenna design. Adjusting the capacitance value of these elements can change the resonant frequency of the antenna.

- Switchable resonant elements: Another approach is to use switchable resonant elements (such as PIN diodes or MEMS switches) to change the resonant frequency of the antenna. These elements can switch in or out parts of the antenna structure, effectively changing its length or shape and thus its resonant frequency.

- Reconfigurable feeding networks: Frequency reconfigurability can also be achieved by using multiple feed points or switchable feed networks in the antenna's design. This can adjust the antenna's resonant frequency and radiation characteristics.

- Metamaterials: Artificial structures known as metamaterials can manipulate electromagnetic waves in unusual ways. By incorporating metamaterials into the antenna design, it is possible to achieve frequency reconfigurability and other advanced functionalities such as beam steering and polarization control.

- Dielectric materials: Another method is to use dielectric materials to change the effective dielectric constant of the antenna substrate and thus its resonant frequency. By embedding tunable dielectric materials (such as ferroelectric materials) into the antenna structure, the resonant frequency can be adjusted.

1.7.2 Reconfigurable antenna based on Radiation-Pattern

Radiation pattern reconfigurability refers to the ability to adjust the shape and direction of the electromagnetic radiation pattern of an antenna or other radiating device. There are several techniques that can be used to achieve radiation pattern reconfigurability, including:

1. Antenna array design: Using an array of antennas, it is possible to steer the direction of the main lobe of the radiation pattern by adjusting the relative phases and amplitudes of the signals feeding each antenna. This technique is often used in radar systems and satellite communications.

2. Active antenna elements: By embedding active elements, such as amplifiers or phase shifters, into the antenna structure, it is possible to adjust the radiation pattern in real time. This approach is commonly used in mobile communication systems and wireless networks.

3. Metamaterials: Metamaterials are artificial materials with unique properties that allow for precise control of electromagnetic radiation. By embedding metamaterial structures into the antenna design, it is possible to achieve pattern reconfigurability.

4. Mechanical adjustments: By physically adjusting the shape or orientation of the antenna, it is possible to alter the radiation pattern. This approach is often used in directional antennas for radio and television broadcasting.

1.7.3 Reconfigurable Antenna based on Polarisation

Polarization reconfigurable antennas are a type of antenna that can be designed to switch between different polarization states, such as linear, circular, or elliptical polarization. These antennas can be useful in situations where the orientation of the receiving or transmitting antenna is not known or may change over time, such as in mobile communications or satellite communications.

Polarization reconfigurability refers to the ability to adjust the polarization of the electromagnetic waves radiated by an antenna. There are several techniques that can be used to achieve polarization reconfigurability, including:

1. Rotating the antenna: One of the simplest ways to achieve polarization reconfigurability is to physically rotate the antenna. By changing the orientation of the antenna, it is possible to adjust the polarization of the radiated wave.

2. Switchable feeds: Using switchable feeds, it is possible to change the orientation of the polarization without physically rotating the antenna. This can be achieved by switching between feeds with different polarization orientations, such as vertical and horizontal.

3. Phase shifters: By using phase shifters, it is possible to adjust the phase of the signal feeding the antenna, which can also change the polarization of the radiated wave. This approach is often used in active electronically steered arrays (AESAs).

4. Metamaterials: As with radiation pattern reconfigurability, metamaterials can be used to achieve polarization reconfigurability. By embedding metamaterial structures into the antenna design, it is possible to control the polarization of the radiated wave.

5. Reflectarrays: Reflectarrays are flat, planar arrays of elements that reflect the incident wave in a specific direction and with a specific polarization. By changing the phase of the elements, it is possible to adjust the polarization of the reflected wave.

1.7.4 Compound Reconfigurable Antenna

A compound reconfigurable antenna refers to an antenna that uses multiple techniques to achieve both frequency and radiation pattern reconfigurability. These antennas are designed to offer advanced functionalities, such as beam steering, polarization control, and multi-band operation. Some of the techniques used in compound reconfigurable antennas include:

1. Multi-band elements: By using multiple resonant elements, such as patches or dipoles, it is possible to achieve multi-band operation. These elements can be switched or tuned to operate at different frequencies, allowing the antenna to cover multiple frequency bands.

2. Tunable elements: Incorporating tunable elements, such as varactor diodes or MEMS switches, into the antenna structure allows for frequency reconfigurability. By adjusting the capacitance or inductance of these elements, the resonant frequency of the antenna can be changed.

3. Metamaterials: Metamaterials can be used to achieve advanced functionalities, such as beam steering and polarization control. By embedding metamaterial structures into the antenna design, it is possible to control the direction and polarization of the radiated electromagnetic wave.

4. Active elements: By using active elements, such as amplifiers or phase shifters, it is possible to adjust the radiation pattern of the antenna in real time. This approach is commonly used in mobile communication systems and wireless networks.

Compound reconfigurable antennas offer several benefits, including improved efficiency, reduced interference, and increased flexibility. They are commonly used in applications such as radar systems, satellite communications, and wireless networks.

1.8 Switchable Devices Used for Reconfiguration

There are several techniques available to implement reconfigurable antennas in different wireless systems like MIMO, cognitive radio communications, and satellite communication. These techniques can be broadly categorized into four groups:

- Electrical reconfiguration
- Optical reconfiguration
- Physical reconfiguration

• Reconfigurable antennas with smart materials.

1.8.1 Electrical Reconfiguration

Electrical reconfiguration is an approach used to alter the electrical properties of an antenna without physically changing its shape or size. By doing so, the antenna's operating characteristics can be changed to meet specific performance requirements. Electrical reconfiguration can be achieved through the use of switchable devices such as diodes, MEMS, and varactors. These devices can be used to modify the electrical properties of the antenna, such as its impedance, radiation pattern, and polarization. The reconfiguration of these properties enables the antenna to operate at multiple frequencies or with different radiation patterns, thereby enhancing its versatility and adaptability to various communication scenarios. The reconfiguration can be achieved through the manipulation of the surface currents on the antenna. By changing the distribution of the surface currents, the parameters of the antenna like frequency, polarization and radiation pattern can be altered. This can be achieved through the use of various techniques, such as the addition of reactive elements or the use of switches to change the antenna geometry.

1.8.1.1 PIN Diodes

A PIN diode, also known as a p-i-n diode, is a type of semiconductor device that has three layers: a p-type layer, an intrinsic layer, and an n-type layer. The intrinsic layer is a lightly doped or undoped region that acts as a high-resistance layer between the p-type and n-type layers. PIN diodes are semiconductor devices that are commonly used in antenna systems for reconfigurability. These diodes operate in reverse bias mode, and their conductive state can be controlled by varying the applied voltage. When used in antenna systems, PIN diodes can be used to switch or tune the antenna's frequency, pattern, or polarization. One of the main advantages of using PIN diodes is their low insertion loss. This means that when the diodes are switched on, the signal loss is minimal, which is important for maintaining signal strength in communication systems. In addition, PIN diodes have a fast switching speed, which allows for rapid

reconfiguration of the antenna. Another advantage of using PIN diodes is their ability to handle high power levels. This is important in applications where the antenna is required to operate at high power levels, such as in radar systems.

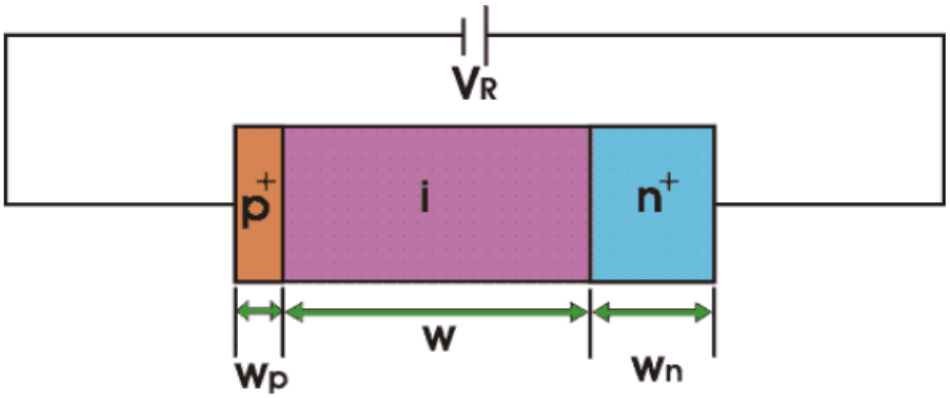

Figure 1.12 PIN Diode diagram

Wp = width of the p-doped region

Wn = Width of the n-doped region

W = Width of depletion region

V_R = Applied voltage

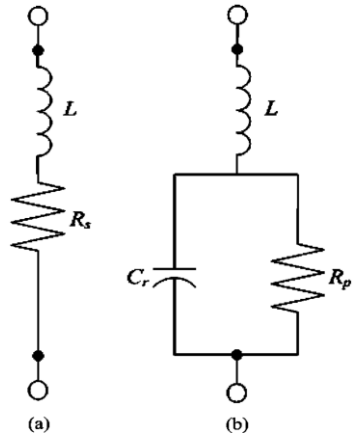

Figure 1.13 Equivalent circuit of a PIN diode

Figure 1.14 PIN diode

Here are some of the most commonly used pin diode models for antennas, along with their typical R, C, and L values:

1. HSMP-382x series: This series of low resistance and low capacitance pin diodes from Broadcom (now Avago Technologies) is commonly used in microwave and RF applications. The typical resistance of the series is 0.6 ohms, the typical capacitance is 0.2 pF, and the typical inductance is 0.1 nH.

2. MA4E1317 series: This series of medium resistance and medium capacitance pin diodes from MACOM (formerly M/A-COM Technology Solutions) is designed for high-frequency applications. The typical resistance of the series is 1.5 ohms, the typical capacitance is 0.4 pF, and the typical inductance is 0.15 nH.

3. BAP50-07 series: This series of high resistance and high capacitance pin diodes from NXP Semiconductors is commonly used in antenna applications where high-power handling and low control voltages are required. The typical resistance of the series is 9 ohms, the typical capacitance is 1.2 pF, and the typical inductance is 0.25 nH.

4. SMS7630-079LF series: This series of ultra-low resistance pin diodes from Skyworks Solutions is designed for high-power applications. The typical resistance of the series is 0.03 ohms, the typical capacitance is 0.6 pF, and the typical inductance is 0.05 nH.

1.8.1.2 Varactor diodes

Varactors function as voltage-controlled capacitors that can adjust capacitance by changing the applied voltage. This ability is useful for tuning antenna performance in reconfigurable designs by enabling frequency tuning. Varactors are known to be nonlinear and have a low dynamic range, which makes them less desirable for certain applications compared to active elements such as PIN diodes or MEMS. However, varactors have advantages such as small current flow and continuous tuning capabilities, which make them suitable for certain applications. The disadvantage of varactors, however, is that they require complex bias circuitry to operate effectively.

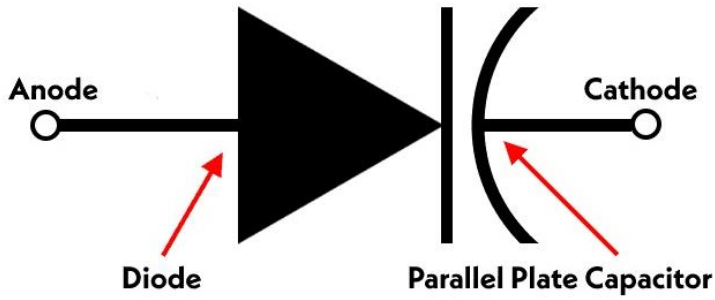

Figure 1.15 Varactor diode

1.8.1.3 MEMS

Microelectromechanical systems (MEMS) are also used for reconfigurability in antennas. MEMS-based reconfigurable antennas offer the potential for compact size, low power consumption, and fast switching speeds. In MEMS-based reconfigurable antennas, the mechanical movement of the MEMS switches changes the antenna's electromagnetic properties, allowing for reconfiguration. MEMS-based switches offer

excellent isolation, high linearity, and low insertion loss, making them suitable for many applications. However, MEMS switches can have high actuation voltage and low reliability due to their moving parts. Despite these limitations, MEMS-based reconfigurable antennas are being actively researched and developed for various applications, including beam steering and frequency tuning in wireless communication systems.

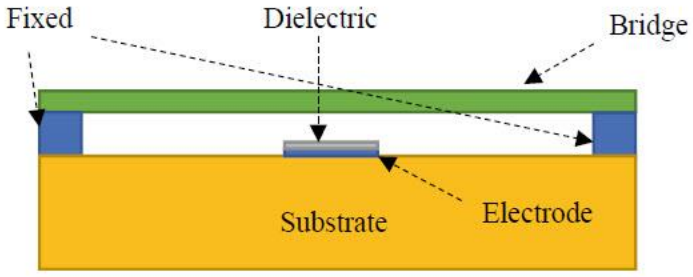

Figure 1.16 MEMS switch

1.8.2 Optical Reconfiguration

Optical reconfiguration is another technique that has been proposed for the design of reconfigurable antennas. This approach is based on the use of materials with photoconductive or electro-optic properties, which can be used to modify the electrical properties of the antenna structure. By controlling the illumination intensity and wavelength, the electrical characteristics of the antenna can be changed, leading to a reconfigurable behaviour. One of the main advantages of optical reconfiguration is its potential for high-speed switching and reconfiguration, as well as low loss and high linearity. However, the need for optical sources and detectors can add complexity and cost to the system. Various materials, including semiconductors, liquid crystals, and polymers, have been investigated for use in optical reconfiguration of antennas, with promising results.

1.8.3 Mechanical Reconfiguration

Mechanical reconfiguration is another technique used for reconfigurable antennas. In this technique, the physical shape of the antenna is changed to achieve the desired reconfiguration. One way of implementing this technique is by using shape memory alloys (SMA) or electroactive polymers (EAP). These materials have the ability to change their shape in response to an electrical or thermal stimulus. By incorporating these materials into the antenna structure, the physical shape of the antenna can be changed in a controlled manner. This can result in a change in the radiation pattern, polarization, or resonant frequency of the antenna.

1.9 Advantages of Reconfiguration

Reconfigurable antennas offer several advantages over fixed antennas, making them increasingly popular in modern wireless communication systems. Some of the advantages of reconfigurable antennas are:

1. Flexibility: Reconfigurable antennas can operate over multiple frequencies and have the ability to adapt to different environments, making them flexible and adaptable to changing conditions.

2. Compact size: By integrating multiple functions into a single antenna, reconfigurable antennas can reduce the overall size and weight of communication systems, making them ideal for portable and handheld devices.

3. Increased efficiency: Reconfigurable antennas can optimize their performance for different frequencies and radiation patterns, resulting in higher efficiency and lower power consumption.

4. Enhanced performance: By adapting to different environments and operating conditions, reconfigurable antennas can improve the performance of wireless communication systems, leading to better signal quality, higher data rates, and improved connectivity.

5. Cost-effective: Reconfigurable antennas can reduce the need for multiple antennas and additional hardware, leading to cost savings in terms of manufacturing, installation, and maintenance.

1.10 Applications of Reconfigurable Antennas

Here are some applications of reconfigurable antennas:

1. Wireless Communication Systems: Reconfigurable antennas are widely used in wireless communication systems to enable multiple frequency bands, polarization, and radiation patterns. They can be used in cellular, satellite, and Wi-Fi networks to improve the overall performance and reliability of the system. For example, in cellular networks, reconfigurable antennas can help minimize interference and improve signal quality in areas with a high density of users.

2. Radar Systems: Reconfigurable antennas are used in radar systems to change the beam shape and direction. They are used in military applications such as surveillance and tracking, as well as in civilian applications such as weather monitoring and air traffic control.

3. Radio Frequency Identification (RFID): Reconfigurable antennas are used in RFID systems to adjust the read range and sensitivity of the system. They can be used in applications such as inventory management, asset tracking, and access control.

4. Electronic Warfare: Reconfigurable antennas are used in electronic warfare to improve the detection and suppression of enemy signals. They can be used in applications such as jamming, direction finding, and countermeasures.

5. Medical Imaging: Reconfigurable antennas are used in medical imaging systems such as magnetic resonance imaging (MRI) and computed tomography (CT) scanners to improve image quality and reduce interference. They can also be used in non-invasive medical procedures such as deep brain stimulation.

6. Space Applications: Reconfigurable antennas are used in space applications such as satellite communication and remote sensing. They can be used to improve the performance and reliability of the system, as well as reduce the size and weight of the antennas.

1.11 Design Equations

The design of an antenna requires consideration of three key parameters: the operating frequency (f), the dielectric constant (εr), and the substrate thickness (h). These parameters are used to determine the antenna's dimensions using the following equations. The width of the patch (W) can be calculated using a specific equation.

The equation to determine the width of the patch:

$$w = \frac{1}{f_r} * \frac{c}{\sqrt{\frac{\epsilon_r + 1}{2}}} \tag{1.13}$$

Where, the width of the patch is denoted by W, where c represents the speed of light, f represents the operating frequency of the antenna, and εr is the relative permittivity of the substrate material utilized to fabricate the patch.

$$L = L_{eff} - 2(0.412h)\left[\frac{\left(\varepsilon_{reff}+0.3\right)\left(\frac{w}{h}+0.264\right)}{\left(\varepsilon_{reff}-0.258\right)\left(\frac{\omega}{h}-0.8\right)}\right] \tag{1.14}$$

Where L_{eff} denoted the effective length of the patch, ε_{reff} represents effective dielectric constant. The equation for the effective length of the patch (L_{eff}):

$$L_{eff} = \frac{c}{2f_r\sqrt{\varepsilon_{reff}}} \tag{1.15}$$

Where C represents velocity of light in free space, f_r is the resonance frequency to which the antenna being designed. The equation for effective dielectric constant ($\varepsilon_{\text{reff}}$):

$$\varepsilon_{eff} = \frac{\varepsilon_r + 1}{2} + \frac{\varepsilon_r - 1}{2}\left(\frac{1}{\sqrt{1 + 12\frac{h}{\omega}}}\right) \quad 1.16$$

1.12 Gain and bandwidth enhancement methods:

Apart from employing diverse feeding techniques, various other methods have been developed in recent times to improve the bandwidth and gain of microstrip antennas. The following is a brief summary of some commonly utilized techniques:

1.12.1 Parasitic Patch

The parasitic patch technique is based on the concept of electromagnetic coupling between two radiating elements. Coplanar parasitic patches are positioned parallel to the driven patch on the same plane. They are designed to be of a specific length and width and placed at a distance from the driven patch. The coupling between the coplanar parasitic patch and the driven patch results in an increase in the effective length of the patch, leading to an increase in gain and bandwidth. On the other hand, stacked parasitic patches are placed above or below the driven patch on a different layer. They can be designed as resonant or non-resonant patches and are placed at a specific distance from the driven patch. The coupling between the stacked parasitic patch and the driven patch results in an increase in the effective aperture of the antenna, leading to an increase in gain and bandwidth.

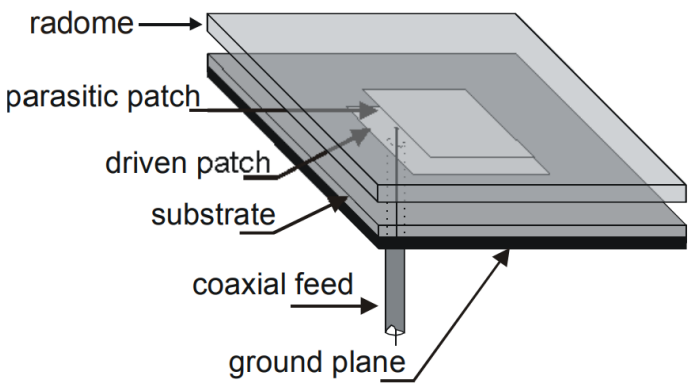

Figure 1.17 Parasitic patch

1.12.2 Air Gap

Air gap is another technique that can be used to enhance the gain and bandwidth of antennas. By introducing an air gap between the radiating patch and the ground plane, the surface wave losses can be reduced, resulting in an increase in the efficiency of the antenna. The air gap technique is commonly used in microstrip patch antennas, where a dielectric substrate is sandwiched between the patch and the ground plane. By increasing the distance between the patch and the ground plane, the capacitance between the two is reduced, resulting in a lower surface wave current and reduced losses. This increases the antenna's radiation efficiency, leading to an increase in gain and bandwidth. However, it is important to note that the introduction of an air gap may also cause a shift in the resonance frequency of the antenna. Therefore, the size and position of the air gap must be optimized to maintain the resonant frequency of the antenna at the desired frequency of operation.

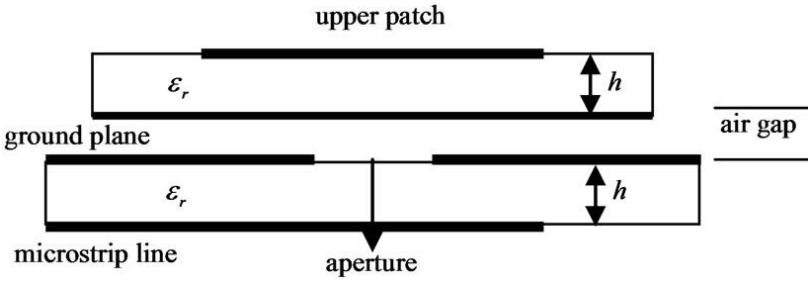

Figure 1.18 Air gap

1.12.3 Slots

Slots are another technique that can be used to enhance the gain and bandwidth of antennas. Slots are small apertures in the conductive surface of an antenna that can modify the current distribution and radiation pattern of the antenna. Slots are commonly used in microstrip patch antennas, where they can be introduced on the radiating patch, the ground plane, or the walls of the substrate. The introduction of slots on the patch or ground plane can modify the current distribution on the patch, resulting in an increase in the effective length of the patch and an increase in gain and bandwidth. Slots on the walls of the substrate can create additional radiation modes, resulting in a broader bandwidth. The size, shape, and position of the slot must be optimized to achieve the desired performance of the antenna. Slot antennas can also be designed as dual-polarized antennas, which are used in applications that require both horizontal and vertical polarization.

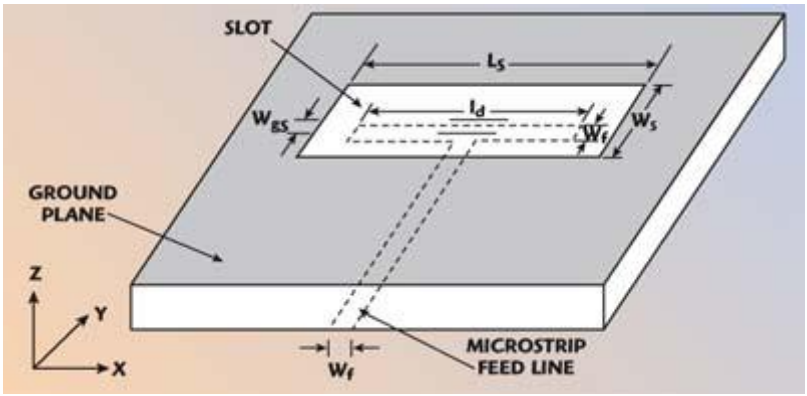

Figure 1.19 Slot antenna

Slot antennas are a type of antenna that uses a slot in a metal surface to radiate or receive electromagnetic waves. The slot can be cut in various shapes, such as rectangular, circular, or triangular, depending on the desired radiation pattern. Here are some design equations for slot antennas:

1. **Length of the slot (L):**

The length of the slot is a function of the operating frequency and the speed of light. It can be calculated using the following equation:

$$L = \frac{\lambda}{2} \tag{1.17}$$

where λ is the wavelength of the operating frequency.

2. **Width of the slot (W):**

The width of the slot determines the bandwidth of the antenna. A wider slot provides a wider bandwidth. The width can be calculated using the following equation:

$$\omega = \frac{\lambda}{2}\left(\frac{1}{\sqrt{\varepsilon_r - 1}}\right) \tag{1.18}$$

where εr is the relative permittivity of the material surrounding the slot.

3. **Position of the slot:**

The position of the slot affects the radiation pattern of the antenna. For example, a slot placed at the center of a rectangular patch antenna will produce a broadside radiation pattern. The position can be calculated using the following equation:

$$x = \frac{L}{2}(m + 0.5) \tag{1.19}$$

where x is the distance from the center of the patch to the center of the slot, and m is an integer that determines the number of half-wavelength resonant modes in the slot.

4. **Impedance matching:**

To ensure efficient power transfer between the antenna and the transmission line, the slot antenna must be impedance matched. The impedance can be adjusted by changing the length or width of the slot, or by placing a matching network between the antenna and the transmission line.

1.12.4 Dual Feed

The basic idea behind dual-feed is to feed the antenna from two different ports with signals that are in-phase. The signals combine to produce a stronger field, resulting in an increase in the gain of the antenna. The two feeds also provide different paths for the currents to flow, resulting in a wider bandwidth. This allows the antenna to operate over a range of frequencies without significant loss of performance. Dual-feed can be used in various types of antennas, such as patch antennas, microstrip antennas, and slot antennas. The technique is particularly useful in high-frequency applications, where the bandwidth of the antenna is limited.

1.12.5 Dielectric Substrate

The substrate material plays a significant role in determining the radiation pattern, resonant frequency, and impedance matching of the antenna. By carefully selecting the dielectric substrate material and its properties, antenna designers can achieve significant improvements in the gain and bandwidth of their designs. A higher dielectric constant substrate material can result in a smaller antenna size, leading to an increase in the gain of the antenna. This is due to the increase in the effective electrical length of the antenna, which in turn increases its resonant frequency. The substrate material can also be used to enhance the bandwidth of the antenna. By using a substrate material with a lower dielectric constant, the operating frequency range of the antenna can be increased. This is because a lower dielectric constant material reduces the electric field within the substrate, leading to a reduction in the resonant frequency and a widening of the operating bandwidth. Antenna designers can also use multiple layers of dielectric substrate to further enhance the performance of the antenna. By stacking multiple substrates with different dielectric constants, the bandwidth of the antenna can be increased even further, while maintaining a compact design.

For microstrip antennas, the substrate thickness (h) is an important design parameter that affects the antenna's bandwidth and radiation characteristics. Therefore, selecting the appropriate substrate material and thickness is a critical step in designing microstrip

patch antennas. The following equations can be used to determine the optimal substrate thickness:

$$h = \frac{0.412\lambda_0}{\sqrt{\varepsilon_\gamma}} \quad 1.20$$

Where λ0 is the free-space wavelength and εr is the relative permittivity of the substrate.

If the substrate is too thick, it can lead to a decrease in antenna efficiency and bandwidth. On the other hand, if the substrate is too thin, it can lead to increased losses due to surface waves. The quality factor (Q) of the substrate is another important parameter that affects antenna performance. The quality factor is a measure of the substrate's ability to store electrical energy without loss. The following equation can be used to determine the quality factor:

$$Q = \frac{\varepsilon_r}{tan\,\delta} \quad 1.21$$

A high-quality factor substrate with a low loss tangent can help to improve antenna efficiency and reduce losses.

1.12.6 Defected Ground Structures (DGS)

Defected ground structures (DGS) have emerged as a recent technique to enhance the performance of microstrip antennas. This method involves creating a simple defect on the ground plane in the form of any shape, which interrupts the current flow and impacts the excitation and propagation of radio waves through the substrate layer. The use of DGS also facilitates the modification of transmission line parameters, including capacitance and inductance, to achieve desired results. Depending on the desired performance, the shape of the defect can range from simple to intricate. In microstrip antennas, DGS offers several benefits, including improved performance in transmission lines, dividers, couplers, oscillators, power amplifiers, and combiners.

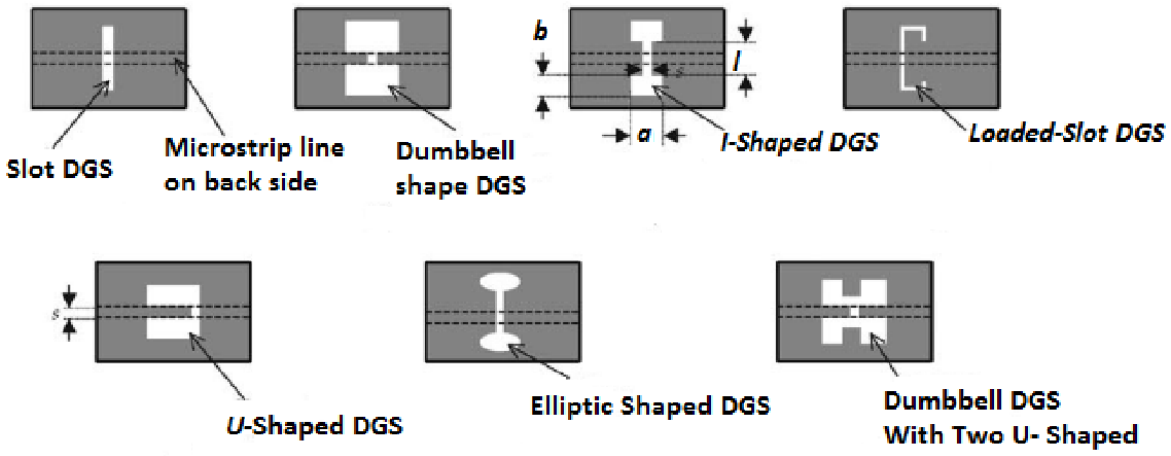

Figure 1.20 Types of Defected ground structures

1.13 Hybrid Coupler

1.13.1 3dB, 90° Hybrid Couplers

A 3 dB, 90° hybrid coupler is a component with four ports that can split an input electromagnetic signal equally into two output ports while also providing a 90° phase shift between them. Alternatively, it can combine two signals while maintaining high isolation between the ports. The coupler provides versatility in signal routing and phase manipulation.

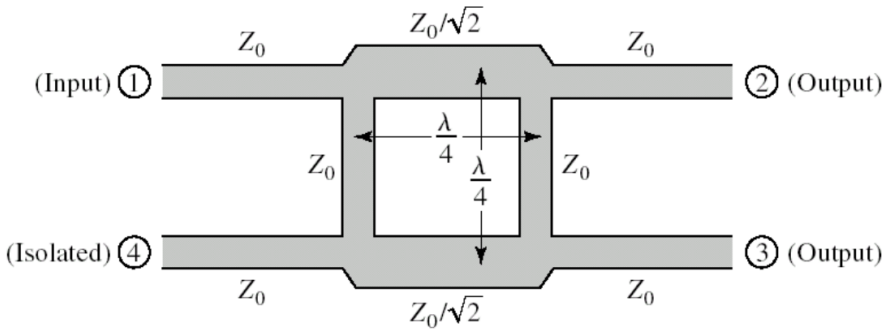

Figure 1.21 3dB, 90° hybrid coupler

Figure 1.21 shows the fundamental design of a hybrid coupler, which consists of two cross-over transmission lines with a length of one-quarter wavelength at the center frequency of operation. When power is introduced at port 1, half of the power (3 dB) flows to port 0°, and the other half is coupled to port 90° in the opposite direction. Any reflections due to mismatches will be sent back to the output ports and will flow directly to the isolated port (2) or cancel at the input, making hybrids useful in applications where high-power signals could damage the driver device through unwanted reflections.

A 3 dB, 90° hybrid coupler is also known as a quadrature hybrid because it can generate two signals of equal amplitude, with a phase difference of 90°, from any input signal. The device is electrically and mechanically symmetrical, meaning that the output relationship between the ports remains the same, regardless of which port is the input. This symmetrical design provides a high degree of isolation between the input and output ports, preventing any unwanted interaction between them.

1.13.2 3dB, 180° Hybrid Ring Couplers

180° Hybrid ring couplers, also known as "rat race" couplers, are four-port devices that can be used to either equally divide an input signal or combine two signals. One advantage of the hybrid ring is that it can provide equally divided output signals with a phase shift of 180 degrees alternately. This feature provides additional flexibility in signal routing and phase manipulation.

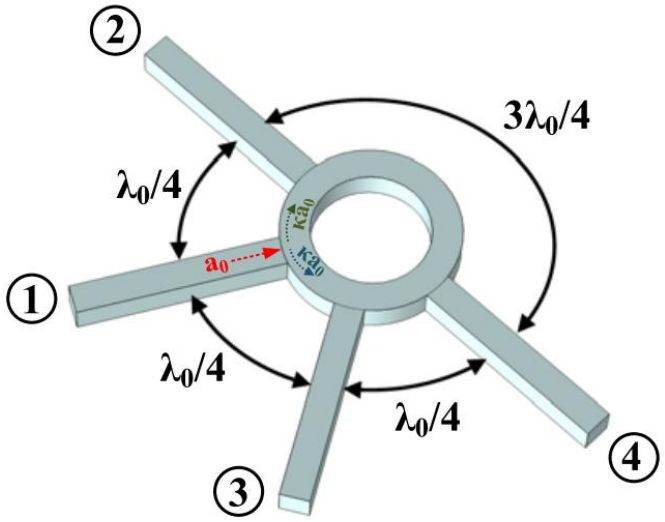

Figure 1.22 3dB, 180° hybrid ring coupler

The 3dB, 180° Hybrid Ring Coupler is composed of a circular ring that has four input/output ports connected to it. The ring is usually made of conductive materials such as aluminum or copper and is designed to have a circumference equal to one wavelength at the operating frequency. Two opposite ports of the ring are used as the input ports, while the other two opposite ports serve as the output ports.

The coupler operates based on the principle of phase cancellation. The signals entering the input ports of the coupler travel around the ring in opposite directions, and when they reach the output ports, they interfere with each other. The signals at one output port add together because they are in phase, while the signals at the other output port are 180 degrees out of phase and cancel each other out.

The 3dB, 180° Hybrid Ring Coupler provides a 3dB power split between the two output ports, and a phase shift of 180 degrees between the output signals. This makes it useful in various applications such as power amplifiers, mixers, and antenna systems. The design of the 3dB, 180° Hybrid Ring Coupler requires the use of transmission line theory and careful consideration of the coupler dimensions and substrate material selection. Design equations are available to calculate the necessary coupler dimensions

based on the desired performance specifications, substrate properties, and operating frequency.

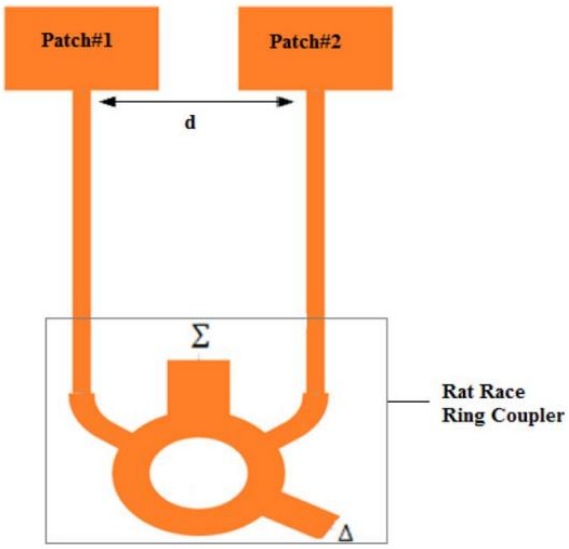

Figure 1.23 Rat race ring coupler

CHAPTER 2:

Literature Survey

C. A. Balanis' "Antenna Theory: Analysis and Design" [1] is a comprehensive textbook that covers the fundamental principles and practical applications of antenna engineering. It includes a broad range of topics such as the basic principles of electromagnetic theory, antenna parameters, radiation pattern analysis, aperture antennas, array antennas, and broadband antennas. Ramesh Garg's "Microstrip Antenna Design Handbook" [2] is a book that serves as a practical guide for designing and analyzing microstrip antennas. It covers various topics such as the basic principles of microstrip antennas, antenna design parameters, feeding techniques, and bandwidth enhancement techniques. In 2006, S. Gao et al. [3] presented an overview of polarization-agile antennas (PAAs) in their publication. These antennas have the capability of changing the polarization of their radiated signal in real-time. They began by emphasizing the significance of polarization in antenna systems and the difficulties associated with achieving polarization diversity in practical systems. The authors then introduced the concept of PAA and provided an overview of various techniques for achieving polarization agility. These techniques included polarization rotation, polarization switching, and dual-polarized antennas. In 2015, M. Saravanan et al. [4] proposed a novel single-fed polarization reconfigurable antenna. The antenna is designed with a radiating patch that has a diagonal slot in its center and utilizes four p-i-n diodes in the diagonal slot region to enable polarization reconfiguration. By applying selective biasing to the p-i-n diodes, the antenna can operate in three distinct states: linear polarization (LP), left-hand circular polarization (LHCP), and right-hand circular polarization (RHCP). In 2016, W. Lin et al. [5] proposed a wideband circularly polarized antenna with polarization reconfigurability. The antenna comprises of a reconfigurable feeding network and four radiating arms. These radiating arms are capable of producing bidirectional radiation patterns in free space, enabling the generation of wideband CP waves.

In 2017, L. Zhang et al. [6] presented a new printed antenna design that offers a broad frequency range, high gain, and the ability to reconfigure circular polarizations. The antenna is constructed by printing a loop antenna on a dielectric substrate on both sides. One side has a dual-p-i-n-diode loaded loop, while the other side has a dual-gap loaded smaller loop. By electronically controlling the on-off states of the p-i-n diodes, the antenna can switch between right-hand circular polarization (RHCP) and left-hand circular polarization (LHCP) across a wide range of frequencies. In 2019, Mahmoud Moubadir et al. [7] presented a new, compact structure designed for wireless communications systems operating at 5.4 GHz. This structure utilizes a dual-fed circular polarization microstrip antenna, which was successfully simulated. By feeding a rectangular patch with two quarter-wavelength transmission lines that are orthogonal to the patch and a microstrip 50Ω transmission line, the antenna is able to achieve dual-polarized radiation, good impedance matching, high port-isolation, and compact feeding. The simulation results indicate that the proposed structure generates circularly polarized radiation with good return loss performance, and the cross-polarization level of the circular polarization radiation for both right-hand circular polarization (RHCP) and left-hand circular polarization (LHCP) is also good. In 2011, Anil Kumar Agrawal et al. [8] proposed a stacked notched rectangular microstrip patch antenna designed for WLAN applications. The antenna's desired band is achieved by adjusting the dimensions of notches and the size of the stacked driven and parasitic patches. In 2021, Wang ST et al. [9] proposed A reconfigurable antenna capable of quad-polarization radiations using a switchable feeding network. To accomplish this, a wideband quad-mode feeding network has been designed, which involves integrating a simple impedance converter with a modified hybrid coupler. In 2019, Q. Chen et al. [10] proposed a novel cut ring microstrip antenna with high gain and polarization-reconfigurability. The antenna comprises a ring radiation patch, two switches (p-i-n diodes), and six nonmetallic columns. By manipulating the switches, the antenna can operate in three polarized states, including linear polarization (LP), left-hand circular polarization (LHCP), and right-hand circular polarization (RHCP). The structure of this microstrip antenna is simple yet effective.

In 2016, H. Sun et al. [11] presented a quad-polarization-agile antenna using a reconfigurable feeding network. By utilizing PIN diodes, the feeding network enables electrical tuning of the four transmission modes with selected phase differences at two output ports. In 2019, P. Kumar et al. [12] presented a novel dual-band circularly polarized slot antenna, which allows for the electronic switching of the far-field polarization between left-hand circular polarization and right-hand circular polarization. In 2021, R. Sharma et al. [13] proposed the design of a circular microstrip patch antenna that operates within the Ultra High Frequency (UHF) band of 470MHz to 806MHz. To improve the antenna's gain, a multilayer structure has been incorporated into the design. In 2018, L. Guo et al. [14] proposed a low-profile patch antenna with dual-linear polarization, which is made up of two stacked substrates, an air gap layer, and a grounded substrate. In 2012, S. T. Fan et al. [15] proposed a printed microstrip-line-fed slot antenna that incorporates a pair of parasitic patches to enhance the antenna's bandwidth. The addition of these patches along the microstrip feed line results in the excitation of an additional resonance, which leads to improved bandwidth performance.

In 2021, L. Kang et al. [16] presented a compact reconfigurable antenna with quad-polarization capability. The antenna employs a switchable feed scheme that allows it to operate in both single-fed and dual-fed modes. In single-fed mode, the feed structure enables the switching of output ports to produce excitations for either slant +45° or -45° linear polarization (LP). In dual-fed mode, the feed structure functions as a switchable phase-shifting power splitter for generating either left-hand circular polarization (LHCP) or right-hand circular polarization (RHCP). In 2021, S. Wang et al. [17] proposed a polarization-reconfigurable antenna is based on the circular polarized mode combination technique. In 2018, J. Hu et al. [18] introduced a low-profile metasurface antenna with the capability of reconfiguring its polarization to four states. This is achieved by incorporating four switchable feeding probes and two SPDT switches. The antenna operates in two orthogonal linear polarization modes and two

orthogonal circular polarization modes, and the polarization state can be changed by controlling the states of the SPDT switches. In 2018, J. Hu et al. [19] introduced a patch antenna with frequency and polarization reconfigurability, which exhibits small gain variation. By switching the shorting pins, the operating frequency can be dynamically selected from eight discrete frequency bands due to the shunt inductive effect. In addition, the polarization can be independently reconfigured among three states, including left-hand circular polarization (LHCP), right-hand circular polarization (RHCP), and linear polarization (LP), by controlling the states of the perturbation segments. In 2016, H. Gu et al. [20] presented a novel probe-fed patch antenna that enables polarization reconfiguration. The antenna comprises a circular radiating patch and a feed network that can be switched by controlling the operating states of four pairs of PIN diodes. This enables the feed point of the circular patch to be switched, thus providing polarization reconfiguration.

CHAPTER 3:

HFSS Software

3.1 Introduction

The Finite Element Method is a numerical tackle used by HFSS (High Frequency Structural Simulator). (FEM). The aforementioned approach divides the structure into several tiny portions which are called finite elements. Tetrahedra are the finite elements employed in HFSS, and every collection of tetrahedra is referred to as a mesh. Maxwell's equations satisfy themselves across the borders between the components in the original structure by finding solutions for the fields within the finite elements concerning one another. The generalized S-matrix solution is discovered following the emergence of the field solution.

Featuring an extensible solver and user-friendly GUI, HFSS (High Frequency Structural Simulator) combines unparalleled effectiveness and profound insight into all 3D EM challenges. HFSS gives a robust and detailed multi-physical analysis of electronic devices to guarantee thermal and structural reliability. It is integrated with ANSYS thermal, structural, and fluid dynamics tools. With auto-adaptive meshing and sophisticated solvers, HFSS was the gold standard for addressing 3D EM difficulties and may be sped up using High-Performance Computing (HPC) technology. HFSS is synonymous with precision and trustworthiness.

3.2 History

It was originally developed by Professor Zoltan Cendes and his students at Carnegie Mellon University. Professor Sendes and his brother Nicholas Sendes founded his Ansoft and bundled and sold his HFSS with his Ansoft product as part of his marketing relationship with Hewlett-Packard in 1989. In 1997, Hewlett-Packard acquired Optimization Systems Associates Inc. (OSA), the company John Bandler founded in 1983. The HP acquisition was prompted by HP's need for HFSS-optimized performance capabilities. After various business relationships from 1996 to

2006, HP (which became EE for his EDA division at Agilent) and Ansoft began to go their separate ways. Ansoft was later acquired by Ansys.

- It uses Finite Element Method
- Simulation tool for complex 3 D geometries
- Adaptive Mesh generation & refinement
- 2 Main Vendors—Agilent & Ansoft
- Transfer to Ansoft HFSS after Nov. 1, 2001

3.3 Finite Element Method

A powerful machine method for addressing differential and integral equations is the finite element method (FEM). A specific field can be seen as an accumulation of uncomplicated geometric components known as finite elements that result in a proximity function. With the use of finite elements, FEM approaches discretize the problem at hand. Finite elements are tetrahedral, hexahedral, or prismatic elements for three-dimensional issues and quadrilaterals or triangles for two-dimensional problems.

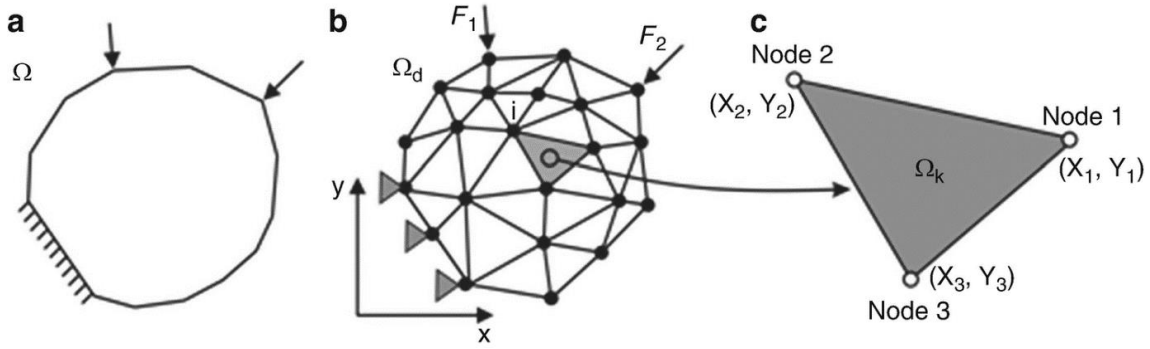

Figure 3.1 FINITE ELEMENT METHOD

FEM models swiftly and efficiently provide correct answers to many differential equations via piecewise approximation. The primary node basis function and its edge element basis can increase accuracy. Microstrip patch antennas may be simulated in multiple dimensions using the time-harmonic vector wave equation. Maxwell's

equations are applied to determine the vector wave equation because the antenna deals with electromagnetic waves. The end product is as follows.

$$\nabla \times B = -JwB \qquad 3.1$$

$$\nabla \times H = J_s + \sigma E + JwD$$

Where, $D = \varepsilon_r \varepsilon_0 E$, and $B=\mu_r \mu_0 H$

In the above equations, H is the magnetic field intensity, E is the electric field intensity and ω is the operating frequency. Furthermore, the permittivity and permeability of free space are ε0 and μ0, respectively, whereas the relative permittivity and permeability are εr and μr . The vector wave equation for E and H is given by eq. 3.2:

$$\nabla \times \left(\frac{1}{\mu_r} \nabla \times E\right) - k_0^2 \varepsilon_r E = -jk_0 \eta_0 Js \qquad 3.2$$

$$\nabla \times \left(\frac{1}{\varepsilon_r} \nabla \times H\right) - k_0^2 \mu_\gamma H = \nabla \times \left(\frac{1}{\varepsilon_r} Js\right)$$

Where, J_s is the current source,

$$\varepsilon_r = \varepsilon_{r'} - j\frac{\sigma}{w\varepsilon_0} \text{ and } k_0 = \omega\sqrt{\varepsilon_0 \mu_0}$$

where k0 is the free space wave number. Consider the substrate's dimensions so that the height of the substrate, h, is very very small with regard to the wavelength of the dielectric. Due to the extremely small substrate height, the field swings through the height is thus taken to be constant. Since the electric field is orthogonal to the patch's surface, only the transverse magnetic (TM) mode has been taken into consideration. As a result, the electric field will be transverse to the ground plane's surface. The patch's four side walls will be seamlessly conducting magnetic walls, while the top and bottom walls are perfectly electric conducting layers. Let r be less than the patch's shares borders with and the substrate's dielectric constant. Equation 3.3 gives the homogeneous wave equation for the vector potential Ax.

$$\nabla^2 A_x + k^2 A_x = 0 \qquad 3.3$$

The solution for this equation using the separation of variables is given as

$$A_x = [A_1 \cos(k_x x) + B_1 \sin(k_x x)] \cdot [A_2 \cos(k_y y) + B_2 \sin(k_y y)] \cdot [A_3 \cos(k_z z) + B_3 \sin(k_z z)] \quad 3.4$$

where the wave numbers along the axis of y, z, and x are, respectively, kx, ky, and kz. Boundary conditions may be utilized to find these. Calculation 3.5 supplies the electric and magnetic field related to the vector potential Ax.

$$E_x = -j\frac{1}{\omega\mu\varepsilon}\left(\frac{\partial^2}{\partial_x^2} + k^2\right)A_x , \quad 3.5$$

$$E_y = -j\frac{1}{w\mu\varepsilon}.\frac{\partial^2 Ax}{\partial x\,\partial y},$$

$$E_z = -j\frac{1}{w\mu\varepsilon}.\frac{\partial^2 A_x}{\partial x\,\partial z},$$

$$H_x = 0,\ H_y = \frac{1}{\mu}\cdot\frac{\partial A_x}{\partial z},\ H_z = -\frac{1}{\mu}\cdot\frac{\partial A_x}{\partial y} \quad 3.6$$

The scattering parameter, which is an essential component of finite element analysis, may be retrieved from the estimated electric field by utilizing the reflection coefficient S11. As a result, the input impedance may be computed as

$$Z = Z_0\frac{1+S_{11}}{1-S_{11}} \quad 3.7$$

where Zo is the characteristic or the matching impedance.

3.4 Ansoft terms

Open the HFSS window. The Ansoft HFSS window has several panels:

3.4.1 Project Manager:

It contains a list of the structure of the project.

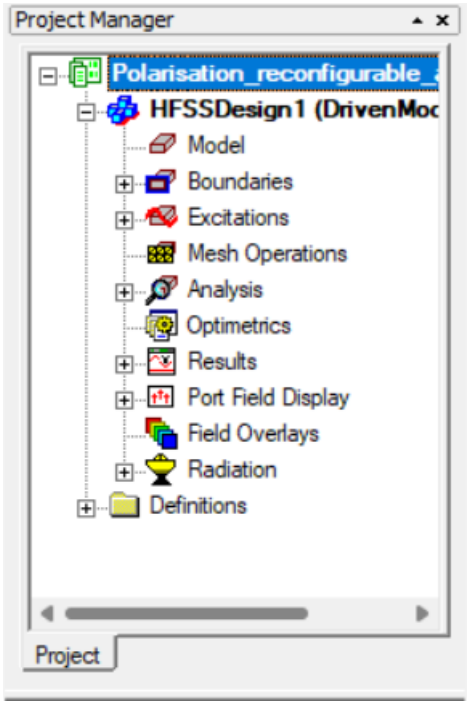

Figure 3.2 Project Manager window

3.4.2 Message Manager

It shows any errors or warnings that occur before you begin a simulation.

3.4.3 Property Window:

It shows and allows you to change model parameters.

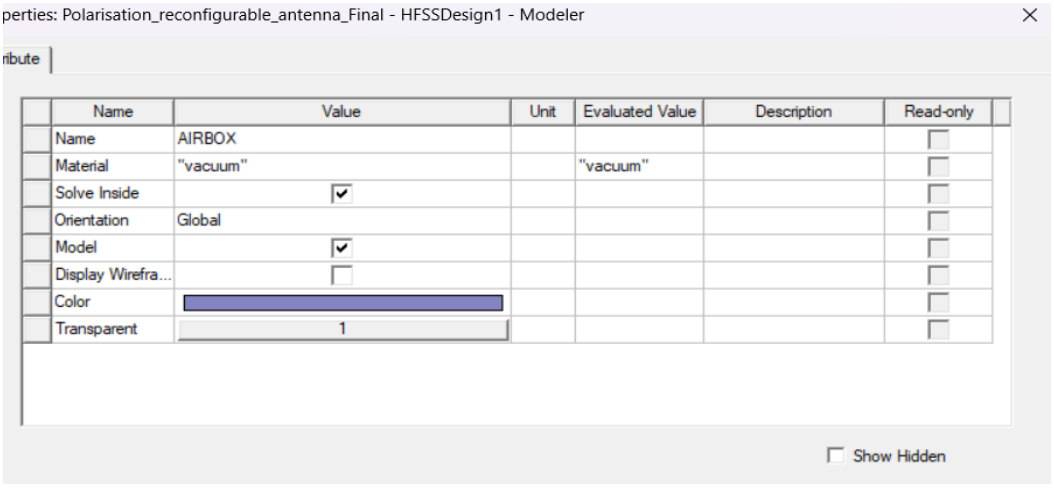

Figure 3.3 Property window

3.4.4 Progress Window

That displays solution progress.

3.4.5 3.4.5 3D Modeler Window

Which contains the model and model tree for the active design.

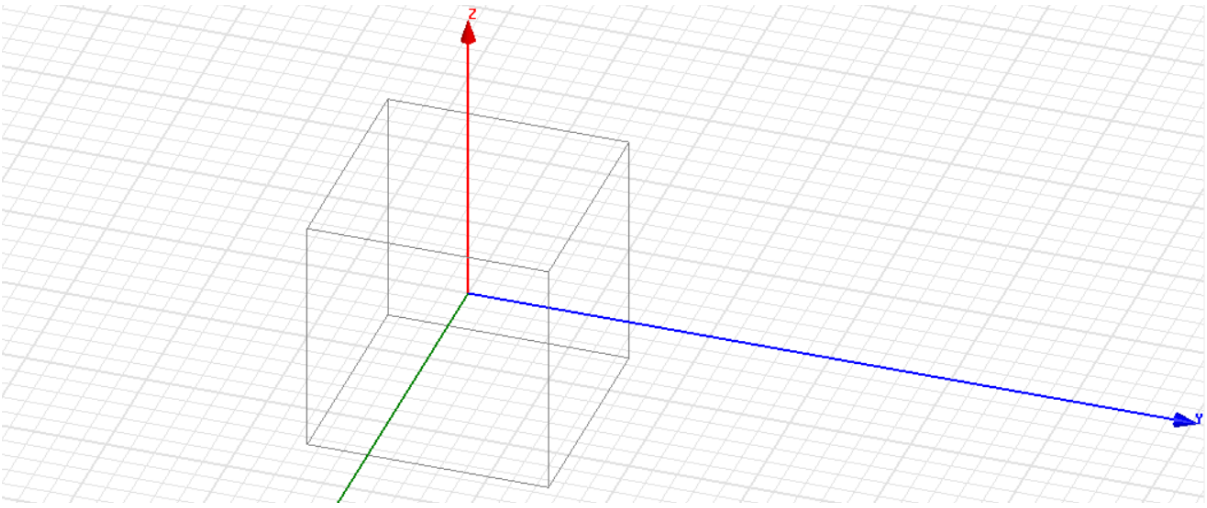

Figure 3.43D Window Modeler

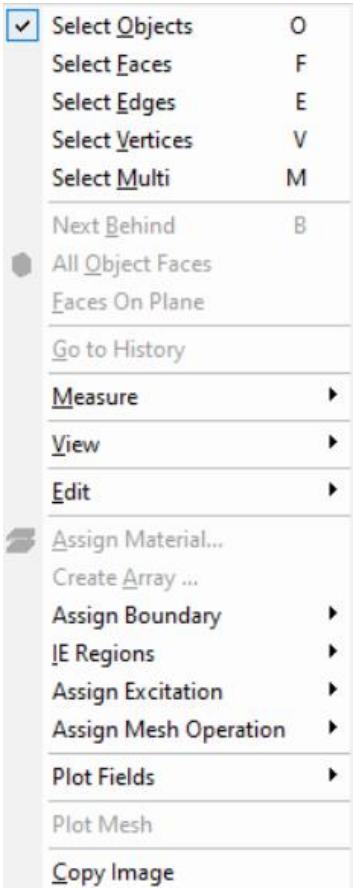

Figure 3.5 Modeller right click options

3.5 Simulation workflow

There are six main steps to creating and solving a proper HFSS simulation. They are:

3.5.1 Create Model/Geometry

The user's physical model for study must be created before an HFSS model may be constructed. A 3D modeler may be used when doing this modeling within HFSS. Because the 3D modeler is entirely parametric, users may design constructions with changing architectural dimensions and characteristics of materials. Therefore, parametric structures come in especially helpful when final dimensions are unknown or when the design needs to be "tuned." As an alternative, 3D structures may be imported from mechanical drawing programs like Solid Works, Pro E, and AutoCAD.

Translated structures, however, do not keep the details of their original. The import mechanism cannot parameterize it, disunity. The user has to edit the imported geometry to allow parameterization if structural parameterization requires modification.

3.5.2 Assign Boundaries

The differential variation on Maxwell's equations is where the wave equation that HFSS solutions come from. The field vector is expected to be single-valued, bounded, and to have a continuous distribution along with its derivatives in order for these equations to be valid. The field is discontinuous along the frontier or source, thus the derivative is pointless. Conditions thereby decide how the field responds across discontinuous boundaries.

Whenever employed effectively boundary conditions can be used infrequently to simplify the model. In reality, HFSS applies boundary conditions automatically to minimize model complexity. For passive RF devices, HFSS can be compared to a virtual prototyping atmosphere. The virtual prototyping environment should be finite, contrasted to the actual world, which has been limited by limitless space. To achieve this finite space, HFSS applies external constraints that apply to the area surrounding the background or geometric model.

Utilising them wherever possible is a competitive advantage since model complexity is normally closely tied to resolution time and processing resources. Boundary events might be of two separate sorts. The first two are largely set by the user, or it is up to them to make sure they are defined effectively. For the user, the material boundary conditions are transparent.

Perfect E - Also known as a perfect conductor, Perfect E is a perfect electrical conductor. The electric field (E-Field) is forced perpendicular to the surface by this kind of obstacles. Also, two automatic Perfect E allocations are made: Any object surface that makes a contact with the backdrop is straight away categorized as a Perfect E boundary and given the label outer for the boundary condition. Any item that is given

the material pec (Perfect Electric Conductor) has the boundary conditions Perfect E and metal automatically applied to its surface.

Perfect H – A perfect magnetic conductor is Perfect H. For the tangential Perfect H and E fields. Natural - This restores the specified region to its original material and removes the Perfect E boundary constraint for a Perfect H boundary that overlaps with a Natural perfect E boundary. It has no real impact on any assignments. For instance, it can be used to simulate a cut-out in a ground plane for a coax feed.

Finite Conductivity – You may define the surface of an object as a lossy (imperfect) conductor using a Finite Conductivity boundary. It is comparable to an idea of a lossy metal drugs and is a deficient E boundary condition. You need leakage and loss parameters in order to model a lossy surface. Loss is computed as a frequency function. It is only for reliable conductors.

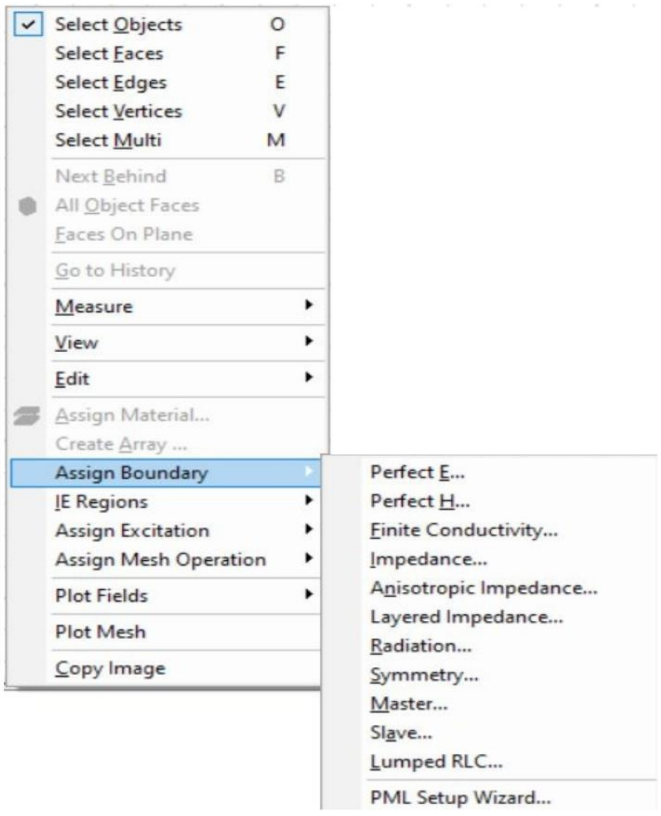

Figure 3.6 Assigning ofBoundary options

3.5.3 Assigning of Excitation

We need the excitation after setting the boundaries. (or ports). Excitation, like limits, has a direct impact on the caliber of the results that HFSS offers for a certain model. We urge you to carefully read the Awakening portion of this text as a result. For the most accurate HFSS findings, proper excitation generation and application are essential, however, there are certain general guidelines that users may adhere to.

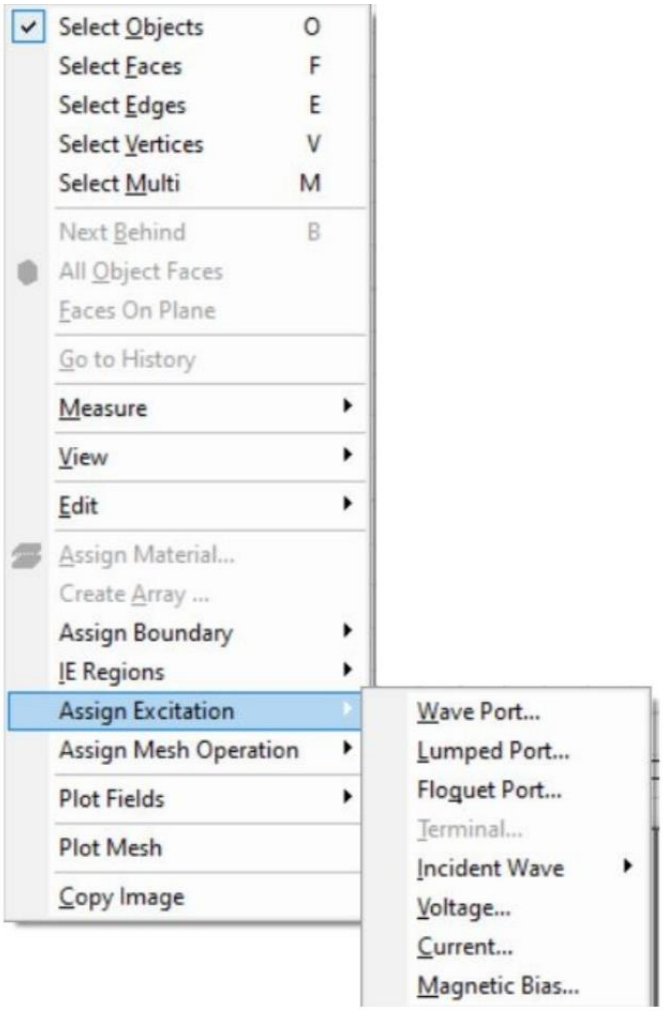

Figure 3.7 Assigning of Excitation options

3.5.4 Solution Type

When using HFSS, a user must initially specify what type of solution HFSS needs to calculate. There are three types of solutions available:

Driven Modal - Calculates the S-parameters. The incident and reflected powers of waveguide modes will be used to represent the S-matrix solutions.

Driven Terminal - Calculates the terminal-based S-parameters of multiconductor transmission line ports. The S-matrix solutions will be expressed in terms of terminal voltages and currents.

Eigen mode – Find a structure's Eigenmodes, additionally referred to as resonances. The structure's resonant frequencies and the fields at those frequencies are found via the Eigenmode solver.

The simulation applying the driven modal solution type produces an S-matrix solution, which distinguishes it from the driven port simulation. The incident and reflected powers of the waveguide mode are used here to represent the driven port. Results from eigenmode solvers can be expressed in terms of a separation's eigenmodes or resonances. This technique offers the fields and resonance frequencies specific resonances.

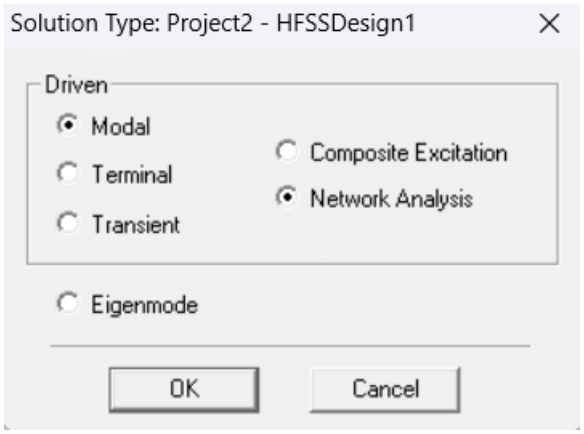

Figure 3.8 Type of the solution

3.5.5 Solve

3.5.5.1

The model may be looked over when the HFSS user has finished the first four phases. The model shape, frequency of solutions, and available computer horsepower all have a major effect on the amount of time needed for analysis. A repair can be performed in as little as a few seconds or as long as it would take to run a cup of coffee for an entire morning. Sending to may frequently be useful. This frees up the PC of the user's girlfriend for other tasks.

3.5.5.2 *Add sweep*

You may also add a Frequency Sweep once a Solution Setup has been created. Right-click Setup in the HFSS Model Tree for doing this. will see the Edit Sweep window open.

Frequency Setup

- After the sweep type has been chosen, the frequencies of interest must be specified.
- There are three Frequency Setup Options:
  - Linear Step --specify a linear range of values with a constant step size.
  - Linear Count -- specify a linear range of values and the number, or count, of points within the variable range.
  - Single Points -- specify a single value for the sweep definition and next step is to validate.
- After setting up the frequency and sweep setup click on the validate option and in this section, it will check for boundary conditions, wave ports and excitations. If any error, it will be shown in a dialog box.
- Analysis Click on analyse all after validation process is completed.

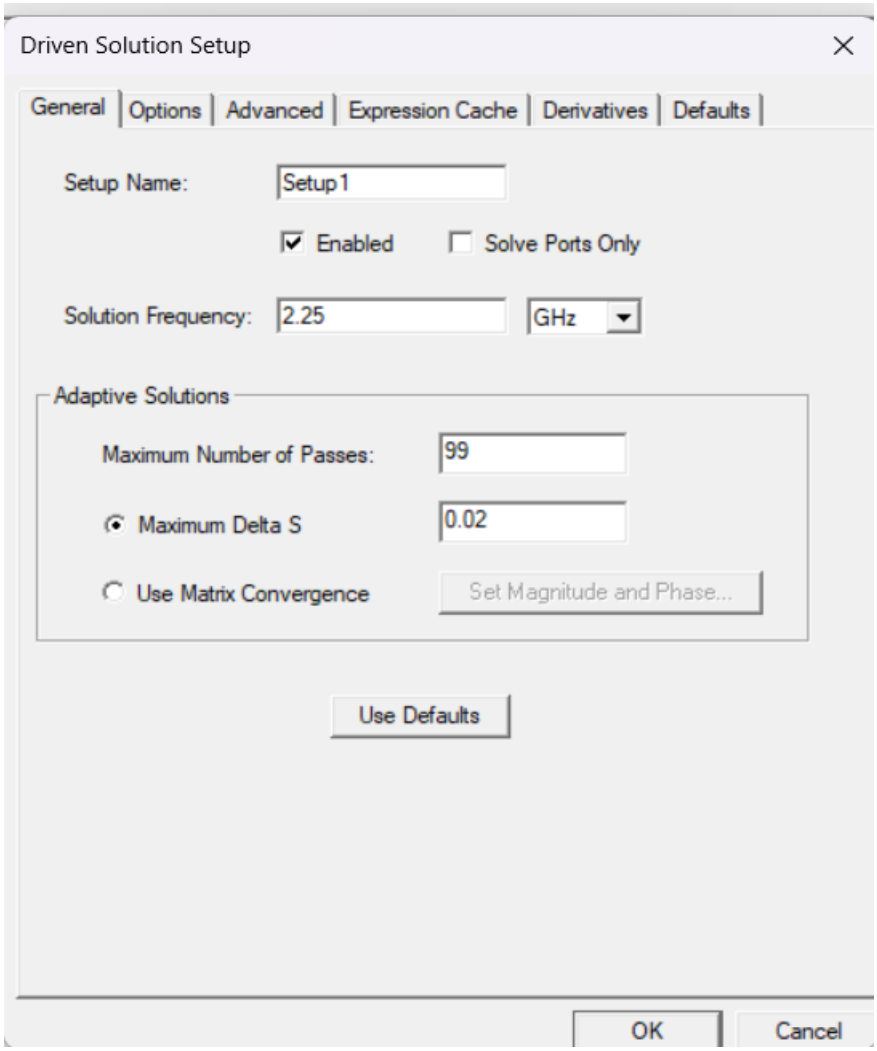

Figure 3.9 Solution Setup

3.6 Plotting Results

3.6.1 Plotting Return loss graph

Step 1: Right-click on the findings following design validation.

Step 2: Select Rectangular Plot after choosing Create Modal Solution Data Report.

Step 3: Next, choose the S11 parameter under the category listed in the dialogue box, and then choose the dB function.

Step 4: Next, select "New Report" and look at the graph.

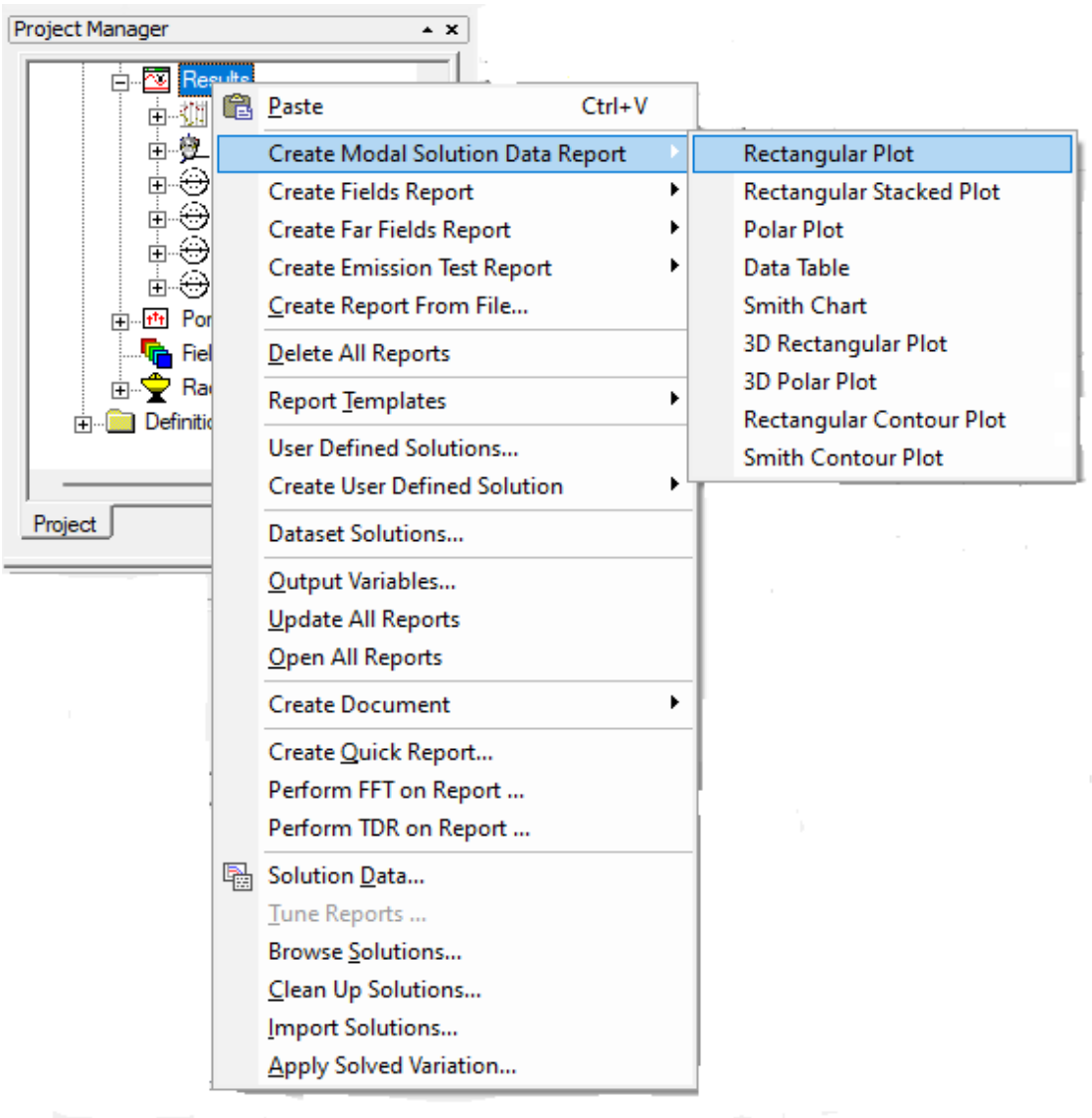

Figure 3.10 Results right click options

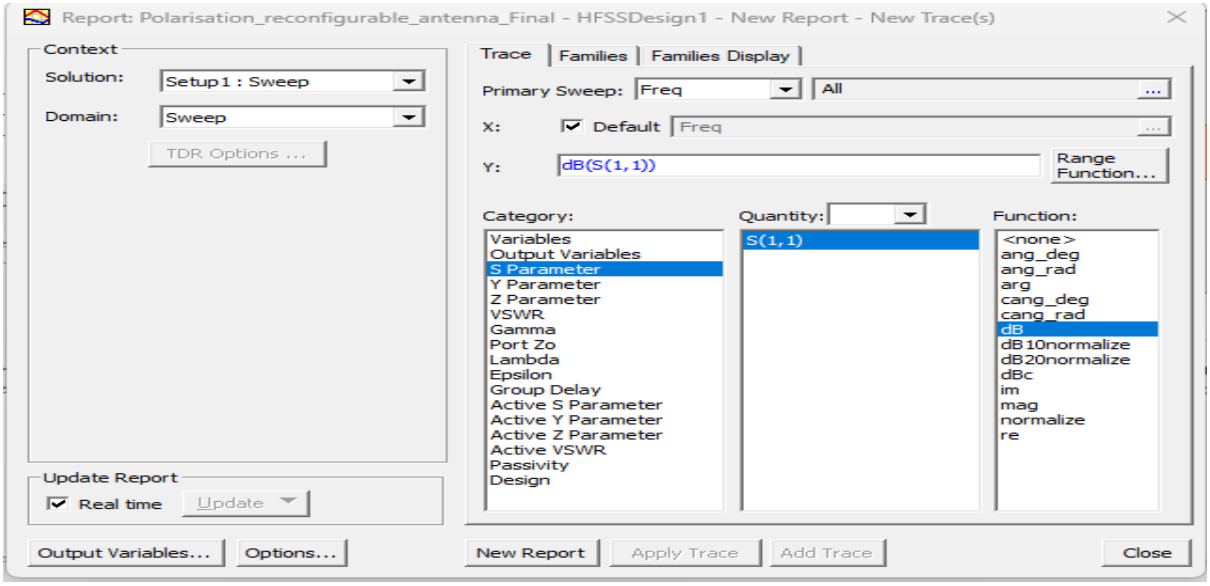

Figure 3.11 Plotting S_{11} Report

3.6.2 Plotting VSWR Graph

Step1: After validation of design right click on results.

Step2: Select Create Modal Solution Data Report and then select Rectangular Plot.

Step3: Now select VSWR in the category shown in the dialogue box and then function as dB.

Step4: Now click on New Report and observe the graph.

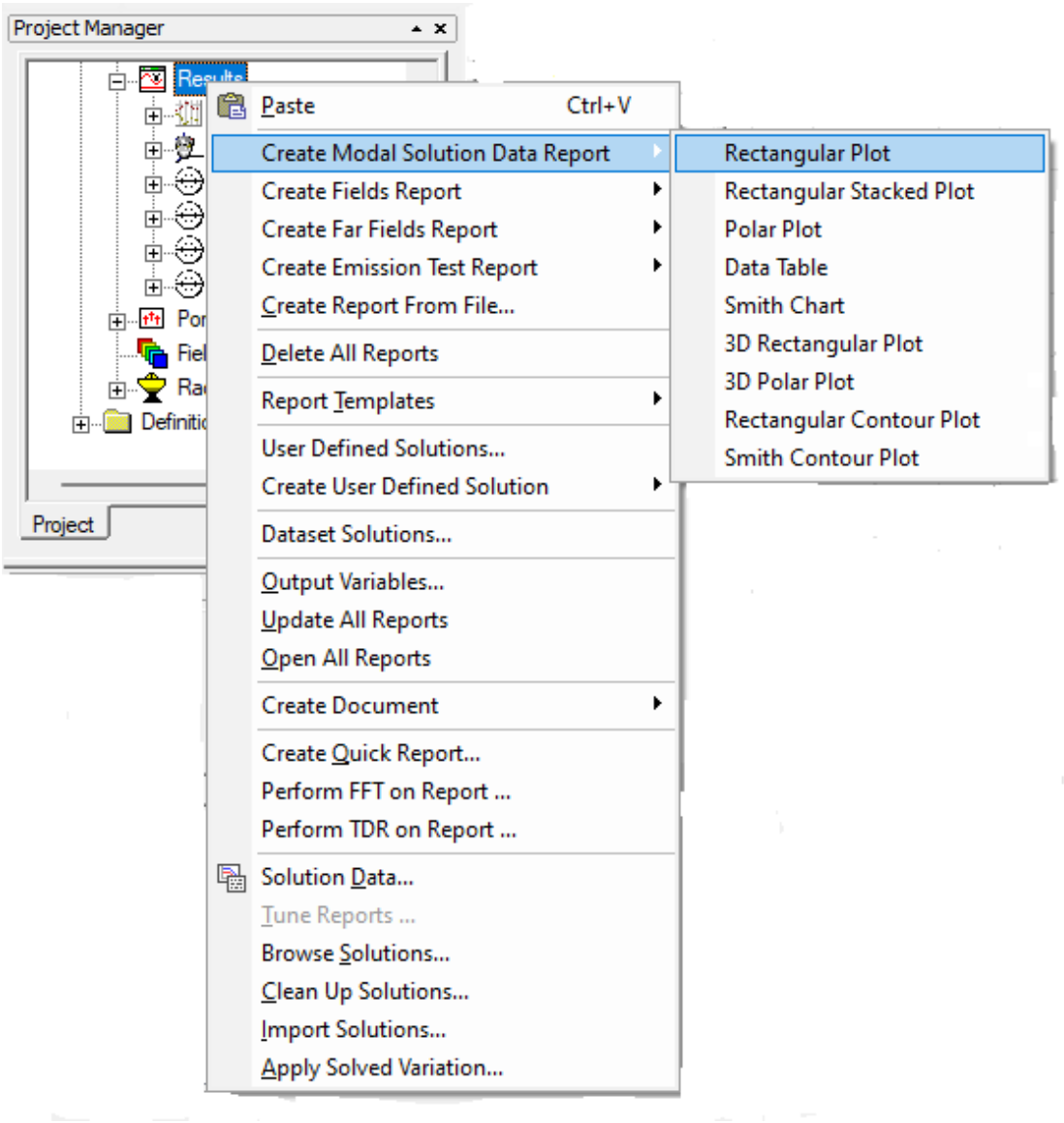

Figure 3.12 Results right click options

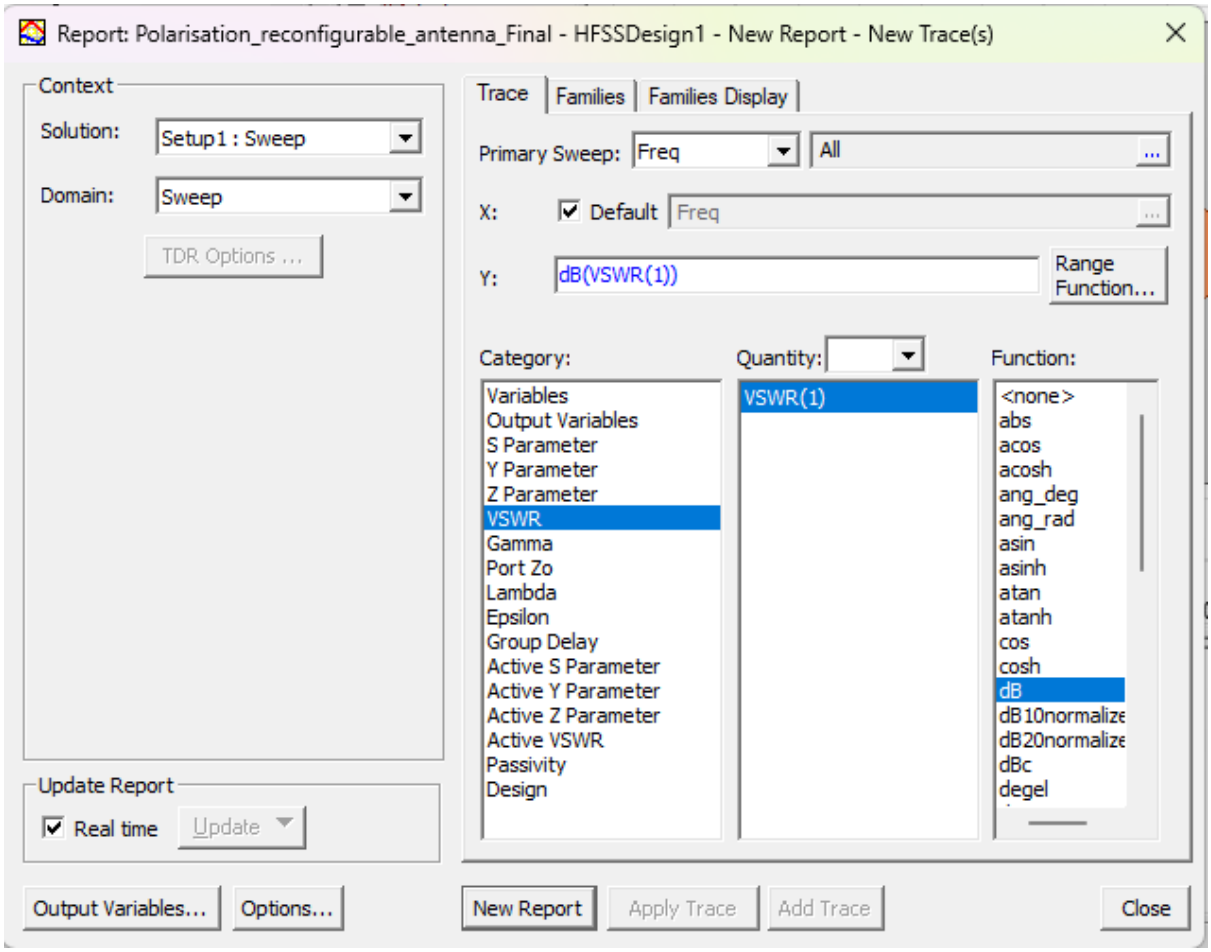

Figure 3.13 Plotting VSWR Report

3.6.3 Plotting Gain Plot

Step 1: Right-click on the outcomes of design validation.

Step 2: Select 3D Polar Plot, then Create Far Field Report.

Step 3: After that, choose Gain from the category listed in the dialogue box, and after this, set the function to dB.

Step 4: Next, click New Report and look at the graph.

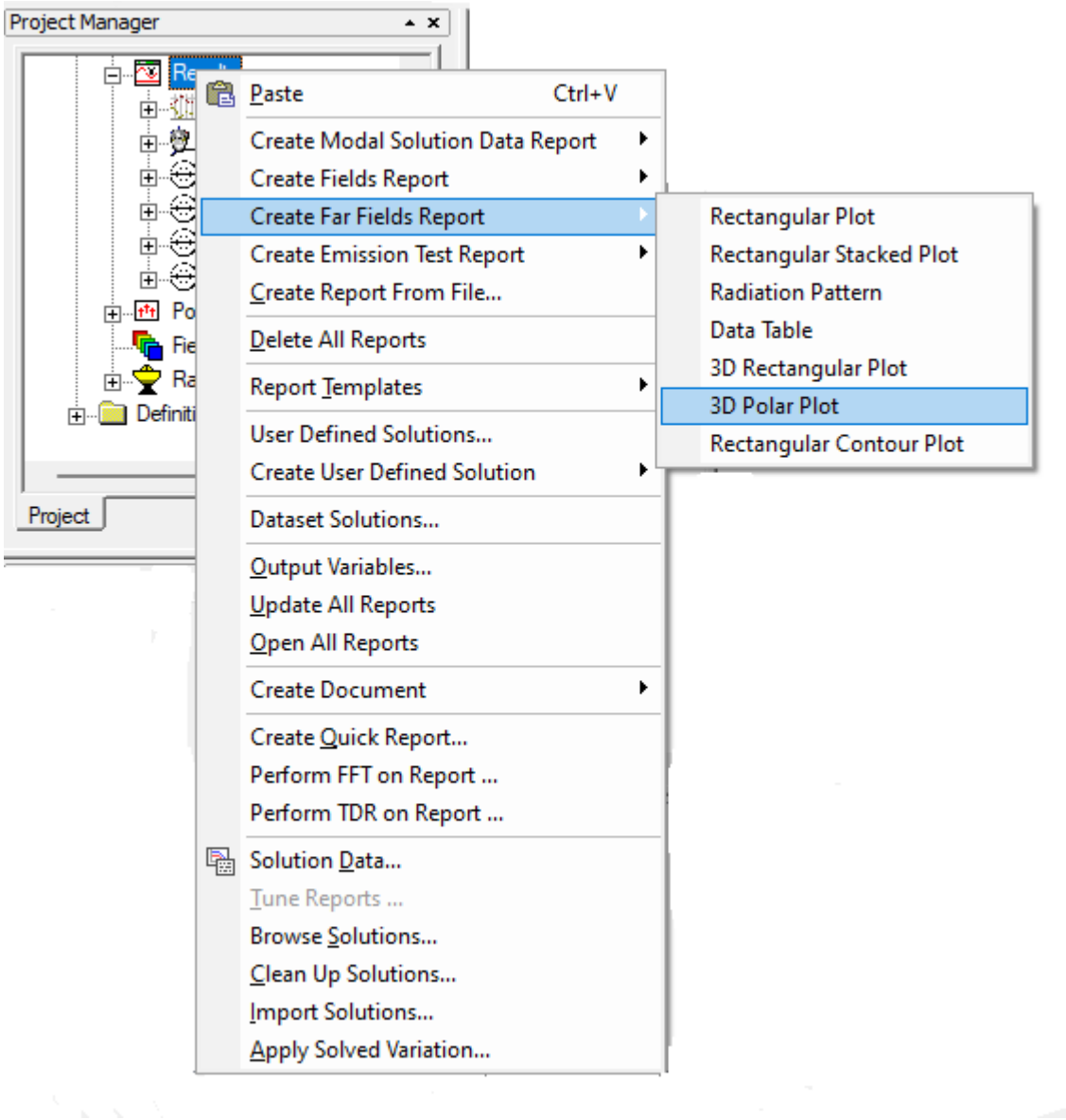

Figure 3.14 Results right click options

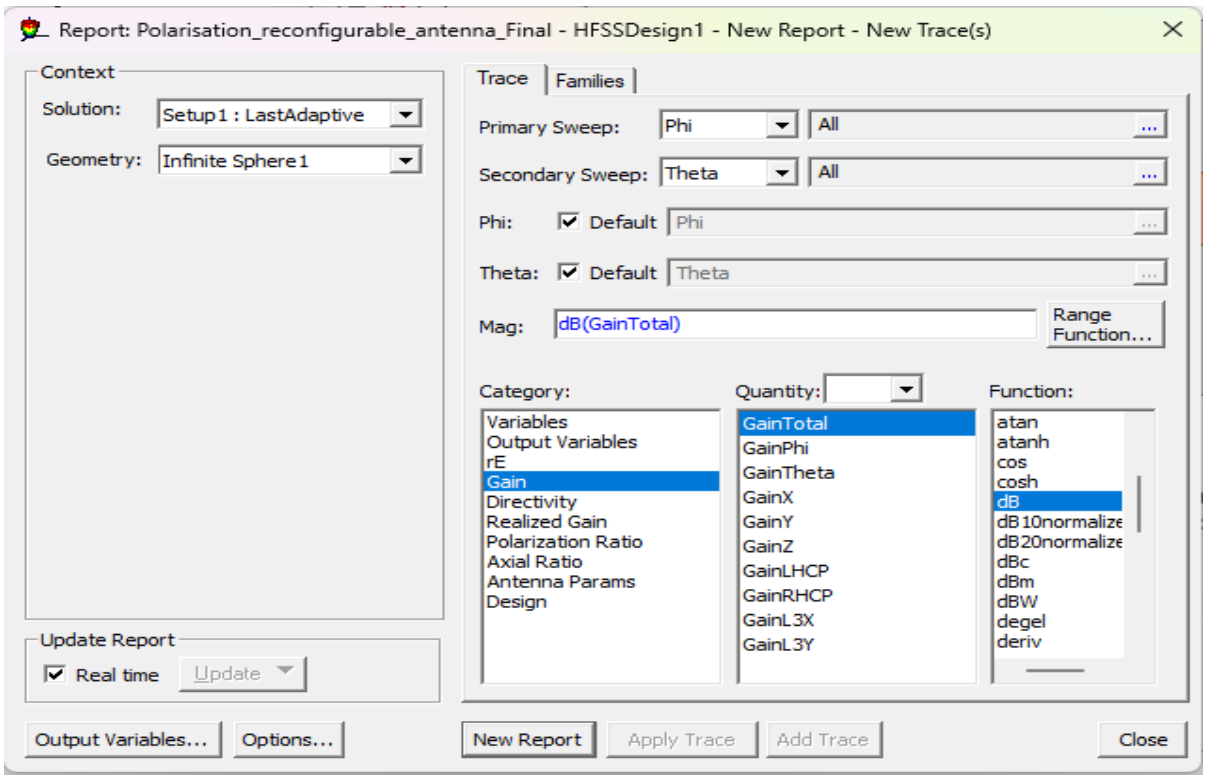

Figure 3.15 Plotting Gain Plot

3.6.4 Plotting Radiation Pattern

Step1: After validation of design right click on results.

Step2: Select Create Far Field Report and then select Radiation Pattern. Step3: Now select Realized Gain in the category shown in the dialogue box and then function as dB.

Step4: Now click on New Report and observe the graph.

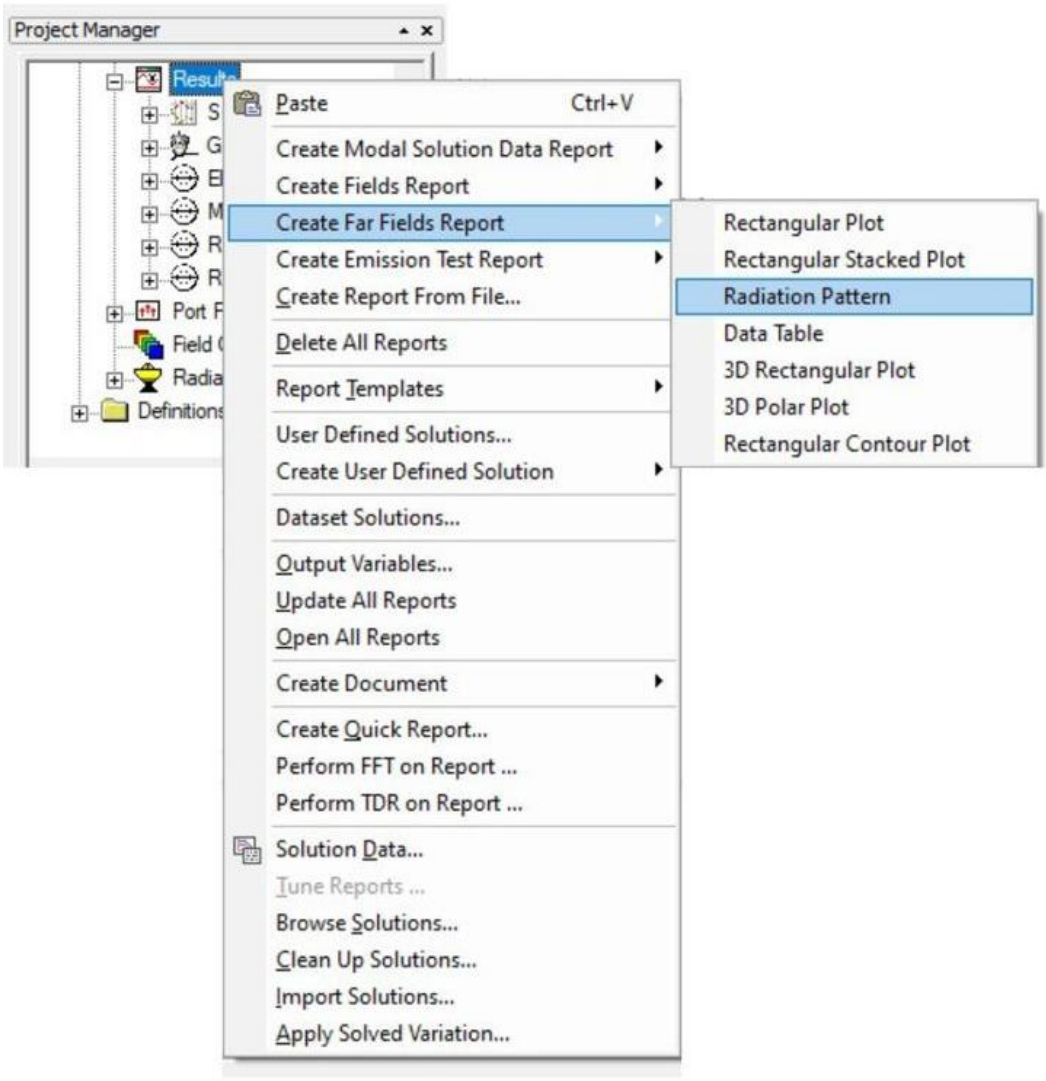

Figure 3.16 Results right click options

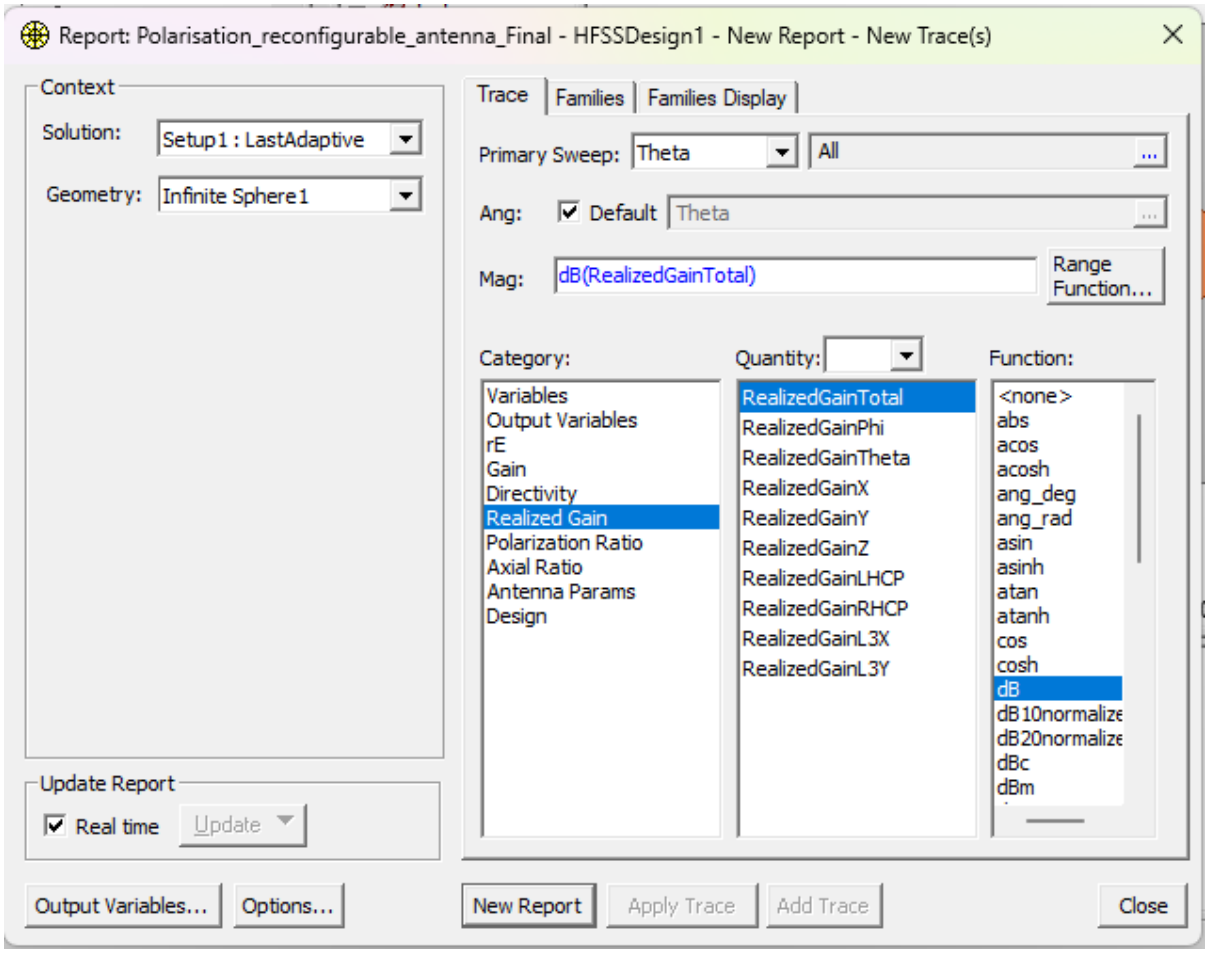

Figure 3.17 Plotting Radiation Pattern

3.6.5 Plotting Axial Ratio Graph

Step 1: Right-click on the findings following design validation.

Step 2: Choose Rectangular Plot after choosing Generate Far Field Report.

Step 3: Next, choose the Axial Ratio option under the category list in the dialogue box, and then choose the dB function.

Step 4: Next, choose the primary sweep as Freq and sweep as the solution type.

Step 5: On the Family box, choose Theta and Phi as .

Step 6: Next, select Create Report and look at the graph.

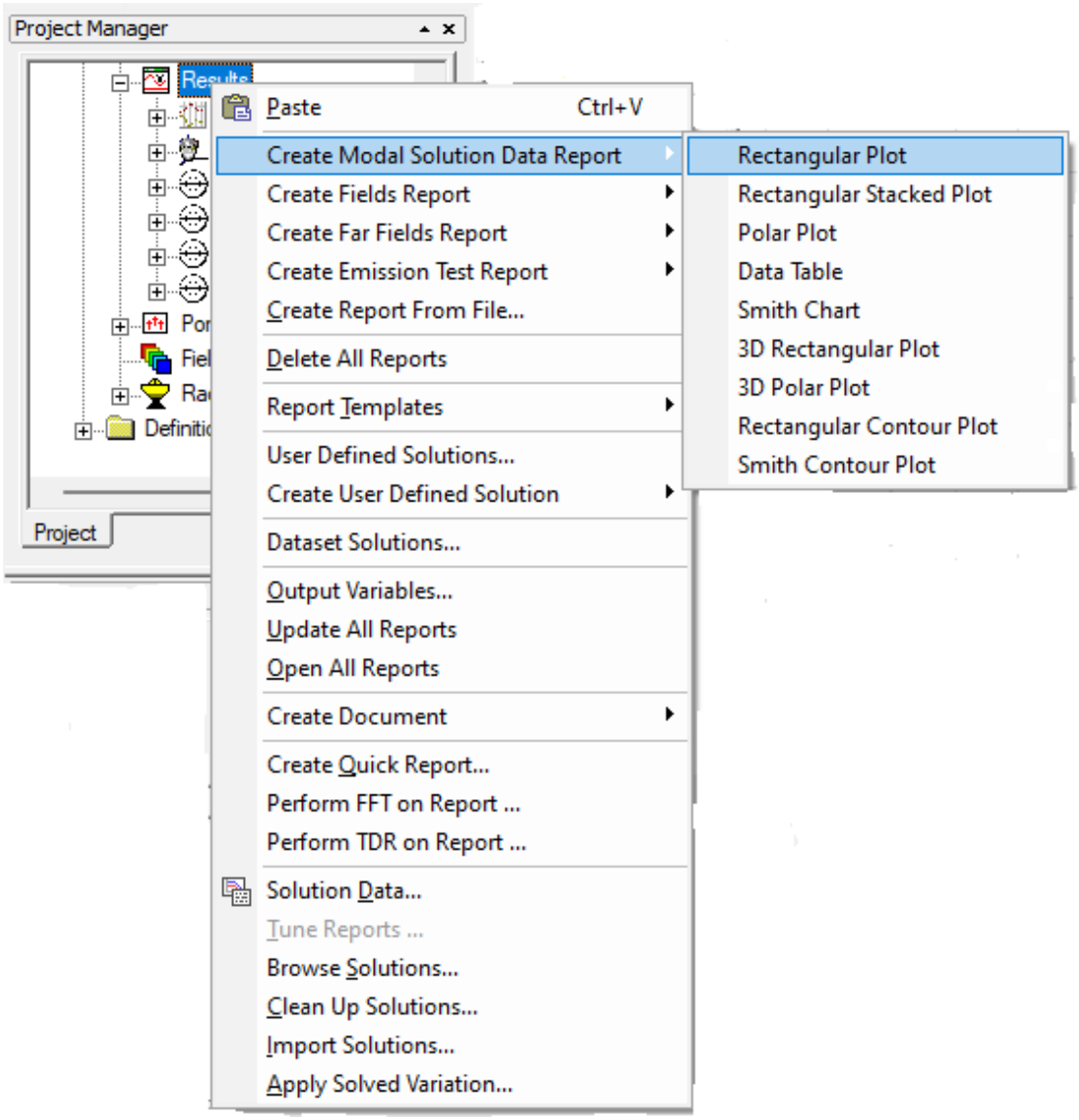

Figure 3.18 Results right click options

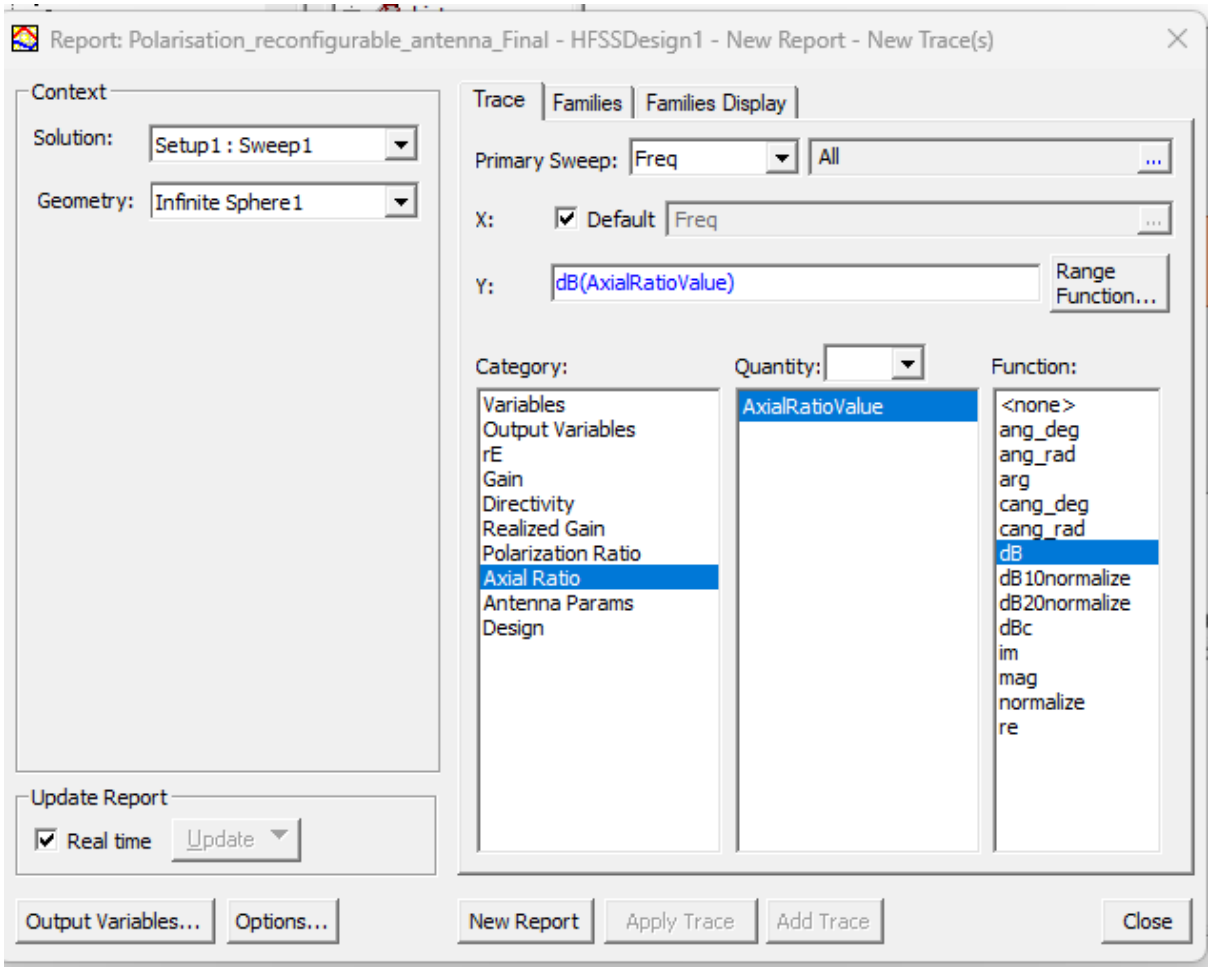

Figure 3.19 Plotting Axial Ratio Report

3.6.6 Plotting Current Distribution

Step 1: When the design has been validated, right-click on the patch and choose Field overlays.

Step 2: Click J after choosing Plot Fields.

Step 3: Next, choose Vector Jsurf and Mag Jsurf to see the magnitude and vector of the current distribution across the chosen region in the design, respectively.

Step 4: To see the outcome, click Done.

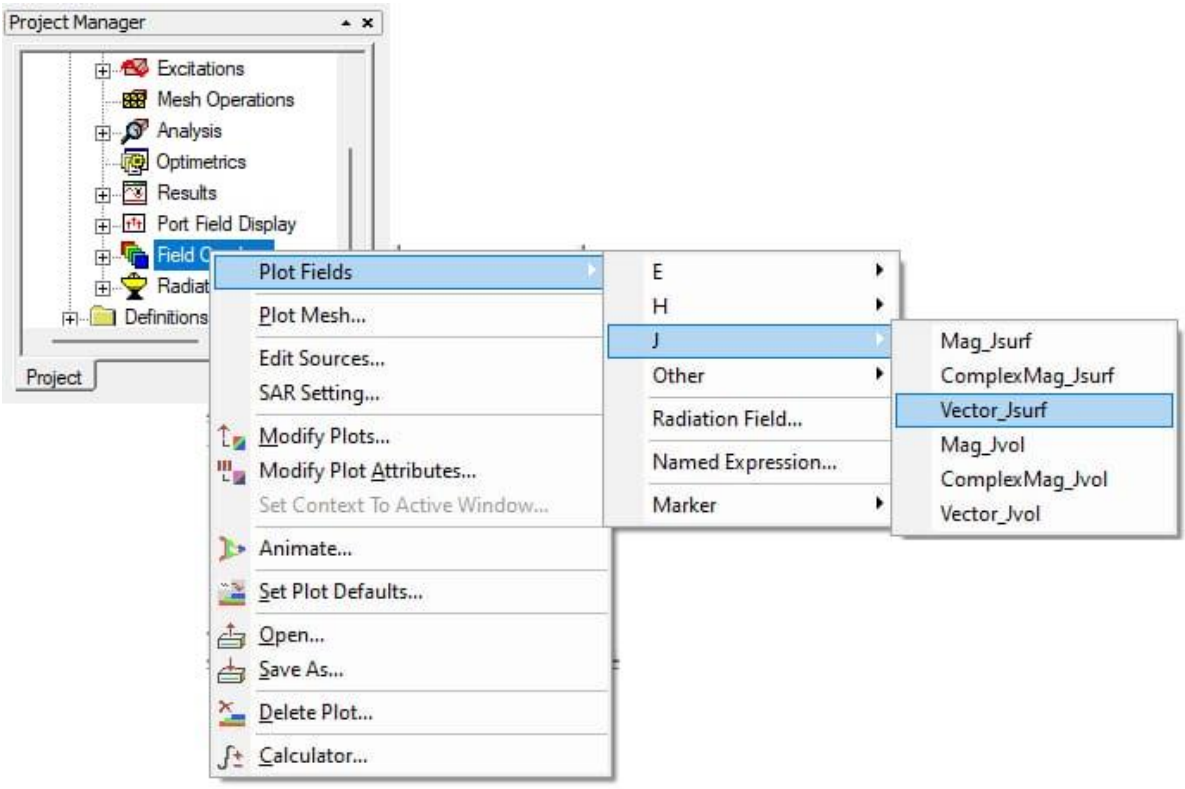

Figure 3.20 Field Overlays Right Click Options

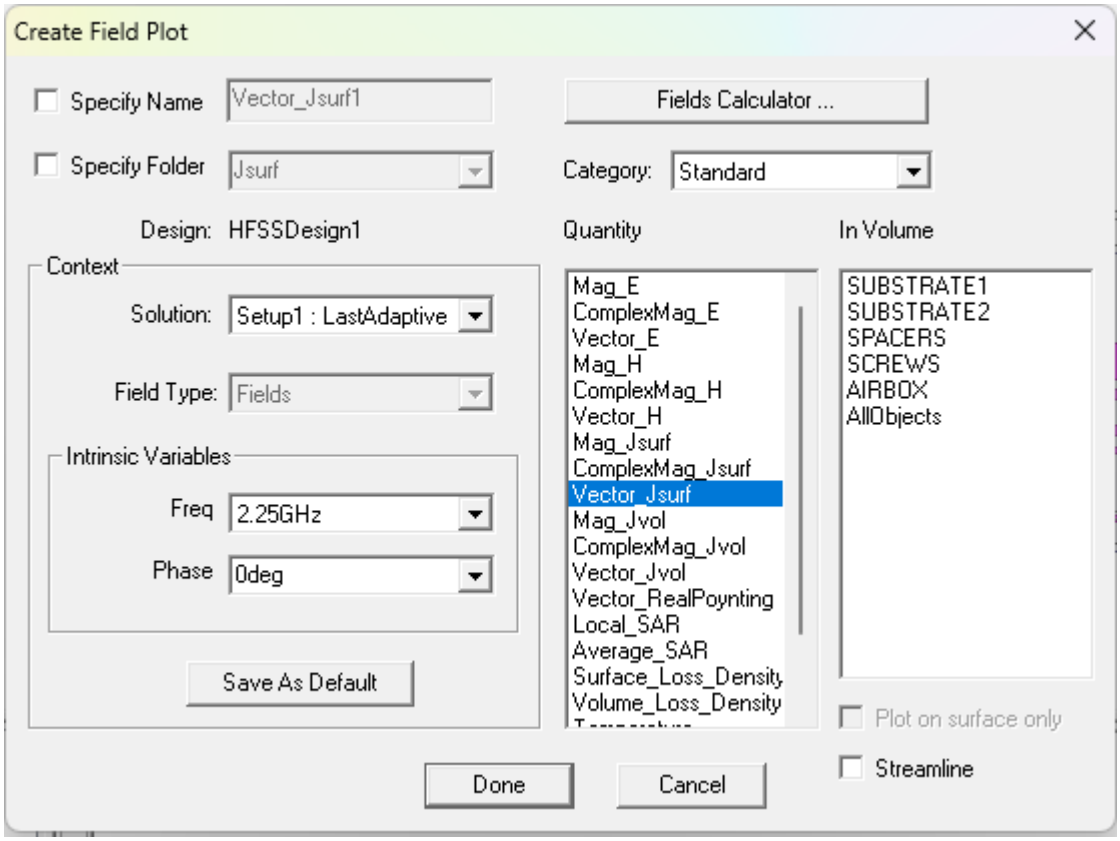

Figure 3.21 Plotting Current Distribution report

3.6.7 Plotting E-Field Distribution

Step 1: When the design has been validated, right-click on the patch and choose Field overlays.

Step 2: Click E after choosing Plot Fields.

Step 3: Next, choose Vector E to observe the electric field's vector and Mag E to observe its magnitude as it is dispersed throughout the chosen region in the design.

Step 4: To see the outcome, click Done.

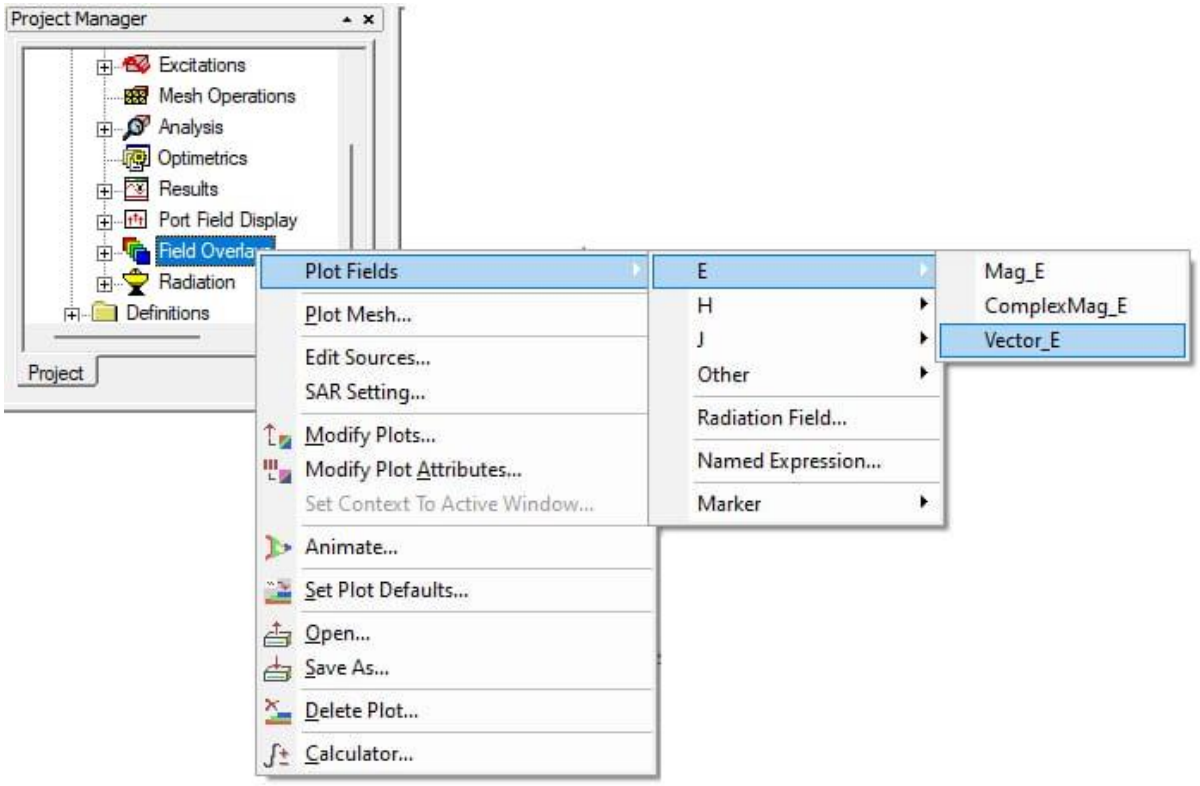

Figure 3.22 Field Overlays right click options

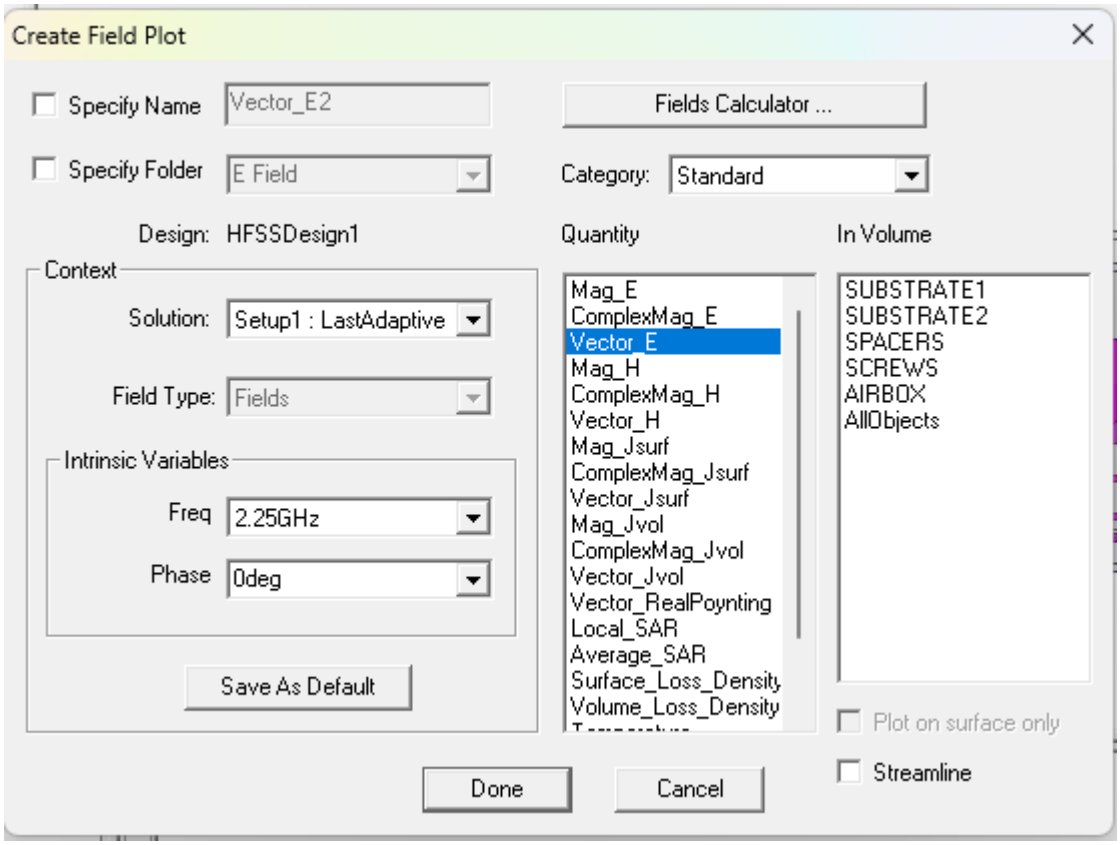

Figure 3.23 Plotting Vector E-Field Report

3.6.8 How to save .csv file for result

Step 1: Plot the results following design validation.

Step 2: Choose Export by doing a right-click anywhere on the outcome.

Step 3: Go to the location where you want to save the file.

Step 4: Choose the file format "Comma delimited data files" (.csv).

Step 5: To save the file, click "OK."….

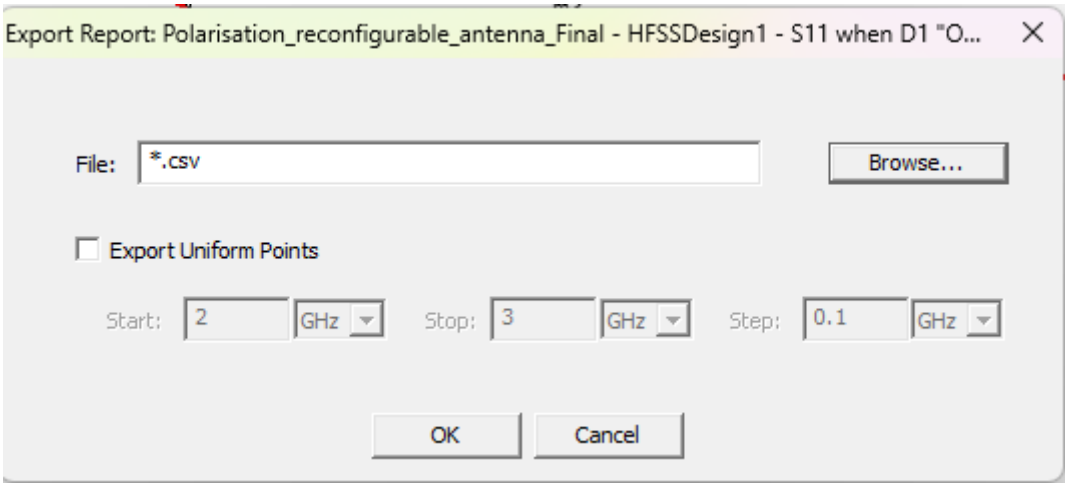

Figure 3.24 Exporting Report

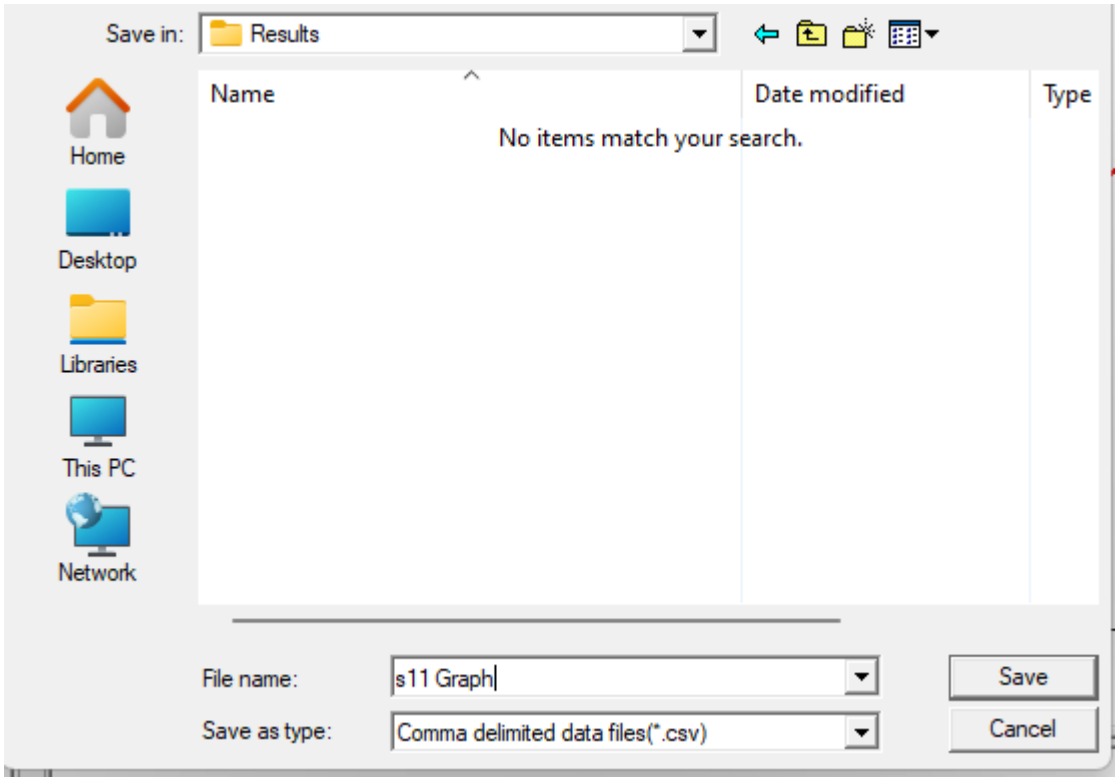

Figure 3.25 Saving csv file

CHAPTER 4:
Reconfigurable Antenna Design

4.1 Introduction

Wireless communication systems require compact, confirmable multi-frequency devices. In terms of reduced size and complexity to achieve various frequency bands, reconfigurable antennas are advantageous since a single antenna can be used over several frequency bands, varied radiation patterns, and multiple polarisations. S and C band frequencies are frequently employed in wireless communication systems for business and security needs. Frequency reconfigurable antennas, radiation pattern reconfigurable antennas, and polarisation reconfigurable antennas are the three most well-known reconfigurable antennas. So many switching mechanisms, including semiconductor diodes operating at microwave frequencies, MEMS, optical switches, microcontroller-based switches, liquid dielectric switches, and FPGA control switches, may be employed to create these types of antennas.

4.2 Hybrid Coupler

In amplifiers, switching circuits, and beamforming antenna networks used in a variety of manufacturing and military applications that require for power or frequency monitoring, balancing, monitoring, or control, hybrid couplers split and combine signals.

Because a signal applied to each input generates two equal amplitude signals in all quadrants, a 3 dB 90-degree hybrid is repeatedly alluded to as a quadrature hybrid (90 degrees apart). The output signals are 90 degrees out of phase from one another and have quite a 3 dB (3 dB) retardation. Only 50% of the input power is evident at one of the outputs when there is a 3 dB attenuation. An even further 50% is dispersed to external dc branches. Also, it is of no consequence whether port is the input because these devices are mechanically and electrically balanced, so the ratio at the output is consistent.

4.2.1 Types of Hybrid Coupler

90-Degree or Quadrature Hybrids:

Due to the fact that a signal given to any input could yield two equal amplitude signals that are both quadrant signals, the 3 dB, 90-degree hybrids are regularly alluded to as quadrature hybrids (90 degrees separated from one another). The output signals are 90 degrees out of phase with one another and have a three decibel (3 dB) retardation.

Due to the other 50% of the input power cascading down to the other output leg, the 3 dB attenuation means that only 50% of the input power can be detected at one of the outputs. The relationship at the outputs remains the same irrespective of which port is the input because these devices are symmetrical both mechanically and electrically. Mismatches send reflections to the isolation port, which prohibits any power from reflecting to the input port. They can be used to combine power signals with a high degree of isolation between the ports in addition to splitting signals. This configuration ensures a high degree of isolation between the two output ports and the two input ports, avoiding potential interaction. 90-degree hybrids are typically used in circuits that necessitate a balanced division of power into two transmission lines with a 90? phase separation. Signal splitters, combiners, balanced mixers, image-rejection mixers, phase shifters, diplexers, switches, and antenna feed networks are applications that have been demonstrated. The rapidly increasing use of broadband microwave systems, as well as the emerging mm Wave and 5G wireless communications systems, has required the creation of broadband 90-degree hybrids with tight output amplitude and phase tracking.

180-degree Hybrids:

The 180-degree hybrids (also known as "rat race" couplers) are four-part devices that are used to either equally divide or add two fused signals. A whole other upside of this hybrid coupler is that it can alternately start providing 1800 phase-shifted output signals. Broadband hybrids have typically been developed in 900 configurations, with less bandwidth available for the greater phase relationship of 1800 hybrids. Systems such as antenna beamforming networks can be designed more efficiently with 1800

hybrids so even though reaction between two divided signals necessitates simpler structure. Four-port components with dual input and output ports are known as hybrids. When a signal is applied to the sum input port, it actually creates two output signals with matched amplitude and phase. Thus every output level in a 3-db hybrid is 3-db lower (less the insertion loss through the hybrid) than the input level. Signals applied to the difference input port yield two equal-amplitude output signals that are out of phase by 180 degrees with one another. As a result of this estate, hybrid circuits are ideal for reducing noise in amplifiers through feedback combining techniques or merging multiple signals from arrays. Four-port components with dual input and output ports are renowned as hybrids. When a signal is applied to the sum input port, it continues to generate two output signals with matched amplitude and phase. Each output level in a 3-db hybrid is 3-db lower (less the insertion loss through the hybrid) than the input level. applied signals to the difference The input port emits two equal-amplitude output signals that are 180 degrees from being in phase with respect to one another. Due to this real estate, hybrid circuits are ideal for reducing noise in amplifiers through feedback combining techniques or merging multiple signals from arrays. 180? hybrids are built using a double-arrow construction technique that funnels two strip line, asymmetric, tapered-line directional couplers. At all frequencies, meandering transmission lines on each side of the hybrid maintain an even 180-degree phase relationship between channels. To generate the double-arrow hybrids, an asymmetric coupler with completely overlapped lines at its coupled end (where the lines cross) is compelled, going to result in an instantaneous transmission from high coupling to no coupling. A three-layer strip line configuration has been employed to build the hybrids. Coupled lines are engraved on opposite sides of a thin coupler circuit board situated between two dielectric boards of comparable thickness.

4.3 Parasitic Patch

At least one parasitic patch is found close to a core patch in a microstrip antenna. The parasitic patch is electrically isolated from the central patch, but it is inductively or otherwise associated to it to facilitate in heat transfer to/from the central patch. The

parasitic patch boosts the antenna's performance in terms of profile reduction, resonance frequency reduction, and bandwidth augmentation. These advancements have been researched and experimentally and computationally substantiated.

4.4 Dimensions of the Proposed Antenna

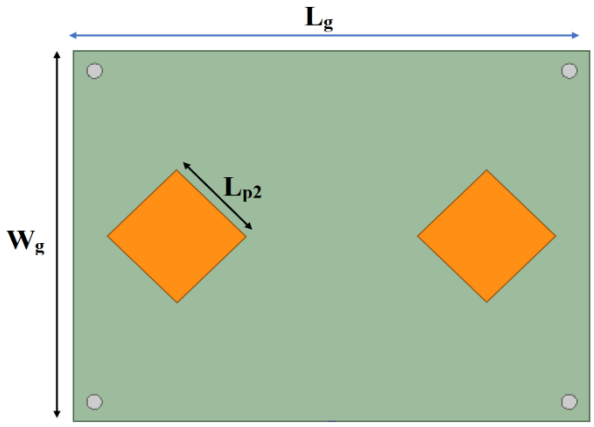

Figure 4.1 Top of the Substrate 2

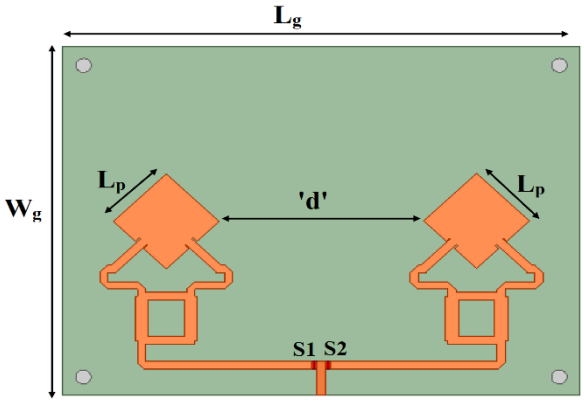

Figure 4.2 Top of the Substrate 1

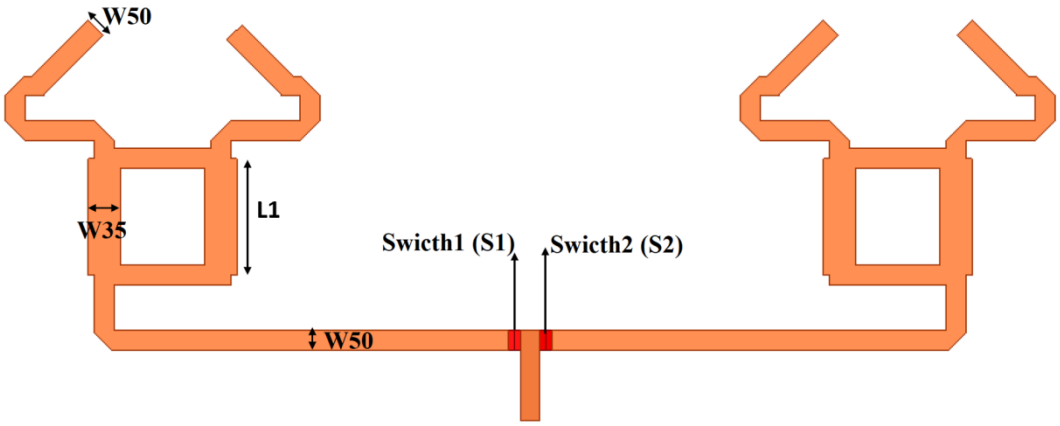

Figure 4.3 Feeding network

Table 4.1 Dimensions of the Proposed Antenna

Parameter	Values (mm)
L_g	200
W_g	150
L_p	29
L_{p2}	38
D_a	80
W_{50}	3.2
W_{35}	5.2
L1	19

4.5 Design of an Antenna

Simulation steps are as below:

Step 1: Start Ansoft HFSS.

Step 2: In an Ansoft HFSS window, select File Create from the menu.

Step 3: Choose Insert HFSS Design from the Project menu.

Step 4: Choose HFSS Solution Type Driven Terminal from the options. Choose 3D Modeller Units mm from the dropdown.

Step 5: Go to the menu and select rectangle. Windows will emerge and you will be capable of explaining all of the details of the ground, such as the kind, dimensions, and name of the sheet as ground. Assign a perfect E to the boundary.

Step 6: Choose cuboid from the menu. Windows will display and describe all of substrate1's attributes, as well as its kind and size. The box will be known as substrate1. Choose FR4 epoxy as the material.

Step 7: Go to the menu and select rectangle. Windows will popup and set all of the specifics of the driven patch, together with its kind, size, and name the sheet Driven Patch. Duplicate the driven patch around the X-axis with 1800 and rotate it with 450. Assign a perfect E to the edge.

Figure 4.4 Substrate of proposed antenna

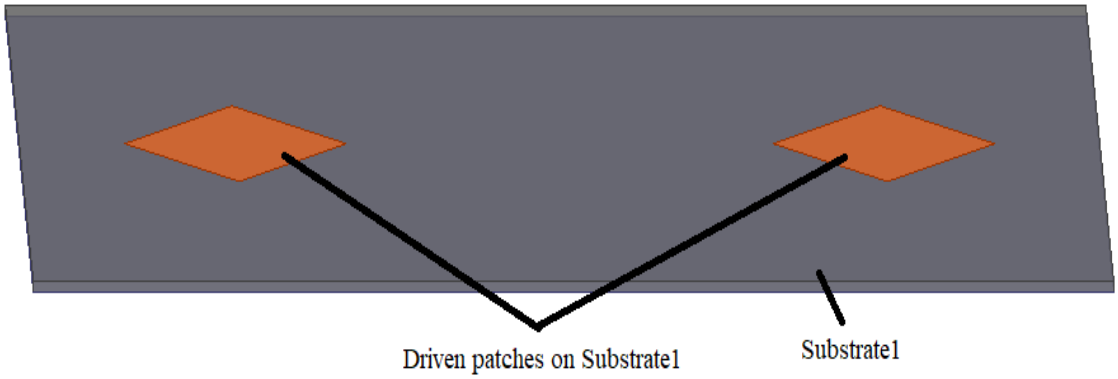

Figure 4.5 Driven Patch in Proposed Antenna

Step 8: Go to the menu and select rectangle. Windows will appear and you will be able to describe all of the requirements needed for the feeding network, the size of each transmission line in the hybrid coupler, and the same hybrid coupler duplicate around the X-axis with 1800. Couple the feeding network with the driven patch.

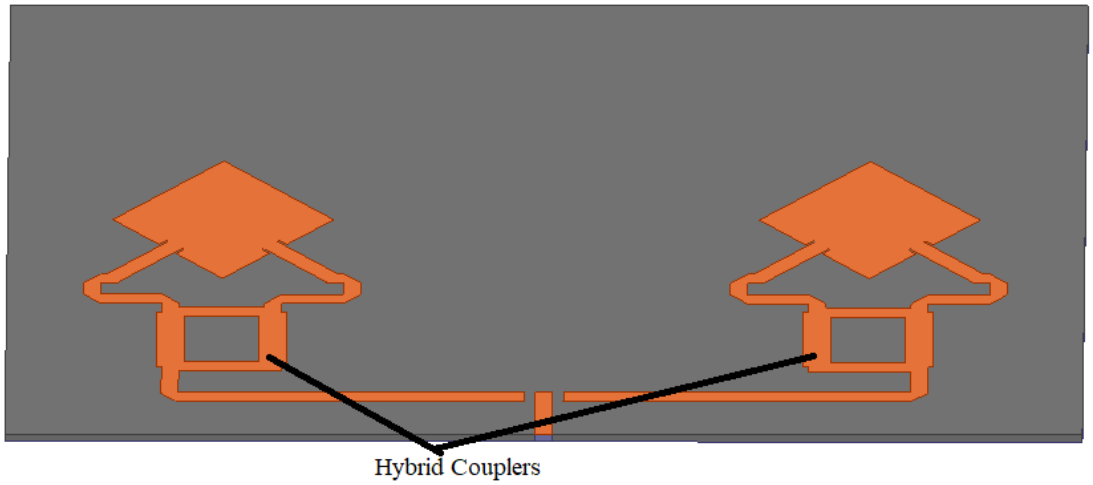

Figure 4.6 Driven Patch along with feeding network in Proposed Antenna

Step 9: Go to the menu and select rectangle. Windows will emerge and you will be allowed to enter all of the specifications of the PIN diode and duplicate along the X-axis to place diodes upon every side of the feeding network in the gaps depicted in the above illustration. Set the barrier to LUMPED RLC.

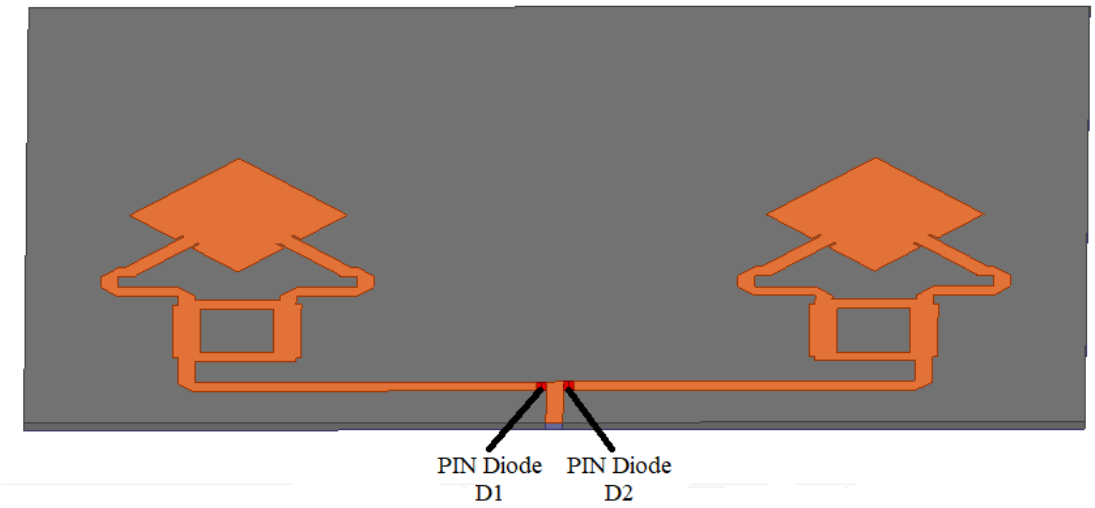

Figure 4.7 Assigning LUMPED RLC in Proposed Antenna

Step 10: Go to the menu and choose the cuboid. Windows will appear and set all specifications of substrate2 as well as its kind and dimensions. The box will also be titled substrate2. Choose FR4 epoxy as the material.

Step 11: Choose rectangle from the options. Windows will open and establish all parasitic patch specifications, as well as its type, measurements, and name. Assign an appropriate range. E.

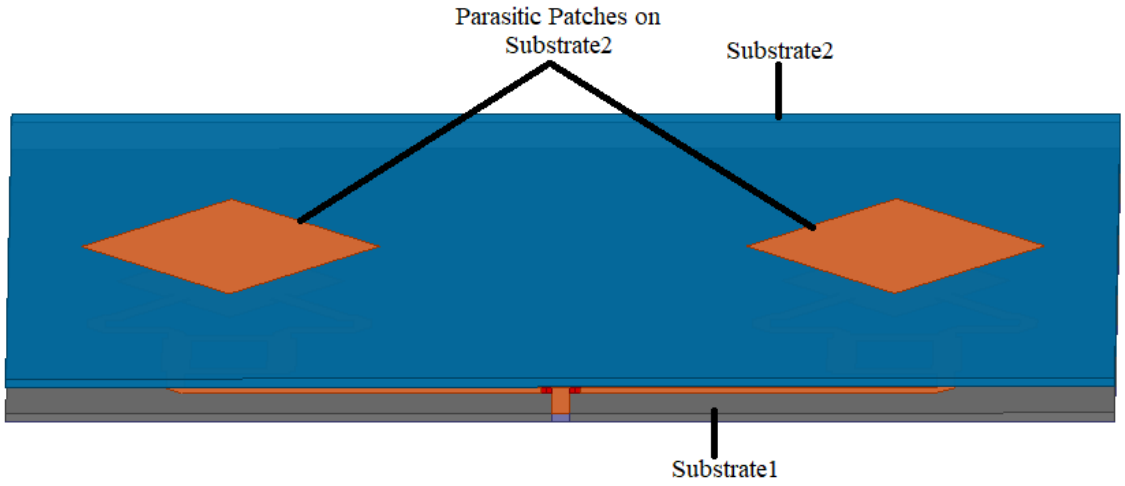

Figure 4.8 Parasitic Patch in Proposed Antenna

Step 12: Choose cylinder as from option. Beforehand to placing spacers at all four corners of the substrates, Windows will popup and provide all spacer characteristics, such as type, size, and duplicate around the X-axis.

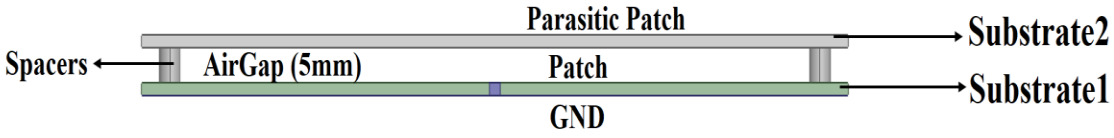

Figure 4.9 Spacers in Proposed Antenna

Step 13: Go to the list and choose the rectangle. Windows will show and define all of the specifications of the lumped port. Therefore provide current direction from the ground to the substrate1.

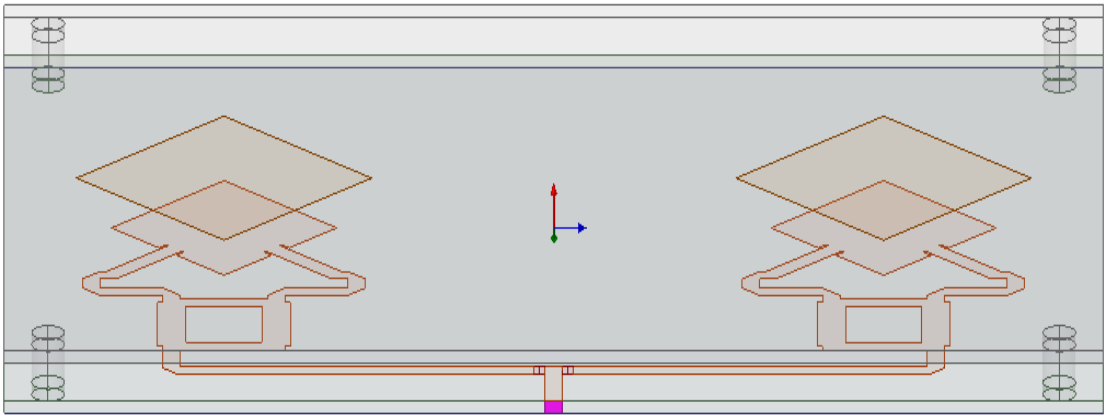

Figure 4.10 Feed in Proposed Antenna

Step 14: Go to the menu and choose box, subsequently specify parameters of 250mm length, 300mm width, and height, and designate the border as radiating box.

Step 15: Choose HFSS then analysis equipment as the solution setup to replicate the planned antenna. The operational rate is set via a window that pops up. To specify the

plot's start and finish wavelengths, go to HFSS, then analysis setup, and finally add frequency sweep.

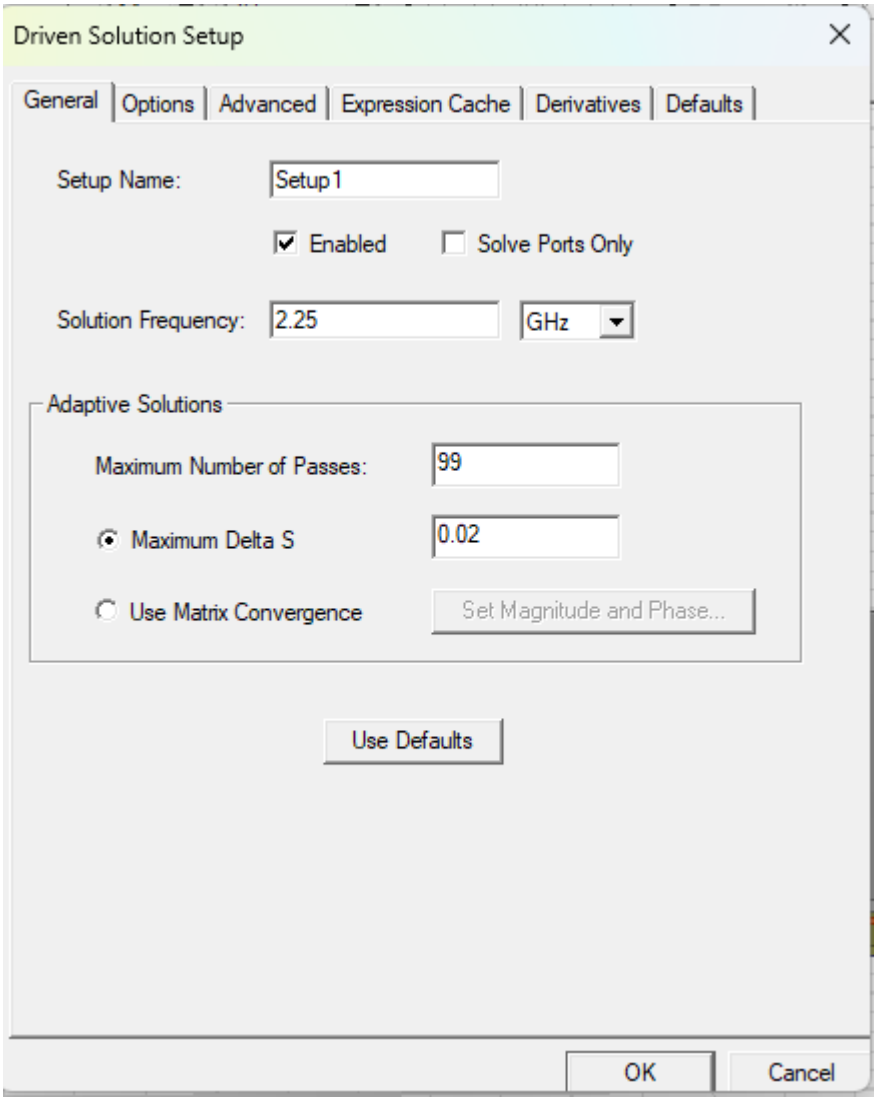

Figure 4.11 Solution setup

Step 16: To identify any faults in the design, go to HFSS and then validation. Check, and then click HFSS then investigate all to examine the design.

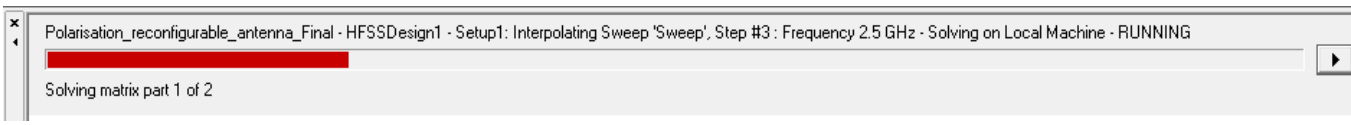

Figure 4.12 Analysis setup

Step 17: On such end of the simulation operation, the facts are assessed via HFSS.

CHAPTER 5:

Results

Using HFSS simulation software, the proposed antenna is modeled and the outputs are tracked. The design incorporates two PIN diodes, D1, D2, in the appropriate locations. One component of the driven patch is linked to diode D1, and another component is connected to diode D2.

The motivated patch Current flows through the matching patch when one diode is on, and through both elements of the array when both diodes are on. Right-handed circular polarization (RHCP) is achieved by turning on diode D1 and turning off diode D2, left circular polarization is achieved by turning on diode D1 and turning on diode D2, and linear polarization is achieved by turning on both diodes D1 and D2. The simulated return losses of the preferred Proposed Antenna in Modes 1 and 2 overlap, whereas the return loss graph in Mode 3 differs slightly. Table2 lists Simulated Values for a variety of modes.

Table 1 displays the Diode D's Changing States. Table 2 displays the resonance frequency, -10dB bandwidth, S11 parameter, and gain in dBi for the three operating modes. The proposed antenna's simulated gains are 6.49 dB, 6.03 dB, and 5.44 dB for each of the three operating modes, respectively. Table 2 shows that three separate re-configurable modes each have a resonance frequency with a return loss S11 of less than -10 dB.

Table 5.1 Switching States

Switching State of Diode D	**Polarization**
Mode 1 (D1 OFF & D2 ON)	LHCP (Left Hand Circular Polarization)
Mode 2 (D1 ON & D2 OFF)	RHCP (Right Hand Circular Polarization)
Mode 3 (D1 ON & D2 ON)	Linear Polarization

Table 5.2 Simulated result values for different switching conditions of proposed antenna

Switching State of Diodes D1 and D2	Resonant Frequency Range (GHz)	Bandwidth (GHz)	Measured Gain(dB)	Polarization
Mode 1 (D1 OFF & D2 ON)	2.20-2.8650	0.665	6.66	LHCP
Mode 2 (D1 ON & D2 OFF)	2.20-2.8510	0.651	6.20	RHCP
Mode 3 (D1 ON & D2 ON)	2.1480-2.3750, 2.5260- 2.7850	0.227,0.259	5.55	Linear Polarization

5.1 Result of Proposed Antenna when PIN Diode D1 “OFF” and D2 “OFF”

5.1.1 Reflection Coefficient

Current does not flow into driven patches and the suggested antenna does not radiate while both PIN diodes are in the OFF condition. An antenna is considered to be transmitting at a given frequency when its reflection coefficient is less than -10 dB. However, the overall S11 graph in this instance is above the -10dB line.

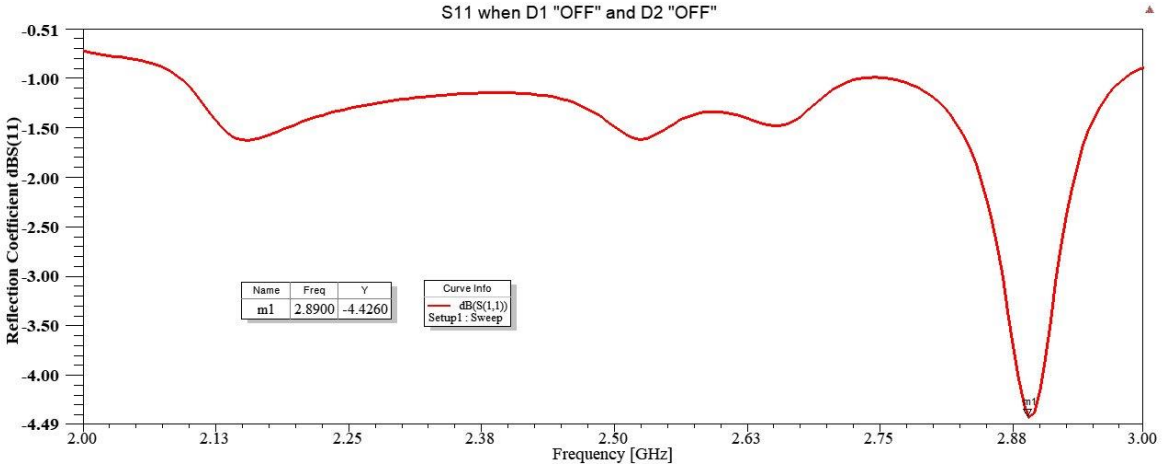

Figure 5.1 S_{11} when PIN Diode D1 “OFF” and D2 “OFF”

5.2 Results of Proposed Antenna when PIN Diode D1 “OFF” and D2 “ON”

5.2.1 Reflection Coefficient

The proposed antenna should have a reflection coefficient (S11) of less than -10 dB, meaning that it should radiate more than 90% of its input power. When the suggested design is in mode 1 (D1 "OFF" and D2 "ON"), the antenna resonates at 2.48GHz with -22.3638dB and at 2.8150 with -20.5862dB and has a bandwidth of 0.510GHz.

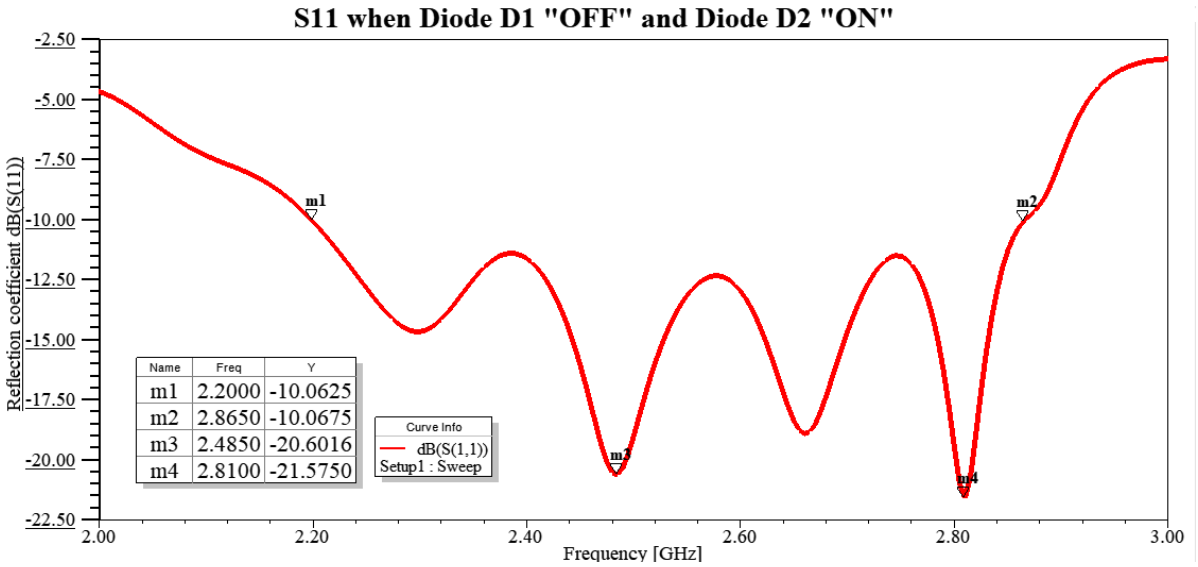

Figure 5.2 S_{11} Plot When D1 OFF & D2 ON

The reflection coefficient graph for an antenna operating in Mode 1 (D1 "OFF" and D2 "ON") is shown in the diagram above.

A constructed antenna operating in this mode (PIN Diode D1 "OFF" & PIN Diode D2 "ON") is able to transmit more than 90% of the input signal in that range, as shown in Fig. 5.2, where S11 graph is below -10 dB line from 2.20 GHz to 2.865 GHz.

5.2.2 Gain

The ratio of the power radiated by the antenna to the power radiated by an isotropic antenna is known as antenna gain. Antenna gain needs to be positive. When the PIN diodes D1 and D2 are in the "OFF" and "ON" states, the antenna radiates with a gain

of 6.4900dB at 2.25GHz. For practical uses, an antenna's gain should be greater than 1.5dB. The obtained gain in this case is greater than 1.5dB, making the suggested antenna practically usable.

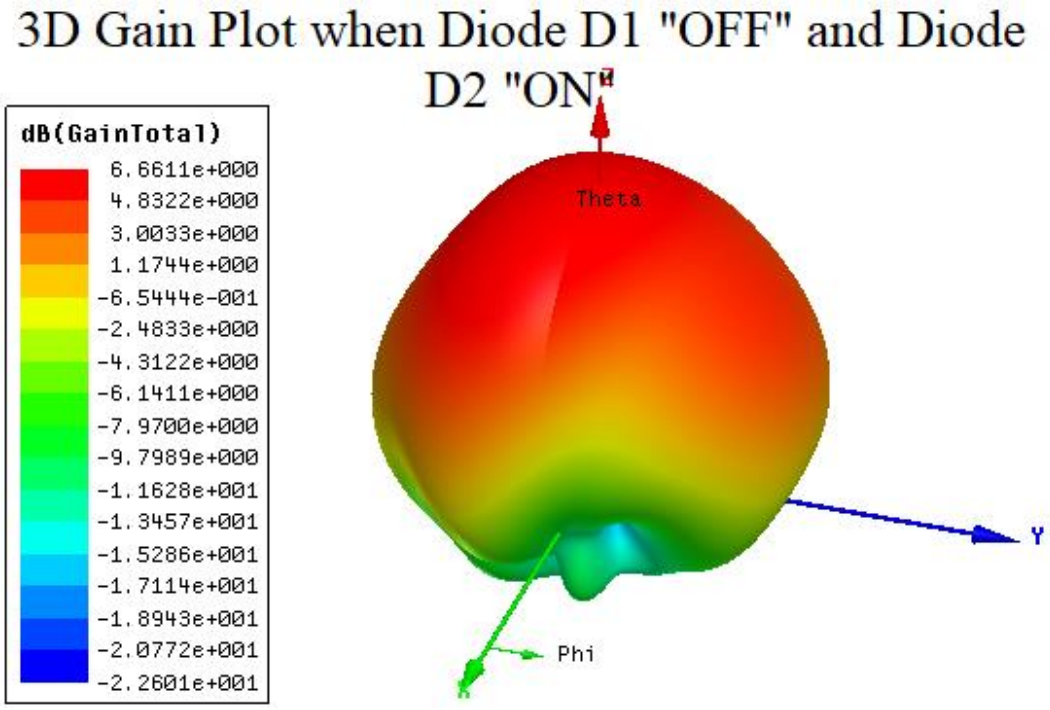

Figure 5.3 Gain Plot when PIN Diode D1 “OFF” and D2 “ON”.

5.2.3 Radiation Pattern

An antenna's radiation characteristics are represented by Radiation Pattern as a function of spatial coordinates. The direction of electromagnetic fields when energy is radiated away from an antenna is known as polarization.

Electric and magnetic fields emanate from the proposed antenna in an anticlockwise direction when it is operating in mode 1, which is when Diode D1 and D2 are both turned off. Thus, it is said that the antenna is in left-hand circular polarization.

As depicted in Fig 5. Right hand circular polarization is represented by the purple line in figure 4, whereas left hand circular polarization is represented by the red line. Here, the LHCP's maximum gain is approximately 6 dB, while the RHCP's maximum gain is a negative number. Thus, it is stated that the antenna is in left-hand circular polarization.

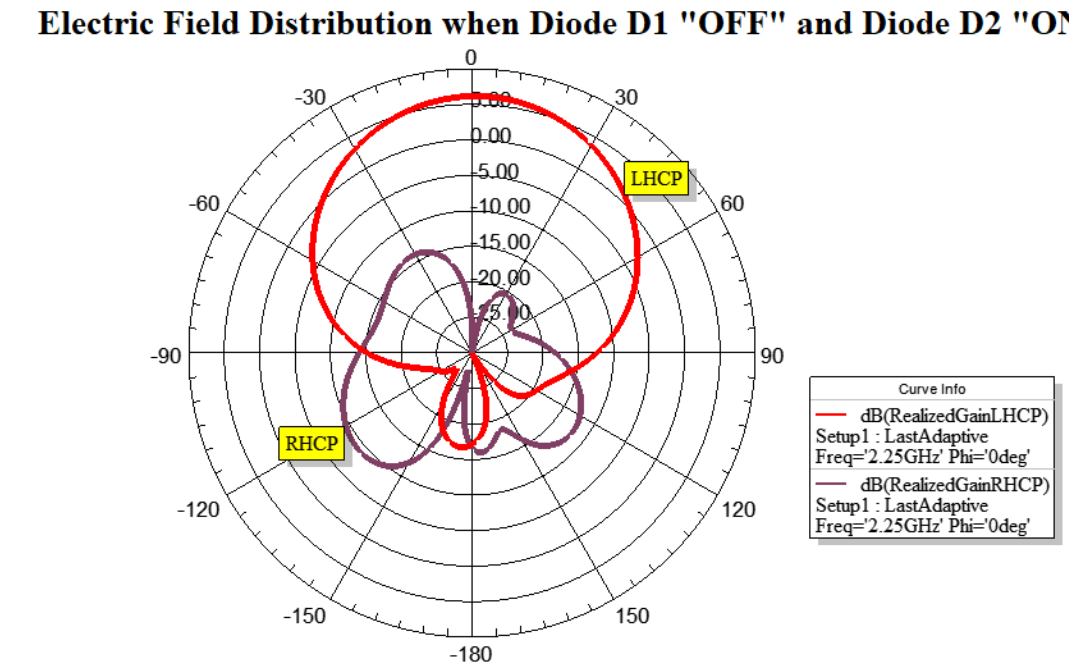

Figure 5.4 Electric Field Distribution when PIN Diode D1 “OFF” and D2 “ON”

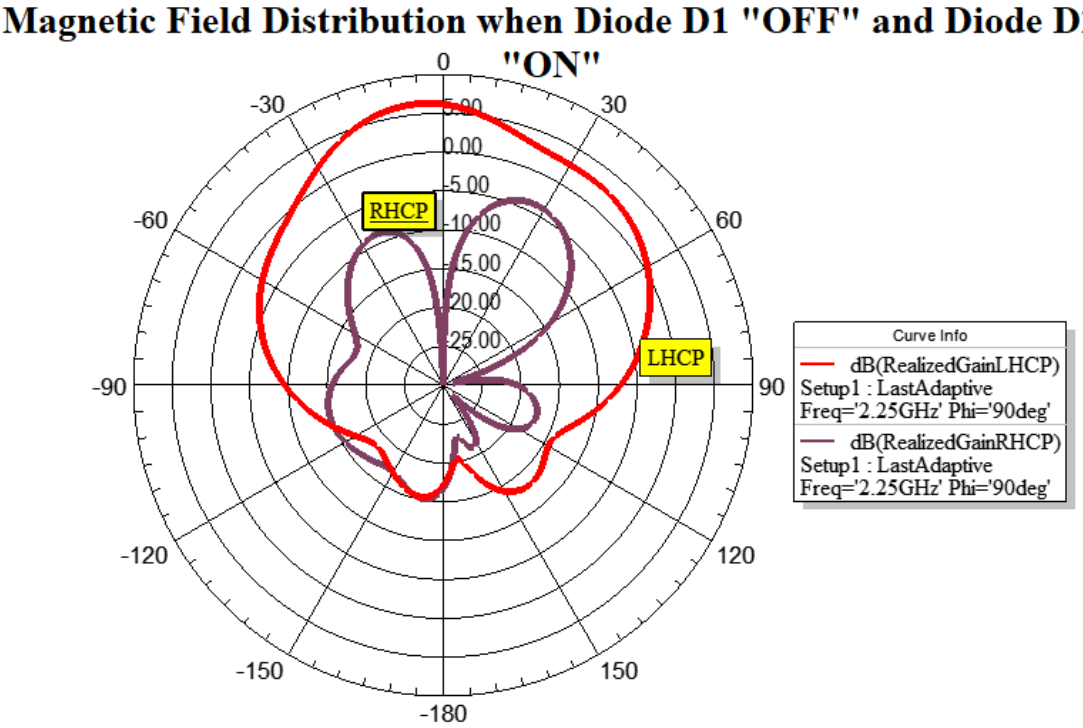

Figure 5.5 Magnetic Field distribution when PIN Diode D1 “OFF” and D2 “ON”

5.2.4 Current Distribution

The diagram below displays the current distribution over the radiating patch when PIN diodes D1 and D2 are turned on and off, respectively, based on the circumstances of the diodes employed in the proposed antenna. The graphics below show the magnitude and vector of the current's distribution over the patch.

As may be seen in the table below from Fig. 5.6's colour mapping, green denotes higher current than blue. In the right side patch of the two element array antenna of the proposed antenna, green hue can be seen. Given that the equivalent PIN Diode D1 is in the OFF condition, it means that there is a greater current flow in the right side patch than the left. As PIN Diode D2 is turned ON, green coloured arrows can be seen on the right-side patch of the vector current distribution diagram (fig. 5.7).

Current Distribution when D1 "OFF" and D2 "ON"

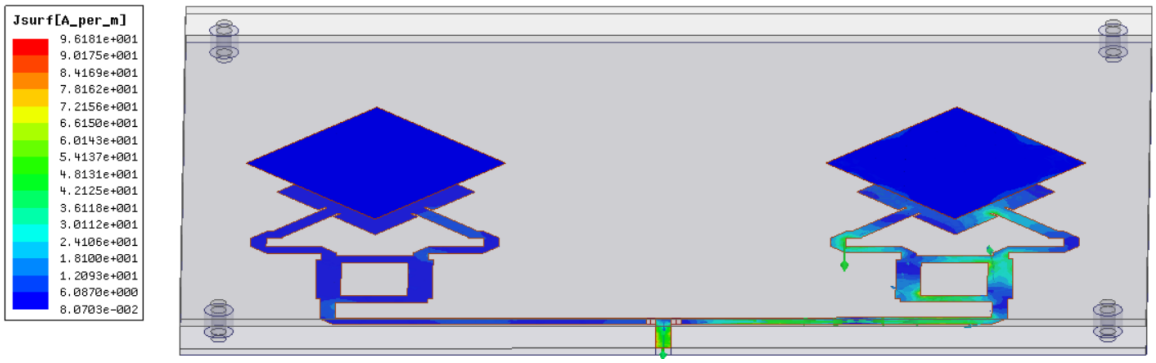

Figure 5.6 Magnitude of current distribution when PIN Diode D1 “OFF” and Diode D2 “ON”

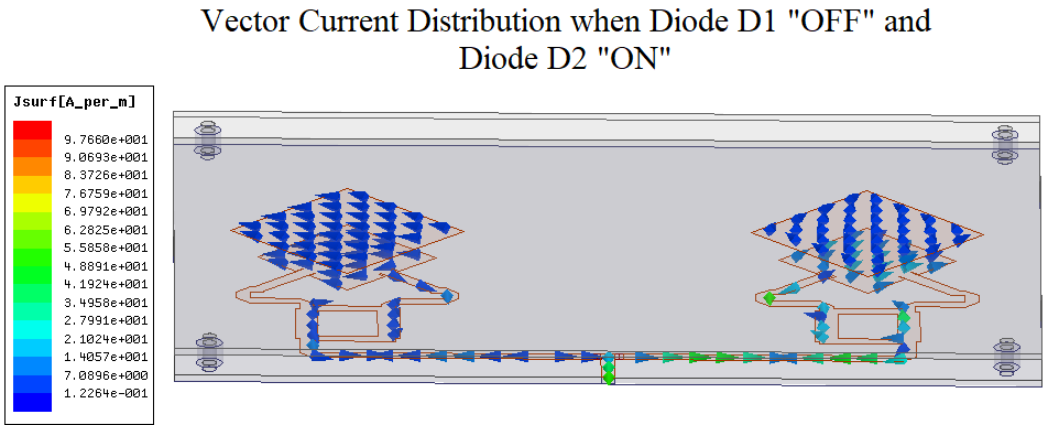

Figure 5.7 Vector Current Distribution when PIN Diode D1 “OFF”and D2 “ON”

5.2.5 E-Field Distribution

Field pattern refers to the field distribution that can be quantified in terms of field intensity. In other words, the plotted radiated power from the antenna is expressed as an electric field, E (v/m). So, it is called a "field pattern."

The voltage delivered to the elements by the antenna causes an electric field, E, to flow from the positive charge to the negative charge.

According to the table below's representation of Fig. 5.8's colour mapping, green denotes more current than blue. Green coloured arrows may be seen on the proposed antenna in the right side patch of the two element array antenna. Given that the equivalent PIN Diode D1 is in the OFF condition, it means that there is a stronger electric field around the right-side patch than the left patch. When PIN diode D1 is "OFF" and D2 is "ON," the proposed antenna's E fields look like the figure below.

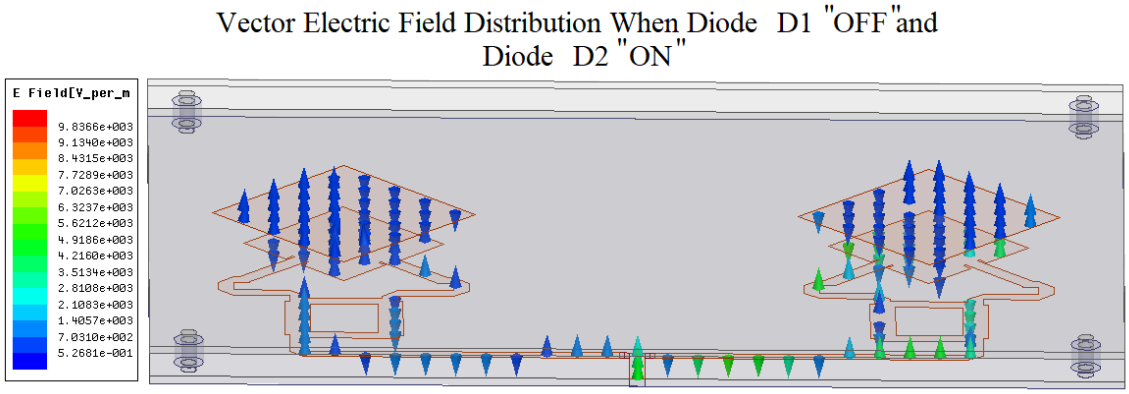

Figure 5.8 Electric Field Distribution when PIN Diode D1 “OFF” and D2 “ON”

5.2.6 Axial Ratio:

The ratio between the major and minor axes of a circularly polarized antenna pattern is known as the axial ratio (AR) of an antenna. This ratio would be 1 if an antenna had perfect circular polarization. (0 dB).

The suggested antenna's axial ratio is obtained as shown below when it is operated in mode 1, which is PIN diode D1 "OFF" and D2 "ON".

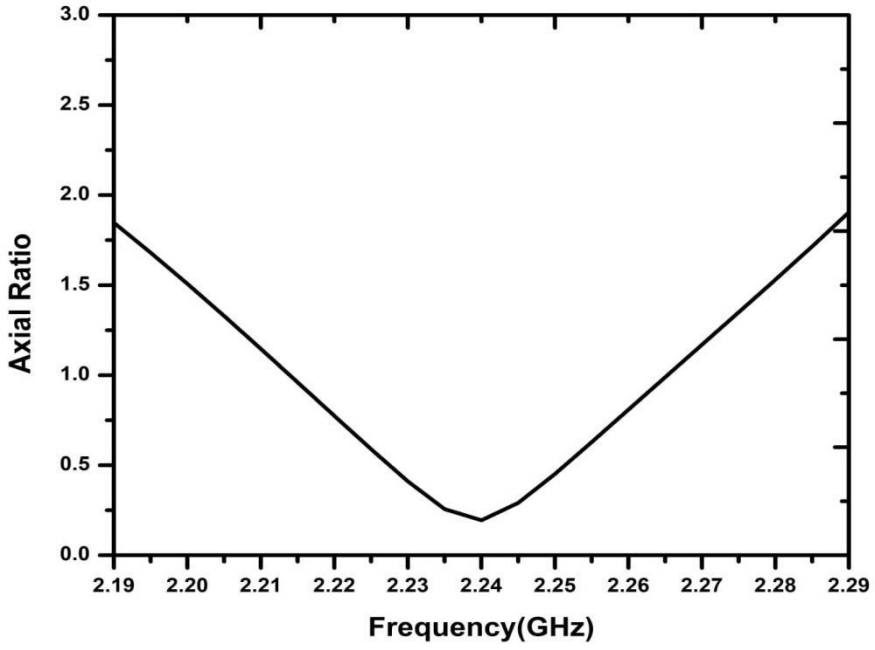

Figure 5.9 Axial Ratio when PIN Diode D1 “OFF” and D2 “ON”

As seen in the axial ratio graph in Fig. 5.8 above, which is below 2.0, it indicates that the antenna is polarized in a circular fashion because the ideal axial ratio is zero. Axial ratio for a circularly polarized antenna must be as little as possible for practical usage.

5.3 Results of Proposed Antenna when PIN Diode D1 “ON” and D2 “OFF”

5.3.1 Reflection Coefficient

The proposed antenna should have a reflection coefficient (S11) of less than -10 dB, meaning that it should radiate more than 90% of its input power. The suggested design's antenna resonates from 2.2090 GHz to 2.8800 GHz with a bandwidth of 0.510 GHz and at 2.49GHz with -21.1441 dB and at 2.8300 with -19.0973 dB when it is in mode 1 (D1 "ON" and D2 "OFF").

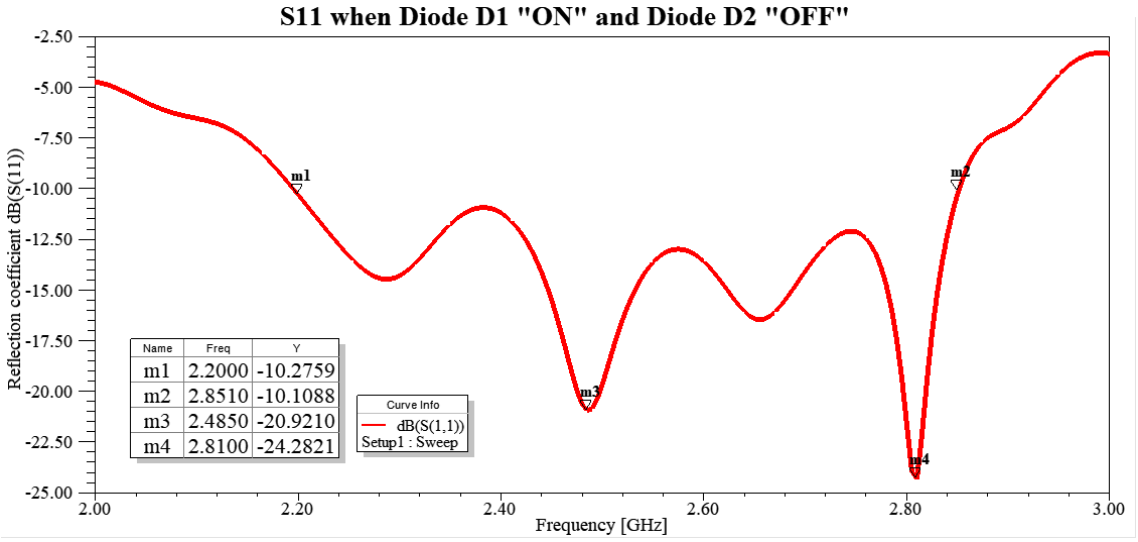

Figure 5.10 S_{11} Plot When PIN Diode D1 ON & D2 OFF

The reflection coefficient graph for an antenna operating in Mode 2 (D1 "ON" and D2 "OFF") is shown in the diagram above.

A constructed antenna operating in this mode (PIN Diode D1 "ON" & PIN Diode D2 "OFF") is able to transmit more than 90% of the input signal in that range, as shown in Fig. 5.10. The S11 graph is below the -10 dB line from 2.20 GHz to 2.851 GHz.

5.3.2 Gain

The ratio of the power radiated by the antenna to the power radiated by an isotropic antenna is known as antenna gain. Antenna gain need to be positive.

When the PIN diodes D1 and D2 are in the "OFF" and "ON" states, the antenna radiates with a gain of 6.0325 dB at 2.25 GHz. For practical uses, an antenna's gain should be greater than 1.5dB. The obtained gain in this case is greater than 1.5dB, making the suggested antenna practically usable.

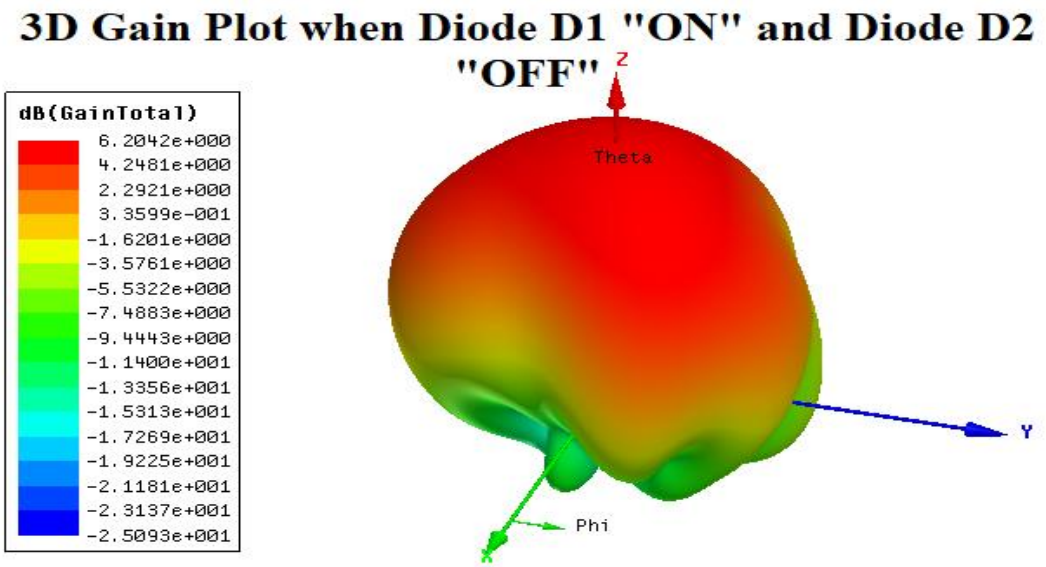

Figure 5.11 Gain Plot When PIN Diode D1 ON & D2 OFF

5.3.3 Radiation Pattern

An antenna's radiation characteristics are represented by Radiation Pattern as a function of spatial coordinates. The direction of electromagnetic fields when energy is radiated away from an antenna is known as polarization. The electric and magnetic fields emitted from the proposed antenna rotate clockwise when it is operated in mode 1, which is when Diode D1 and D2 are both turned on. Thus, it is claimed that the antenna is in right-hand circular polarization.

As depicted in Fig 5.12 Red lines indicate the radiation pattern for left-hand circular polarization, while purple lines indicate right-hand circular polarization. Here, the

RHCP's maximum gain is approximately 6 dB, while the LHCP's maximum gain is a negative number. Thus, it is claimed that the antenna is in right-hand circular polarization.

Electric Field Distribution when Diode D1 "ON" and Diode D2 "OFF"

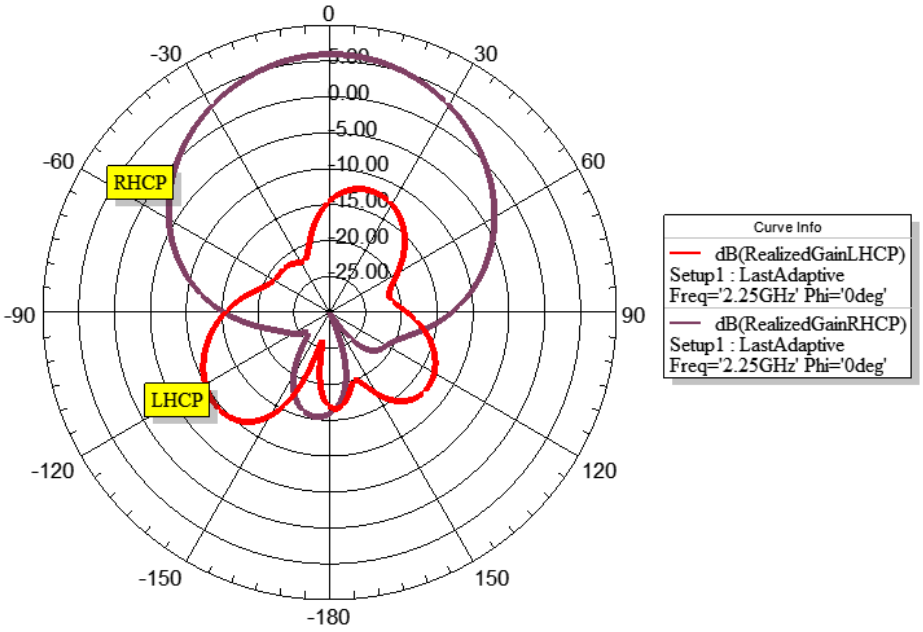

Figure 5.12 Electric Field When PIN Diode D1 ON & D2 OFF

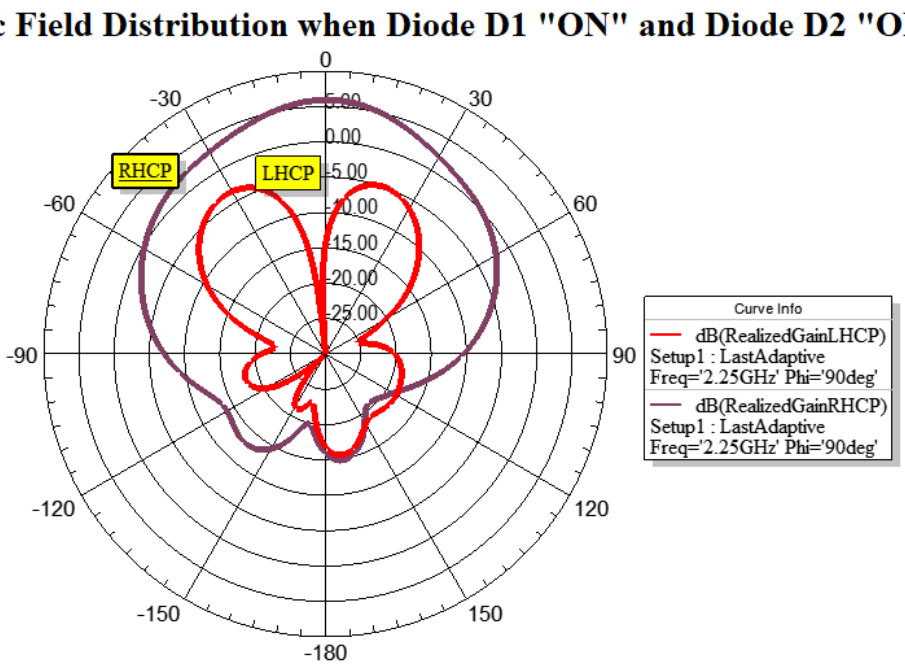

Figure 5.13 Electric Field When PIN Diode D1 ON & D2 OFF

5.3.4 Current Distribution

The diagram below displays the current distribution over the radiating patch when PIN diodes D1 and D2 are turned on and off, respectively, based on the circumstances of the diodes employed in the proposed antenna. According to the table below's representation of Fig. 5.14's colour mapping, green denotes more current than blue. On the suggested antenna, the left side patch of the two element array antenna may be seen to be green in hue. Given that the equivalent PIN Diode D2 is in the OFF condition, it means that there is a greater current flow in the left side patch than the right side patch. As PIN Diode D1 is turned ON, green coloured arrows can be seen on the patch on the left in the vector current distribution diagram (fig. 5.15).

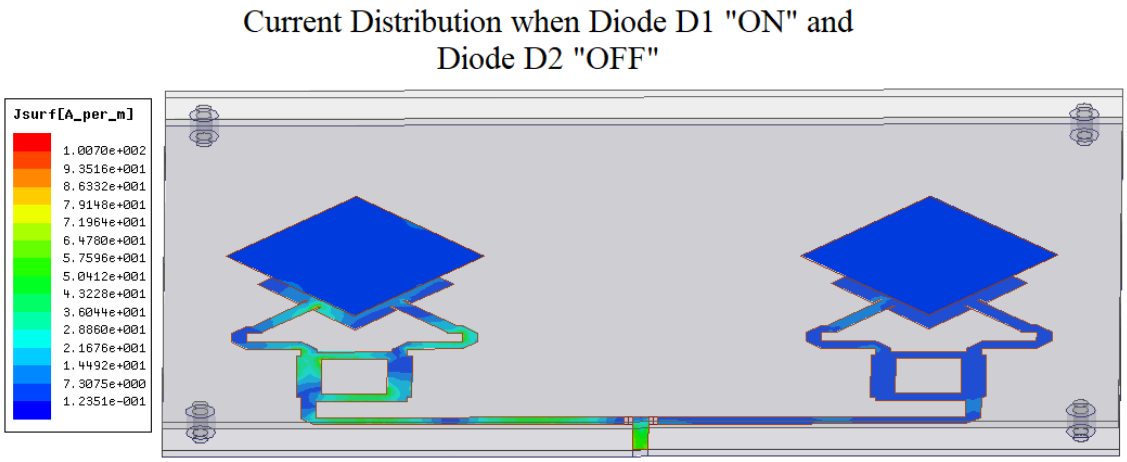

Figure 5.14 Magnitude of current Distribution When PIN Diode D1 ON & D2 OFF

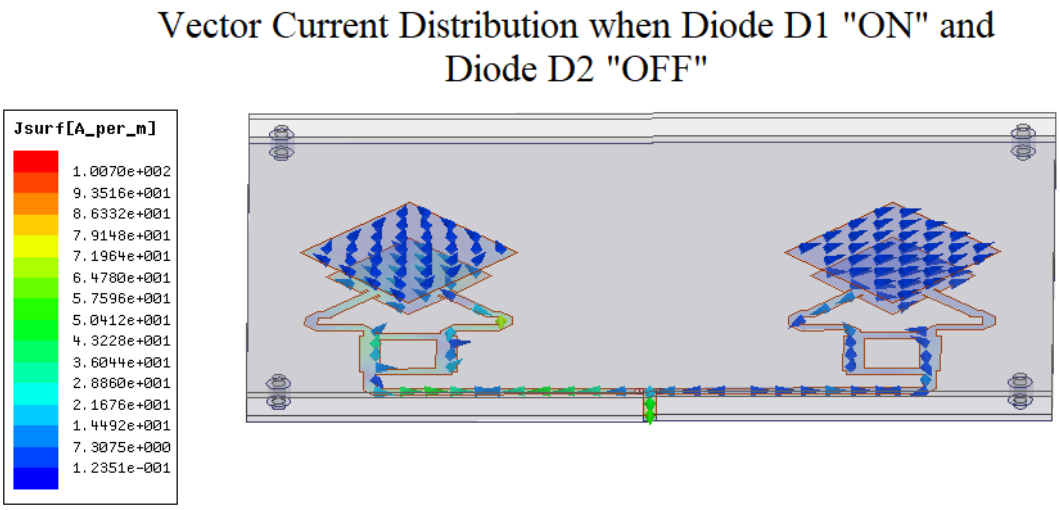

Figure 5.15 Current Distribution When PIN Diode D1 ON & D2 OFF

5.3.5 E-Field Distribution

Field pattern refers to the field distribution that can be quantified in terms of field intensity. In other words, the plotted radiated power from the antenna is expressed as an electric field, E (v/m). So, it is called a "field pattern."

The voltage delivered to the elements by the antenna causes an electric field, E, to flow from the positive charge to the negative charge.

When PIN diode D1 is "ON" and D2 is "OFF," the proposed antenna's E fields are as illustrated in the below image.

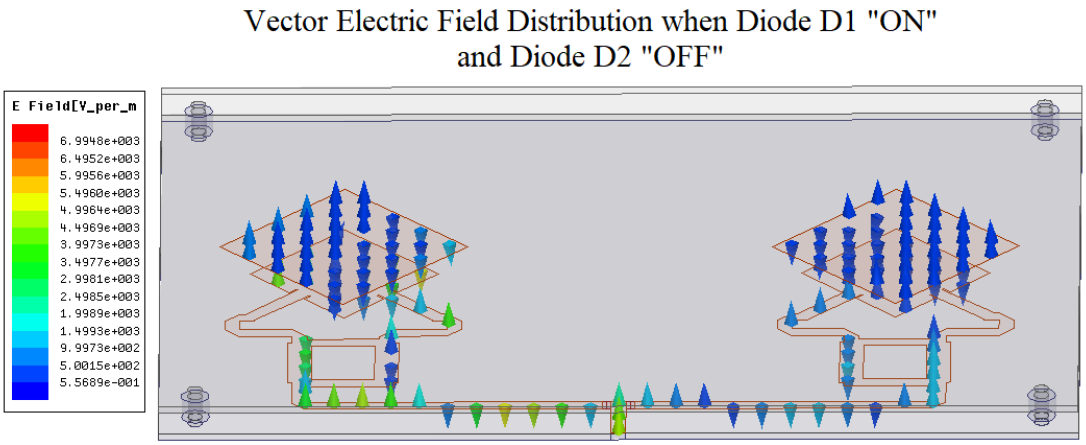

Figure 5.16 Electric Field Distribution When PIN Diode D1 ON & D2 OFF

5.3.6 Axial Ratio

The ratio between the major and minor axes of a circularly polarized antenna pattern is known as the axial ratio (AR) of an antenna. This ratio would be 1 if an antenna had perfect circular polarization. (0 dB).

When the proposed antenna is used in mode 1, which turns PIN diode D1 "ON" and D2 "OFF," the axial ratio is obtained as shown below.

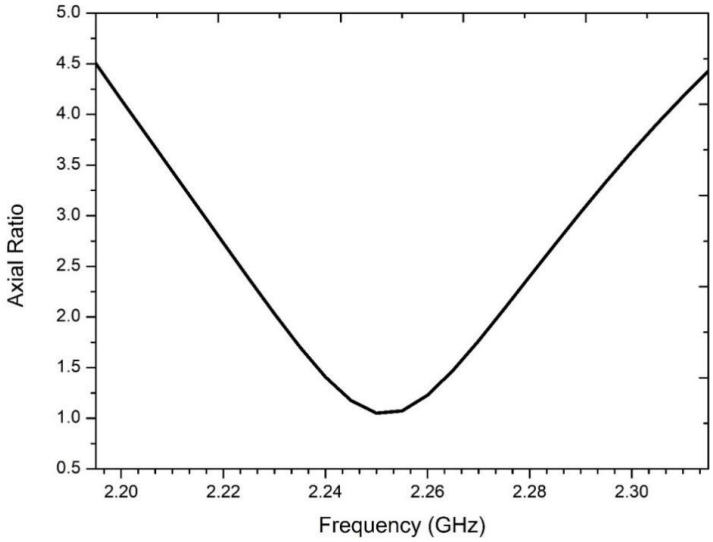

Figure 5.17 Axial Ratio when Diode D1 “ON” and Diode D2 “OFF”

5.4 Results of Proposed Antenna when PIN Diode D1 “ON” and D2 “ON”

5.4.1 Reflection Coefficient

The proposed antenna should have a reflection coefficient (S11) of less than -10 dB, meaning that it should radiate more than 90% of its input power. The suggested design's antenna resonates from 2.2090 GHz to 2.8800 GHz with a bandwidth of 0.510 GHz and at 2.49GHz with -21.1441 dB and at 2.8300 with -19.0973 dB when it is in mode 1 (D1 "ON" and D2 "OFF").

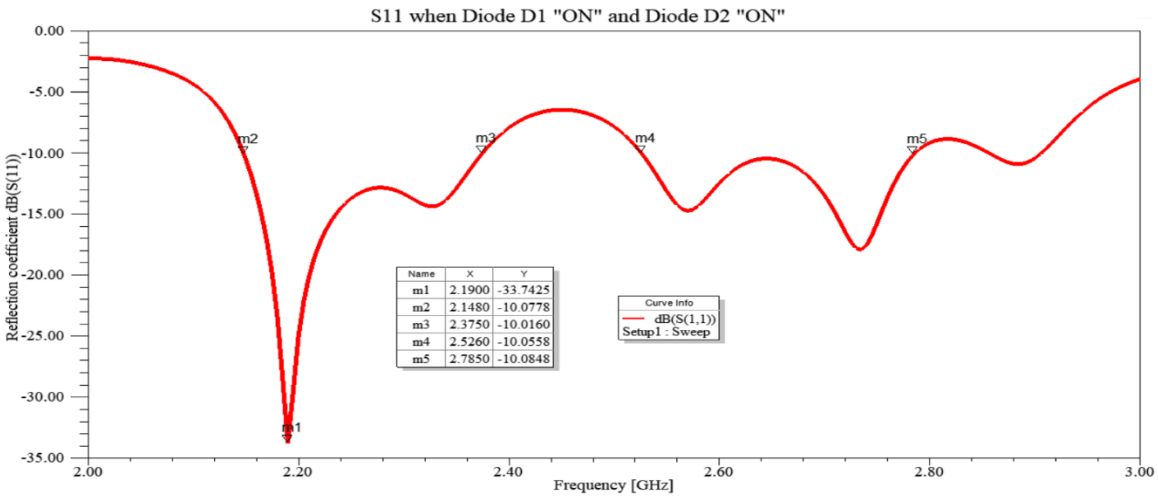

Figure 5.18 S_{11} Plot PIN Diodes When D1 ON & D2 ON

The reflection coefficient graph for an antenna operating in Mode 3 (D1 and D2 turned on) is shown in the diagram above.

In Fig. 5.18, we can see that the S11 graph from 2.14 GHz to 2.375 GHz is below the -10 dB line, indicating that the designed antenna used in this mode (PIN Diode D1 "ON" & PIN Diode D2 "ON") is capable of transmitting more than 90% of the input signal in that frequency range.

5.4.2 Gain

The ratio of the power radiated by the antenna to the power radiated by an isotropic antenna is known as antenna gain. Antenna gain need to be positive.

When both PIN diodes are turned on, the antenna radiates at 2.25GHz with a gain of 5.44dB. For practical uses, an antenna's gain should be greater than 1.5dB. The obtained gain in this case is greater than 1.5dB, making the suggested antenna practically usable.

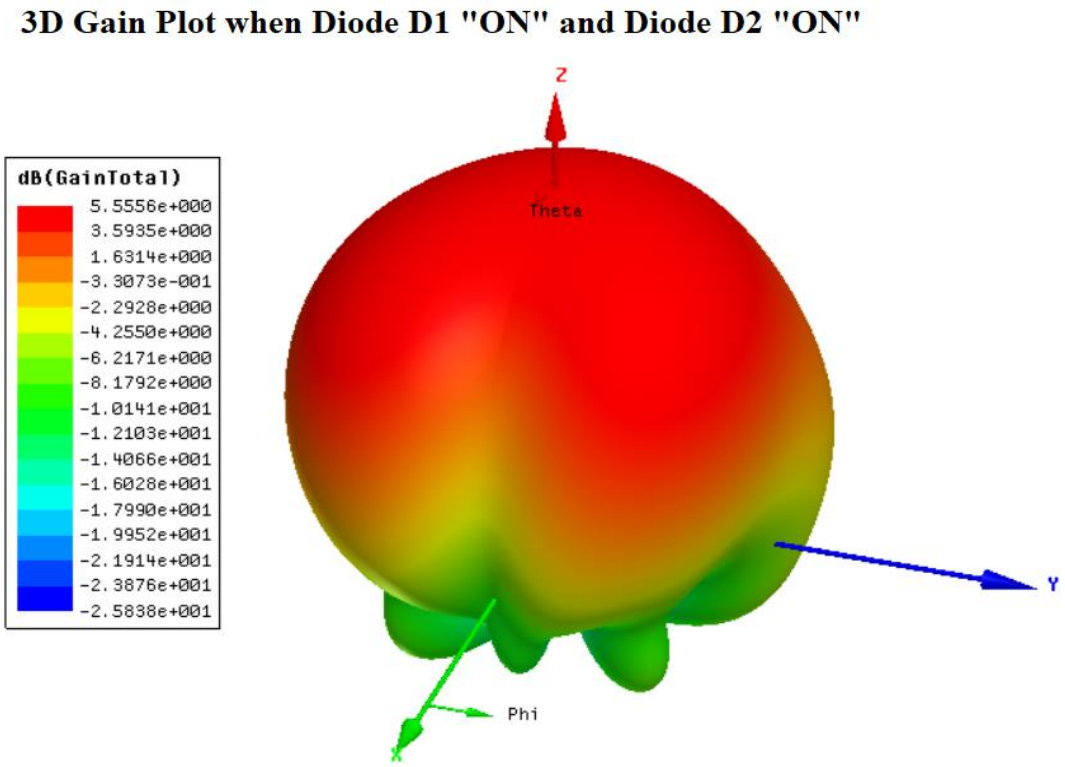

Figure 5.19 Gain Plot PIN Diodes When D1 ON & D2 ON

5.4.3 Radiation Pattern

An antenna's radiation characteristics are represented by Radiation Pattern as a function of spatial coordinates. The direction of electromagnetic fields when energy is radiated away from an antenna is known as polarization. The proposed antenna's electric and magnetic fields radiate in a linear direction when it is in mode 1, which is the condition where Diode D1 and D2 are turned on. Thus, it is claimed that the antenna is in linear polarization.

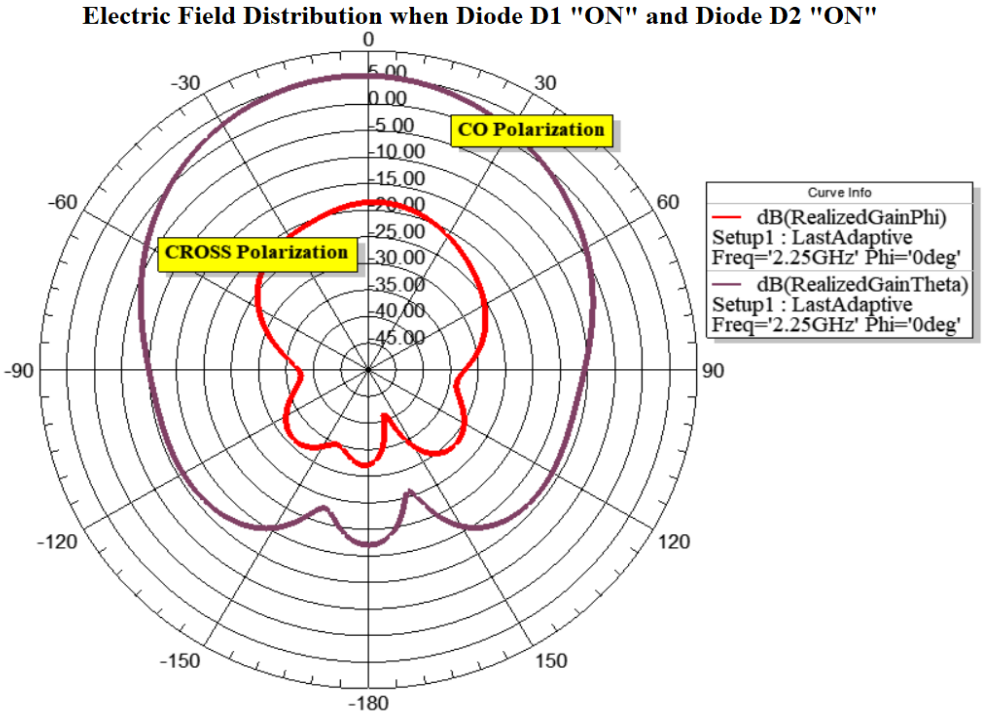

Figure 5.20 Electric Field Distribution PIN Diodes When D1 ON & D2 ON

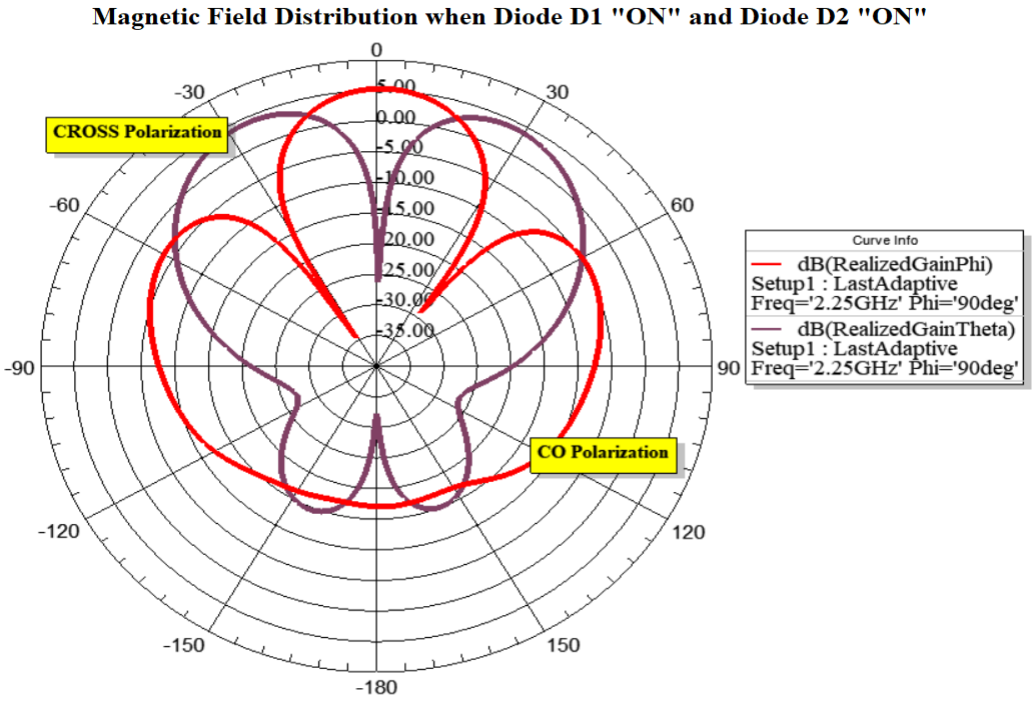

Figure 5.21 Magnetic Field Distribution PIN Diodes When D1 ON & D2 ON

5.4.4 Current Distribution

Current distribution throughout the radiating patch varies depending on the diode conditions utilized in the proposed antenna, as shown in the diagram below when PIN diodes D1 and D2 are turned on.

According to the table below's representation of Fig. 5.22's colour mapping, green denotes more current than blue. On the suggested antenna, both patches of the two element array antenna can be seen to be green in hue. As both PIN diodes are turned on, green arrows in the vector current distribution (fig. 5.23) may be seen on both patches.

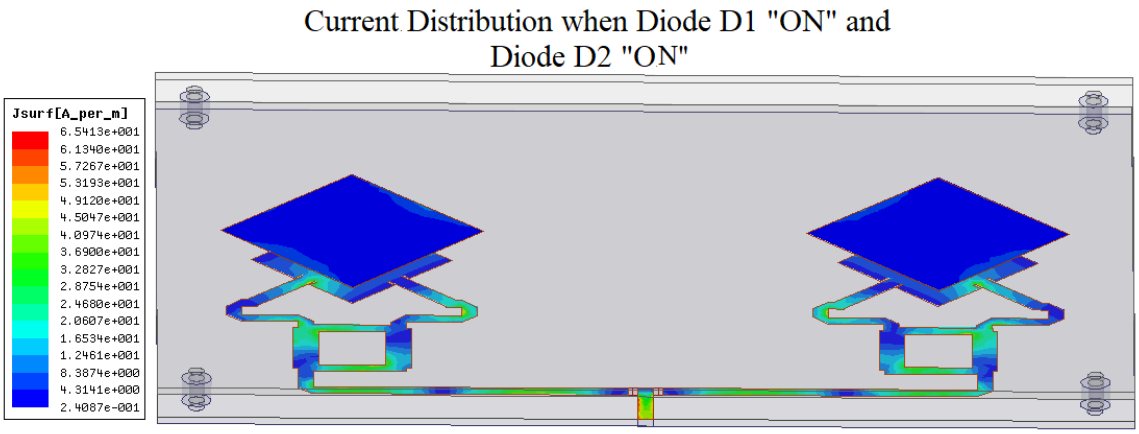

Figure 5.22 Magnitude of current Distribution PIN Diodes When D1 ON & D2 ON

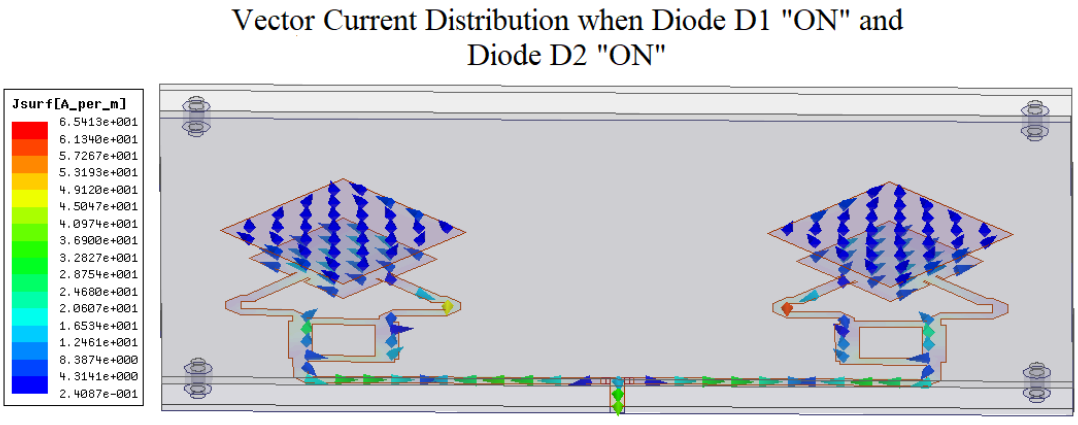

Figure 5.23 Current Distribution PIN Diodes When D1 ON & D2 ON

5.4.5 E-Field Distribution

Field pattern refers to the field distribution that can be quantified in terms of field intensity. In other words, the plotted radiated power from the antenna is expressed as an electric field, E (v/m). So, it is called a "field pattern."

The voltage delivered to the elements by the antenna causes an electric field, E, to flow from the positive charge to the negative charge.

When PIN diodes D1 and D2 are turned on, the proposed antenna's E fields will look like the picture below.

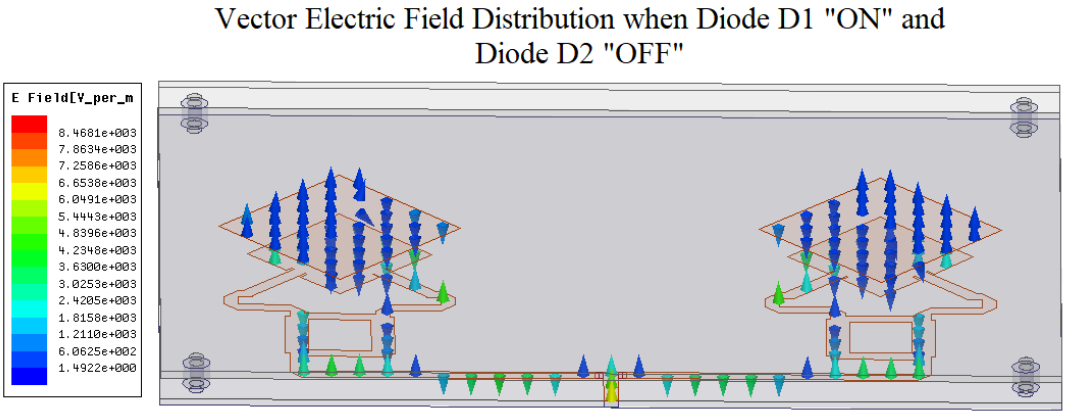

Figure 5.24 Electric Field Distribution PIN Diodes When D1 ON & D2 ON

5.4.6 Axial Ratio

The ratio between the major and minor axes of a circularly polarized antenna pattern is known as the axial ratio (AR) of an antenna. This ratio would be 1 if an antenna had perfect circular polarization. (0 dB).

The suggested antenna's axial ratio is obtained as shown below when it is operated in mode 1, with PIN diodes D1 and D2 turned on.

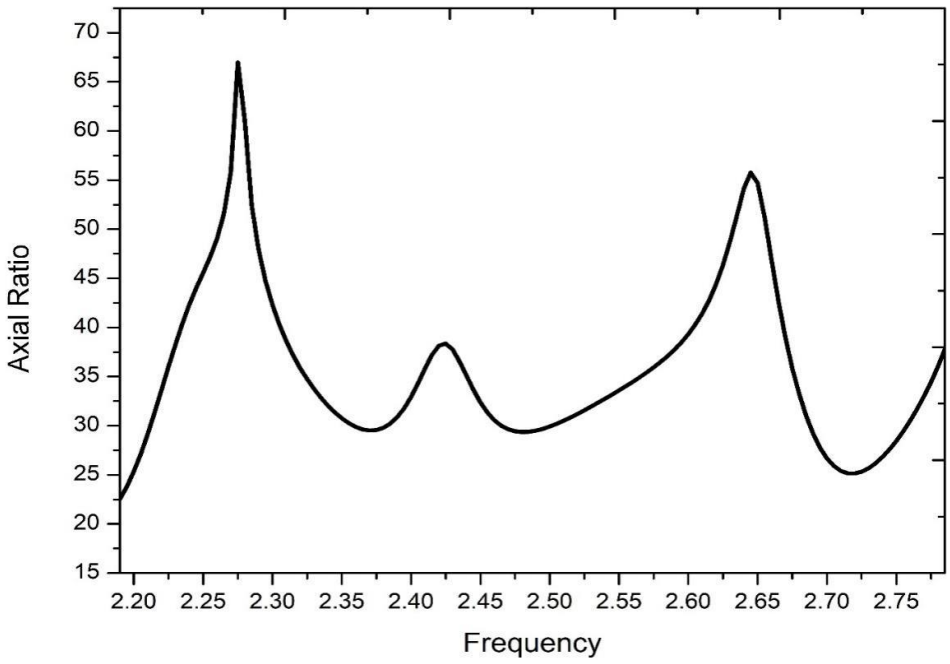

Figure 5.25 Axial Ratio when Diode D1 "ON" and Diode D2 "ON"

CONCLUSION

The proposed Polarization Agile Reconfigurable Antenna is simulated in HFSS. Two PIN diodes are used to achieve Polarisation Reconfigurability. In different operating modes, when the Diode D1 “OFF” and D2 “ON” state, the antenna is in Left Hand Circular Polarisation with a gain of 6.66 dB and resonating frequency range 2.2-2.8650GHz. When the PIN diode D1 “ON” and PIN diode D2 “OFF” state antenna is in Right Hand Circular Polarisation with gain 6.20 dB and resonating frequency range 2.2-2.8510GHz. When both PIN diodes D1 and D2 are in “ON” state the antenna is in linear polarization with gain 5.55dB and resonating frequency 2.1480-2.7850 GHz. The achieved modes of operation will be used for applications in S band.

REFERENCES

[1] C. Balanis, Antenna Theory. Wiley, 1997.

[2] Garg, Ramesh. Microstrip Antenna Design Handbook. United Kingdom, Artech House, 2001.

[3] S. Gao, A. Sambell and S. S. Zhong, "Polarization-agile antennas," in *IEEE Antennas and Propagation Magazine*, vol. 48, no. 3, pp. 28-37, June 2006.

[4] M. Saravanan and M. J. S. Rangachar, “Polarization Reconfigurable Square Patch Antenna for Wireless Communications”, *AEM*, vol. 7, no. 4, pp. 103–108, Sep. 2018.

[3] W. Lin and H. Wong, "Wideband Circular Polarization Reconfigurable Antenna," in *IEEE Transactions on Antennas and Propagation*, vol. 63, no. 12, pp. 5938-5944, Dec. 2015.

[4] L. Zhang, S. Gao, Q. Luo, P. R. Young and Q. Li, "Wideband Loop Antenna With Electronically Switchable Circular Polarization," in *IEEE Antennas and Wireless Propagation Letters*, vol. 16, pp. 242-245, 2017.

[5] Mahmoud Moubadir, Imane Badaoui, Naima Amar Touhami, Mohamed Aghoutane, Mohssine El Ouahabi, “A new circular polarization dual feed microstrip square patch antenna using branch coupler feeds for WLAN/HIPERLAN applications”, Procedia Manufacturing, Volume 32,2019, Pages 702-709,ISSN 2351-9789.

[6] Anil Kumar Agrawal, Shyam Sundar Pattnaik, S Devi & J G Joshi (2011). Broadband and high gain microstrip patch antenna for WLAN. *Indian Journal of Radio & Space Physics Vol 40 October 2011.*

[7] Wang, S. T., Sun, S., Sun, H., Yang, S., & Hu, J. (2021). A quadrature-hybrid-integrated reconfigurable feeding network for wideband quad-polarization-agile Antenna Design. *International Journal of RF and Microwave Computer-Aided Engineering*, *31*(6).

[8] Q. Chen, J. -Y. Li, G. Yang, B. Cao and Z. Zhang, "A Polarization-Reconfigurable High-Gain Microstrip Antenna," in *IEEE Transactions on Antennas and Propagation*, vol. 67, no. 5, pp. 3461-3466, May 2019.

[9] H. Sun and S. Sun, "A Novel Reconfigurable Feeding Network for Quad-Polarization-Agile Antenna Design," in *IEEE Transactions on Antennas and Propagation*, vol. 64, no. 1, pp. 311-316, Jan. 2016.

[10] P. Kumar, S. Dwari, R. K. Saini and M. K. Mandal, "Dual-Band Dual-Sense Polarization Reconfigurable Circularly Polarized Antenna," in *IEEE Antennas and Wireless Propagation Letters*, vol. 18, no. 1, pp. 64-68, Jan. 2019.

[11] R. Sharma, N. S. Raghava and A. De, "Design of Compact Circular Microstrip Patch Antenna using Parasitic Patch," 2021 6th *International Conference for Convergence in Technology (I2CT)*, Maharashtra, India, 2021, pp. 1-4.

[12] L. Guo and M. -C. Tang, "A Low-Profile Dual-Polarized Patch Antenna with Bandwidth Enhanced by Stacked Parasitic Elements," 2018 *International Conference on Microwave and Millimeter Wave Technology (ICMMT)*, Chengdu, China, 2018, pp. 1-3.

[13] S. T. Fan, Y. Z. Yin, B. Lee, W. Hu and X. Yang, "Bandwidth Enhancement of a Printed Slot Antenna With a Pair of Parasitic Patches," in *IEEE Antennas and Wireless Propagation Letters*, vol. 11, pp. 1230-1233, 2012.

[14] L. Kang, H. Li, B. Tang, X. Wang and J. Zhou, "Quad-Polarization-Reconfigurable Antenna With a Compact and Switchable Feed," in *IEEE Antennas and Wireless Propagation Letters*, vol. 20, no. 4, pp. 548-552, April 2021.

[15] S. T. Fan, Y. Z. Yin, B. Lee, W. Hu and X. Yang, "Bandwidth Enhancement of a Printed Slot Antenna With a Pair of Parasitic Patches," in *IEEE Antennas and Wireless Propagation Letters*, vol. 11, pp. 1230-1233, 2012.

[16] L. Kang, H. Li, B. Tang, X. Wang and J. Zhou, "Quad-Polarization-Reconfigurable Antenna With a Compact and Switchable Feed," in *IEEE Antennas and Wireless Propagation Letters*, vol. 20, no. 4, pp. 548-552, April 2021.

[17] S. Wang, D. Yang, W. Geyi, C. Zhao and G. Ding, "Polarization-Reconfigurable Antenna Using Combination of Circular Polarized Modes," in *IEEE Access*, vol. 9, pp. 45622-45631, 2021.

[18] J. Hu, G. Q. Luo and Z. -C. Hao, "A Wideband Quad-Polarization Reconfigurable Metasurface Antenna," in *IEEE Access*, vol. 6, pp. 6130-6137, 2018.

[19] J. Hu and Z. -C. Hao, "Frequency and Polarization Reconfigurable Patch Antenna Using Switchable Shorting Pins," 2018 *IEEE Asia-Pacific Conference on Antennas and Propagation* (APCAP), Auckland, New Zealand, 2018, pp. 418-419.

[20] H. Gu, J. Wang, L. Ge and C. -Y. -D. Sim, "A New Quadri-Polarization Reconfigurable Circular Patch Antenna," in *IEEE Access*, vol. 4, pp. 4646-4651, 2016.

PUBLISHED PAPERS

1) Bammidi Deepa, Villa Vidya Sri Sai Kiran, Chilla Sandeep Reddy and Kondapalli Yasaswini, “Design of Dual L-Slot Asymmetric I-Shaped Frequency Reconfigurable Antenna”, 2022 *International Conference on Advancement in Electronic Systems and Communication Technologies*, 2022 November.

2) Bammidi Deepa, Gatreddi Bhavana Sai Sree and Madimi Dhanush Karthik , “Automation Of Vehicle To Vehicle Distance Measurement Using IOT ”, 2022 *International Conference on Advancement in Electronic Systems and Communication Technologies*, 2022 November.

Design of Dual L-Slot Asymmetric I-Shaped Frequency Reconfigurable Antenna

Bammidi Deepa
ECE *department*
ANITS
Anil Neerukonda Institute of Technology and Sciences
Visakhapatnam, India
deepa.ece@anits.edu.in

Villa Vidya Sri Sai Kiran
ECE *deartment*
Anil Neerukonda Institute of Technology and Sciences
Visakhapatnam, India
vidyasrisaikiran.2018.ece@anits.edu.in

Chilla Sandeep Reddy
ECE *deartment.*
Anil Neerukonda Institute of Technology and Sciences
Visakhapatnam, India
sandeepreddy.2019.ece@anits.edu.in

Kondapalli Yasaswini
ECE *deartment*
Anil Neerukonda Institute of Technology and Sciences
Visakhapatnam, India
yasaswini.2019.ece@anits.edu.in

Abstract—Reconfigurable antennas are advantageous in terms of reduced size and complexity to achieve multiple operating frequency or multiple radiation patterns or multiple polarization. A dual I-shaped frequency reconfigurable antenna is discussed in the paper. The proposed antenna is simulated on the FR4_epoxy substrate material having εr=4.4 with a size about 25 x 15 x 1.6 mm. A dual L-slot I-shaped frequency reconfigurable antenna is proposed to switch at different frequency bands between 2 to 4 GHz (S-band) & 4 to 8 GHz (C-band) with the help of a two asymmetric L- slot structures on the I-shaped design. It is planned to achieve frequency reconfigurability using one RF PIN diode SMP 1346-079LF at an appropriate location on the patch. The two operating modes of the PIN diode i.e., ON/OFF states would result in different current distribution, causing antenna resonance at different frequencies. The designed antenna is suitable for wireless applications like Wi-Fi and WLAN.

Keywords—Frequency reconfigurable antenna, switching states, WLAN, C-band, S-band, Asymmetric Slot.

I. INTRODUCTION

Compact, confirmable and multi operating frequency devices are the requirement of wireless communication systems. Reconfigurable antennas are advantageous in terms of reduced size and complexity but can achieve different frequency bands, polarization and radiation pattern. In wireless communication systems, S band and C band frequencies are widely used for commercial and security applications.

The performance of a microstrip patch antenna and its resonant frequency depends on the current distribution on the radiating patch structure [1]. By switching the PIN diodes on the patch structure it is possible to change the electrical equivalent circuit of the antenna, thus the resonant frequency can be changed [2]. The antenna controlling concepts using programming were discussed by Christodoulou et al. [3]. Achieving single directional radiation patterns with low cross polarization for UHF band applications is discussed by Yogesh kumar Choukiker et al[4]. A slot antenna is designed, which is utilized for frequency and pattern reconfiguration is discussed by Wenmei Zhang et al[5]. Dual L-Slot was discussed by Bhaben Saikia [6]. I-shaped patch structure was discussed by Nikolaou et al [7]. A compatible dual band reconfigurable antenna was discueed by Yasir et al [8]. The working of frequency and pattern reconfigurable antennas was discussed by Majid et al [9]. A slot antenna with frequency reconfiguration was discussed by Han et al [10].DRA structure with frequency reconfiguration was discussed by Danesh et al [11]. A Dielectric resonator antenna with a Co-Planar Waveguide structure to achieve frequency reconfigurability is discussed by Danesh et al[12].WLAN software defined radio antenna was discussed by Tekin et al [13]. Design of portable wireless devices was discussed by Aberle et al [14]. Youcef has discussed about U shapped antenna [15]. A two element reconfigurable antenna was discussed by Zainarry et al [16].

An I-shaped antenna is proposed which is operated in multiple frequencies using a PIN diode. The proposed design causes the antenna to resonate at two distinct frequency bands i.e., S and C band which includes WiMAX, WLAN and satellite communications. To obtain frequency reconfiguration, I-shaped asymmetric structures are used with one PIN diode which acts as a switch. So by using the PIN diode at an appropriate location on the patch the required frequency reconfiguration is achieved.

II. DESIGN OF ANTENNA

The antenna measurements, technique used to design the antenna and the transitioning between states of the PIN diode of the presented antenna is discussed. The frequency reconfigurability is acquired by inserting RF pin diode in the proposed design.

A. Designing Procedure Of The Antenna

The proposed antenna with I-shaped has a ground of size 25mm x 15mm and the size is same for the substrate. The material used for the substrate of FR4_epoxy material

with dielectric constant of εr = 4.4 and thickness of h = 1.6mm. Figure 1 shows the overall view of the proposed antenna. In this proposed antenna, we have used strip line feeding technique in which the patch is directly attached to the feed line. In this design, we have introduced DGS (Defective Ground Structure) which is used to optimize gain and bandwidth and to enhance the radiating properties of the micro strip antenna. The length of the defective ground structure is Lg = 10mm. To achieve frequency re-configurability, we have introduced a RF PIN Diode (SMP 1345 079LF) at an appropriate location on the patch. The Table 1 represents the parameter values that we have used for the proposed antenna design.

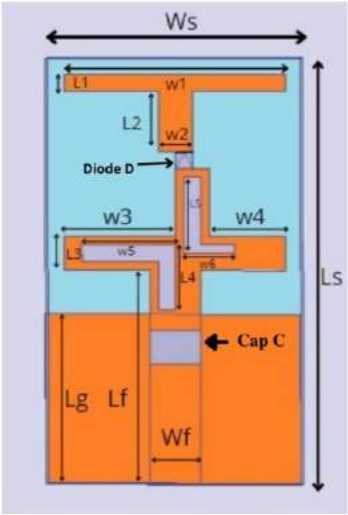

Fig. 1. Overall view of proposed antenna

The length and width of the feedline can be adjusted to achieve appropriate impedance matching at the desired resonant frequency. Two Asymmetric L-slots are introduced on the patch and One PIN Diode is placed in between the upper part of I- Shaped patch and the lower part of I-Shaped Patch. The Two L-slots dimensions, feed line's length and width can be optimized for good impedance matching and for maximization of -10dB frequency reconfigurable range using HFSS software. The RF p-i-n Diode works as a switch and changes surface current distributions across the slots made, in order to attain frequency re-configurability. The two operating modes of the PIN diode i.e., ON/OFF states would result in different current distribution thus causing antenna resonance at different frequencies.

The value of L4 and L5 can be optimized for better impedance matching and for improving the return loss to acquire the resonant frequency of 3.2GHz when pin diode D is in OFF condition and 3.4GHz and 6.8GHz when pin diode D is in ON condition. The chosen value of L4 is 3.8mm and L5 is 4.5mm to achieve better frequency re- configurability. We can also optimize the position of the Capacitor C which is on the feed line. After optimizing, the feed line's length and width is chosen as 12.5mm and 3mm.

TABLE 1 PROPOSED ANTENNA PARAMETER

Variables	Value(mm)
L_s	25
W_s	15
L_1	1
W_1	13
L_2	3.5
W_2	2
L_3	2
W_3	6.5
W_4	4.5
L_4	3.8
W_5	5.5
L_5	4.5
W_6	3
L_f	12.5
W_f	3
L_g	10

VALUES

B. The Pin Diode Used And It's Biasing Circuit

The equivalent circuit of the PIN Diode is shown in Figure 2. When pin diode D is in OFF condition (Reverse Bias Condition) , diode D acts as an Open Circuit with resistance Rp=5kΩ in parallel with capacitance Cp=0.19pF and the combination is in series with inductance Ls=0.7nH as given in Figure 2(a). When the pin diode D is in ON condition (Forward Bias Condition) , The Diode D acts as an Short Circuit and offers very low resistance with Rs=1.5Ωwith a series inductance of Ls=0.7nH as given in Figure 2(b) . The above values of the elements in RF pin diode when the diode is in ON/OFF condition is taken as shown in datasheet of pin diode of Skyworks solutions of the diode model (SMP 1345-079LF). The pin diode is introduced in order to acquire frequency reconfigurability of the presented antenna. A 1mm slot is used to introduce the RF PIN diode D at an appropriate location on the patch. A capacitor C of value 10pF is introduced on the feed line to block the DC voltage and to remove unwanted noise.

SWITCH OFF **SWITCH ON**

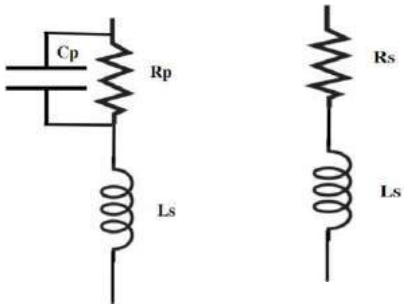

Fig. 2. (a) Equivalent Circuit of PIN diode in OFF state (b) Equival Circuit of PIN diode in ON state

III. RESULTS AND DISCUSSION

The Frequency Reconfigurable Patch Antenna (FRPA) is simulated, and outputs are observed using HFSS simulation software. One PIN Diode D is inserted in between the Upper and Lower part of the I-shaped Patch Antenna in such a way that the cathode of Diode D touches the Upper part and the Anode of Diode D touches the Lower part i.e., current direction of PIN Diode D is from Lower part to Upper part of I-shaped Patch Antenna which leads to two distinct reconfigurable operating modes, i.e., Mode 1 (OFF) and Mode 2 (ON). The simulated return losses of preferred FRPA under 2 different modes of operation (OFF and ON) is shown in Figure 3 and Figure 4. Switching States of the Diode D is given in Table 2. Resonant Frequency, -10dB Bandwidth, S11 parameter and gain dB for the 2 operating modes is given in Table 3. The FRPA Simulated Gains for the 2 operating modes (OFF and ON) are 1.5374dB,1.25dB and 1.8804dB. From Table 3 , it is observed that 2 distinct reconfigurable modes offers resonant frequency with return loss/reflection coefficient S11< -10dB.

TABLE 2
TRANSITIONING BETWEEN STATES

State of Switching of Diode D	Resonant Frequency in GHz
Mode 1 (OFF condition)	3.2
Mode 2 (ON condition)	3.4 and 6.8

The resonant frequencies are found to be distinct and operating in 2 different bands i.e., S band and C band.

TABLE 3 SIMULATED RESULTS OF PREFERRED ANTENNA TABLE 3.1: SIMULATED RESONANT FREQUENCY AND FREQUENCY BAND

Switching State of Diode D	Resonant Frequency	Frequency Band
Mode 1 (OFF State)	3.2	3.0589GHz to 3.3898GHz
B. Mode 2 (ON State)	3.4 and 6.8	Pass Band- 3.1612GHz to 3.7162GHz Stop Band- 6.8766GHz to 6.9741GHz

TABLE 3.2
SIMULATED BANDWIDTH AND S_{11}

Switching State of Diode	Bandwidth	). Measured S_{11} (dB)
Mode 1 (OFF State)	330.9MHz	-20.8868
Mode 2 (ON State)	Pass band bandwidth - 555MHz Stopband Bandwidth- 97.5MHz	-27.3191 and -24.2098

TABLE 3.3
MEASURED GAIN OF THE PROPOSED ANTENNA

Switching State of Diode D	Measured Gain(dB)
Mode 1 (OFF State)	1.5374
Mode 2 (ON State)	1.25 and 1.8804

FREQUENCY AND FREQUENCY BAND

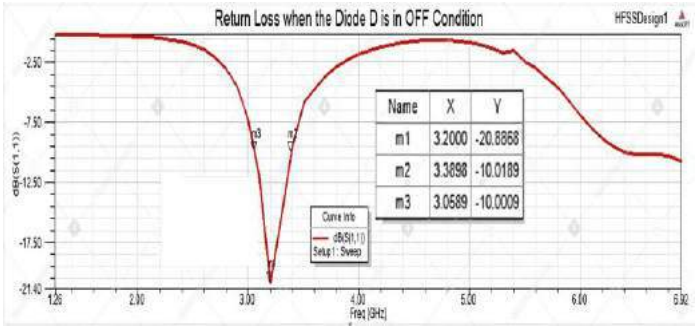

Fig. 1. S_{11} plot when D is in OFF State

In Mode 1, when D is in OFF State, the antenna resonates at 3.2GHz frequency which is a single band with impedance matching bandwidth of 330.9MHz (from 3.0589GHz to 3.3898GHz) and the resonant frequency is in S band (2 to 4 GHz).

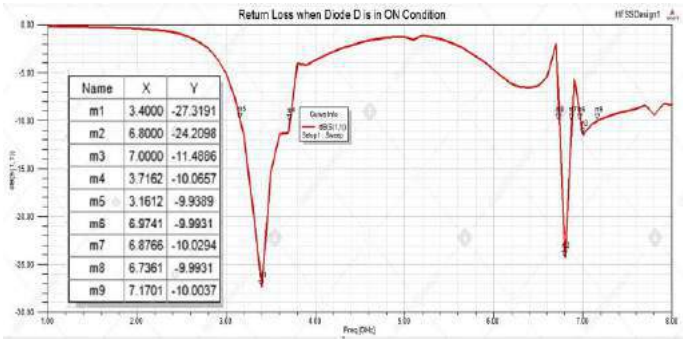

Fig. 4. S11 plot when D is in ON State

For Mode 2, when D is in ON condition, the antenna is resonating at 2 different frequencies i.e., 3.4GHz and 6.8GHz frequency which is a dual band with pass band bandwidth of 555MHz (from 3.1612GHz to 3.7162GHz) and stop band bandwidth of 97.5MHz (from 6.8766GHz to 6.9741GHz) and the resonant frequencies are in S-band (2 to 4GHz) and C-band (4 to 8GHz).Surface Current Distribution is represented for 2 distinct states of switching of Diode D(OFF and ON) which clearly displays the effective resonance lengths in the radiating structure that are responsible for

different frequencies is shown in Figure 5, Figure 6 and Figure 7.

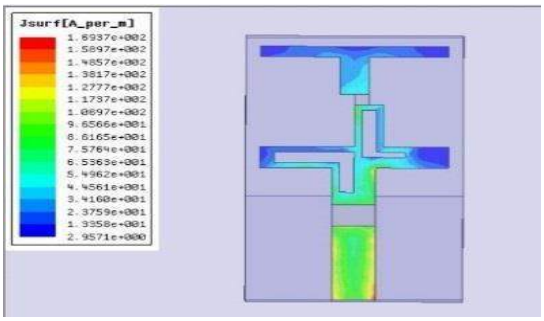

Fig. 5. Surface Current Distribution at 3.2GHz when D is in OFF State

When the diode D is in OFF condition, at 3.2GHz the more current is distributing in the feedline that represents the returns loss is improved.

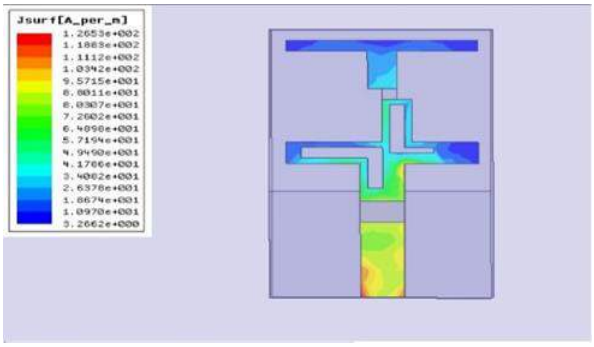

Fig. 6. Surface Current Distribution at 3.4GHz when D is in ON state

When the diode D is in ON condition, at 3.4GHz more current is distributed in the feedline when compared to current distribution in pin diode OFF condition and also the return loss is improved, and bands are changed when switched from OFF state to ON state.

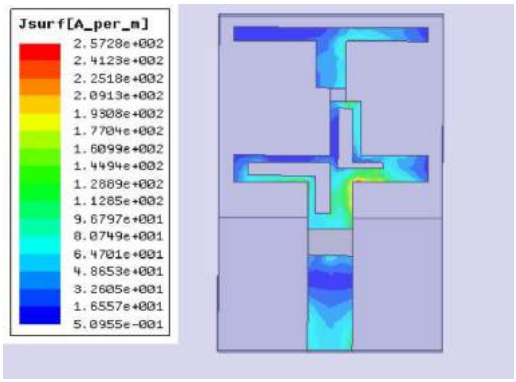

Fig. 7. Surface Current Distribution at 6.8GHz when D is in ON State

When the diode D is in ON condition, at 6.8GHz more current is distributed in the feedline and in the upper part of the I-shaped patch when compared to the current distribution in p-i-n diode OFF condition and bands are changed when switched from OFF to ON state. The simulated VSWR in dB of preferred FRPA under 2 different operating modes (OFF and ON) is shown in Figure 8 and Figure 9.

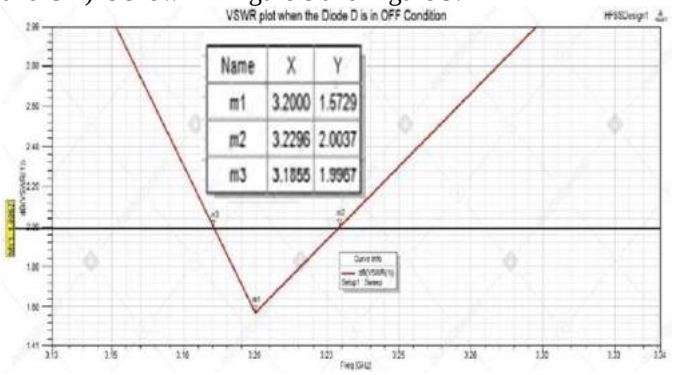

Fig. 8. VSWR in dB when D is in OFF condition

When the pin diode D is in reverse bias condition (OFF condition), the antenna is radiating nearly with a VSWR of 1.5729dB at 3.2GHz for S-band frequency range with partial S-band of bandwidth 44.1MHz.

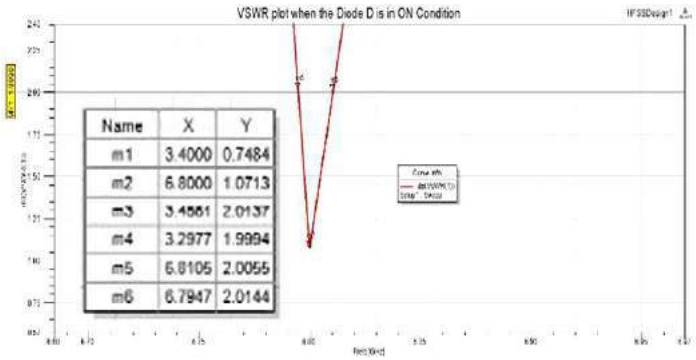

Fig. 9. VSWR in dB when D is in ON condition

When the pin diode D is in forward bias condition (ON State), the antenna is radiating nearly with a VSWR of 0.7484dB for S-band frequency range with partial S-band of bandwidth 158.4MHz and 1.0713dB for C-band frequency range with partial C-band of bandwidth 15.8MHz. The simulated 3D Polar Plot in dB of preferred FRPA under 2 different operating modes (OFF and ON) is shown in Figure 10, Figure 11 and Figure 12.

The antenna is radiating with a maximum gain of 1.5374dB at 3.2GHz when the diode D is in OFF condition. The resultant 3D gain plot when the diode D is in OFF state is almost equal to the plot of the omnidirectional antenna.

The antenna is radiating with a gain of 1.25dB at 3.4GHz when the pin diode D is in ON condition. The resultant 3D gain plot when the diode D is in ON state is almost equal to the plot of the omnidirectional antenna.The antenna is radiating with a gain of 1.8804dB at 6.8GHz when the pin diode D is in ON condition. The resultant 3D gain plot when

the diode D is in ON state is almost equal to the plot of the omnidirectional antenna.

TABLE 4
COMPARISON OF PRESENTED DESIGN IN TERMS OF SIZE WITH THE PREVIOUSLY PUBLISHED PAPERS ON FRPA

Ref No.	Size (mm^2)	Switch Type and Quantity	
[2]	280 x 280	Varactor Diode	2
[10]	30 x 40	PIN Diode	2
[8]	50 x 50	PIN Diode	2
[5]	80 x 40	PIN Diode	4
Proposed Design	25 x 15	PIN Diode	1

TABLE 4.1
COMPARISON OF PROPOSED DESIGN PERFORMANCE WITH THE PREVIOUSLY PUBLISHED PAPERS ON FRPA

Ref No.	Maximum Bias Voltage	Operating Frequencies(GHz)	Peak gain (dB)
[2]	14V	2.56,2.88,3,3.1,3.15,3.46	-0.70 to 5.50
[10]	5V	3.38,3.88,3.69 and 4.2	2.21 to 2.8
[8]	3V	5.2 and 6.4	2.30 to 3.00
[5]	1.5V	2.8,3 and 3.9	1.87 to 3.30
Proposed Design	3V	3.2,3.4 and 6.8	1.25 to 1.8804

Table 4 compares the new research with earlier findings in terms of frequency reconfiguration, antenna size, and switching type quantity. The proposed antenna is clearly smaller and more reliable than current antenna designs, with fewer switching types.

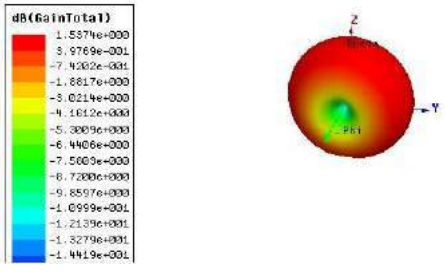

Fig. 10. 3D polar plot in dB at 3.2GHz when OFF State

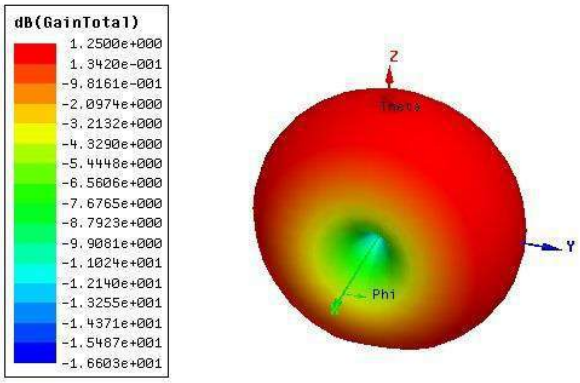

Fig. 11. 3D polar plot in dB at 3.4GHz when ON state

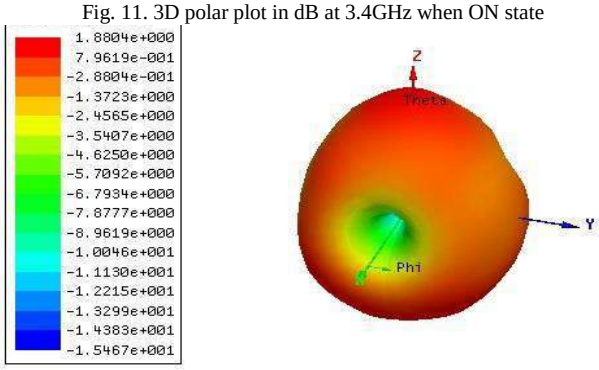

Fig. 12. 3D polar plot in dB at 3.4GHz when ON state

IV. CONCLUSION

The proposed Dual L-Slot Asymmetric I-Shaped Frequency Reconfigurable Patch Antenna is simulated in HFSS software. One pin diode is used to acquire frequency re-configurability. In different operating modes, When the diode D is in OFF condition, the antenna is resonating in a single band at 3.2GHz with the pass band bandwidth of 330.9MHz. When the diode D is in ON condition, the antenna is resonating in a dual band one is at 3.4GHz with the pass band bandwidth of 555MHz and other is at 6.8GHz with the stop band bandwidth of 97.5MHz. The antenna is radiating with gain of 1.5374dB and with a VSWR of 1.5729dB at 3.2GHz frequency when diode is in OFF state. The antenna is radiating with a gain of 1.25dB and with a VSWR of 0.7484dB at 3.4GHz frequency and with a gain of 1.8804dB and with a VSWR of 1.0713dB at 6.8GHz frequency when diode is in ON state. The achieved modes of operation will be used for applications in S-band and C-band.

V. REFERENCES

[1] Balanis, C. A., Antenna Theory, Analysis andDesign,2nd Ed., J. Wiley& Sons, New York, USA, 1997.

[2] Nguyen-Trong, N., A. Piotrowski, and C. Fumeaux, "A frequency-reconfigurable dual-band low profile monopolar antenna," IEEE Trans. Antennas Propag., Vol. 65, No. 7, 3336 3343, Jul. 2017.

[3] Christodoulou, C. G., Y. Tawk, S. A. Lane, et al., "Reconfigurable antennas for wireless and space applications,"Proceedings of the IEEE, Vol. 100, No. 7, 2250–2261, 2012.

[4] Choukiker, Y. K. and S. K. Behera, "Wideband frequency reconfigurable Koch snowflake fractal antenna," " IET Microwaves, Antennas & Propagation, Vol. 3, No. 1, 203-208, 2016.

[5] Zhang, L., T. Jiang, and Y. Li, "Dual-band printed antenna for WLAN applications," PIERS Proceedings, 1020{1023, Prague, Czech Republic, July 6{9, 2015.

[6] Bhaben Saikia, Pulin Dutta, and Kunal Borah J. T., S. H. Oh, D. T. Auckland,et al., "A Compact Dual Asymmetric L-Slot Frequency Reconfigurable Microstrip Patch Antenna," Progress in Electromagnetics Research C, Vol. 113, 59-68, 2021.

[7] Nikolaou, S., B. Kim, and P. Vryonides, "Reconfiguring antenna characteristics using PIN diodes," 2009 EuCAP 2009 3rd European conference on Antennas and Propagation, 3748-52, IEEE, 2009.

[8] Yasir, L. A., A. O. George, S. A. Abdulkareem, J. M. Husham, A. A. Ramzy, A. A. A. Raed, and M.N. James, Design of frequency reconfigurable multiband compact antenna using two PIN diodes for WLAN/WiMAX applications," IET Microwaves, Antennas & Propagation, Vol. 11, No. 8,1098-1105,2017.

[9] Majid, H. A., M. K. A. Rahim, M. R. Hamid, and M. F. Ismail, "Frequency and pattern reconfigurable slot antenna," IEEE Trans. Antennas Propag., Vol. 62, No. 10, 5339-5343, 2014.

[10] Han, L., C. Wang, et al., \Compact frequency-reconfigurable slot antenna for wireless application,"IEEE Antennas Wirel. Propag. Lett., Vol. 15, 1795{1798, 2016.

[11] Danesh, S., S. K. A. Rahim, M. Abedian, M. Khalily, and M. R. Hamid, "Frequency-reconfigurable rectangular dielectric resonator antenna," IEEE Antenna Wirel. Propag. Lett., Vol. 12, 1331-1334, 2013.

[12] Zhu, Z., P. Wang, S. You, and P. Gao, "A flexible frequency and pattern reconfigurable antenna for wireless systems," Progress In Electromagnetics Research Letters, Vol. 76, 63-70, 2018.

[13] Tekin, I. and M. Knox, "Reconfigurable microstrip patch antenna for WLAN software defined radio applications,"Microwave and Optical Technology Letters, Vol. 54, No. 3, 644–649, 2012.

[14] J. T. Aberle, S.-H. Oh, D. T. Auckland, and S. D. Rogers,"Reconfigurable antennas for wireless devices," IEEE Antennas Propag. Mag., vol.45, no. 6, pp. 148–154, Dec. 2003.

[15] Youcef B. Chaouche, Farid Bouttout, Mourad Nedil, Idris Messaoudene and Ismail Benmabrouk, "A Frequency Reconfigurable U-Shaped Antenna for Dual-Band WIMAX/WLAN Systems", Vol. 87, 63-71, 2018.

[16] Zainarry, S. N. M., N. Nguyen-Trong, and C. Fumeaux, "A frequency and pattern reconfigurable two-element array antenna," IEEE Antenna Wirel. Propag. Lett., Vol. 17, 617-620, 2018.

AUTOMATION OF VEHICLE TO VEHICLE DISTANCE MEASUREMENT USING IOT

Mrs Deepa Bammidi
Assistant professor
Department of ECE
Anil Neerukonda Institute Of Technology and Sciences
Visakhapatnam, INDIA
deepa.ece@anits.edu.in

Gatreddi.Bhavana sai sree
Electronics and Communication Engineering
Anil Neerukonda Institute of Technology and Sciences
Visakhapatnam, INDIA
bhavanasaisree.2019.ece@anits.edu.in

Madimi Dhanush Karthik
Electronics And Communication Engineering
Anil Neerukonda Institute Of Technology and Sciences
Visakhapatnam, INDIA
dhanushkarthik.2019.ece@anits.edu.in

***Abstract*— A prototype is presented to know the distance between vehicle to vehicle using an Arduino microcontroller to avoid accidents. During high fog climate conditions, heavy traffic situations, while parking & back out and to maintain convoy, it is always important to know the distance between the surrounding vehicles. With the help of an ultrasonic sensor HC-SR04, the distance between two vehicles can be sensed and the Arduino device would suggest the safe distance. The sensor is based on the measurement of the time of flight of an ultrasonic pulse, which is reflected by the obstacle like a vehicle. The automation of vehicular distance measurement through IOT device is explained in the paper.**

Keywords— Ultrasonic Sensors, Vehicular distance, IoT, Obstacle Identification, Alerting System, Traffic Management.

I. INTRODUCTION

Digital vehicle monitoring system is very essential in the present day traffic management, due to increased population of vehicles on road. An IoT controlled obstacle identification and alerting system would make the vehicular driving safer and easier. By placing ultrasonic sensor at the required directions, it is possible to identify the objects at different directions from all directions to a specific vehicle. The driver needs to know how far an object is from a moving vehicle that is in front of it or to its side. Such systems for measuring distance employ a variety of sensors and technologies. In the majority of applications, speed, precision, and low cost are all crucial. When measuring distance, ultrasound sensors are incredibly flexible.They are also offering the most affordable solutions.

Both above and below water, ultrasound waves are helpful. For the majority of everyday uses, ultrasonic sensors are also rather quick. It is also possible to employ a less expensive microcontroller in systems that are simpler in order to reduce costs.

The paper presents a prototype designed with an ultrasonic sensor HC-SR04, interfaced with Arduino UnoR3. The ultrasonic sensor transmits the sound waves and would receive an echo signal, if it encounters an obstacle. The sound waves are used for distance measurement and speed calculation of the obstacle. Arduino UnoR3 is used as the microcontroller to write code to calculate the distance and speed. The result is displayed on an LCD display. One red colour and a green colour LEDs to indicate the unsafe or safe distance between the vehicles. Measurement using ultrasonic signal in air includes the continuous pulse-echo transmission method, a burst of the pulse is sent through the medium and is reflected by an object kept at a specific distance. The time taken for the sound wave to propagate from transmitter to receiver is proportional to the distance of the object.

The paper discusses the literature study done by the authors before developing the prototype, in section-2. The next section presents the A) implementation steps involved in the prototype development B) flowchart for the code written in Arduino UnoR3. Section-4 discusses the results obtained by the prototype. Finally, the work done and the results obtained were concluded.

II. LITERATURE SURVEY

Ultrasonic sensors are important because they can be used to determine how far an obstacle is. In terms of measuring distance, ultrasonic sensors are quite versatile. They offer affordable solutions. Both underwater and in the air, ultrasound waves are useful [1]. A method for obstacle identification and collision control of a moving unmanned quadrocopter has been discussed by Nils Gageik et al [2]. Using an ultrasonic sensor, an Internet of Things-based system for vehicle obstacle detection and alerting was discussed by Harish Kumar et al [3]. Distance measurement of a blockage by using separate ultrasonic transmitter, receiver and a microcontroller in robotic sewer blockage detection system was discussed by A. K. Shrivastava [4]. The effectiveness of fast non-hierarchical stereo correspondence algorithm producing sparse disparity information for obstacle avoidance in a common outdoor setting was discussed by Sumit Badal [5]. Ultrasonic distance measuring system based on S3C2410, its operation principle, procedure design along with additional temperature compensation circuit to the hardware to improve its precision was discussed by Hongjiang He[6]. The use of HCSR-04 ultrasonic sensor in automobile prototype for distance measurement of obstacles that appear or lie in the path of the prototype and its implementation in python was discussed by D.S. Vidhya [7]. An obstacle avoidance algorithm for unmanned vehicles in unknown environment using the concept of danger zone along with an ultrasonic sensor and a servo motor which rotates from 0 to 180 degrees was discussed by Ta-Chung Wang [8]. A pulsed ultrasonic distance measurement system (UDMS) for use in air and a new form of signal processing for timing of a BFSK signal based upon phase digitizing the received signal was discussed by David Webster [9]. Several digital signal-processing algorithms including L1, L2 norm, and correlation with different approaches for envelope extraction

to overcome the low bandwidth of current ultrasonic transducers has been discussed by M. Prailla [10]. A technique resolving the location of solid surfaces with ultrasonic sensors and obtaining the true direction to a planar surface using three sensors or three positions of one sensor was discussed by Micahel K. Brown [11]. Estimation of optical flow to detect static obstacles during the motion of mobile robot based on correlation scheme algorithm was discussed by N. Ancona [12].

III. Methodology and Implementation

A. Implementation steps

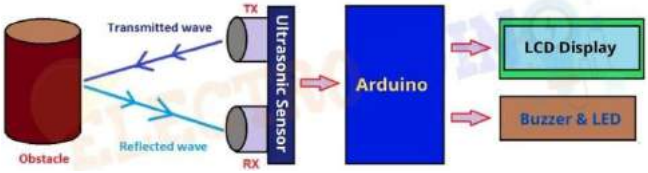

Fig. 1. Schematic diagram of the prototype proposed

Figure1 shows the steps involved in the proposed prototype. As described in Fig.1, when ultrasonic sensor HC-SR04, receives the input, sensor transmits sound waves, when sound waves produced by sensor hits the obstacle sensor receives the reflected signal. This reflected signal is received by echo pin it produces electrical signal which can be used for further processing and electrical signal is sent to Arduino. Arduino is an electronics platform and easy to use hardware and software. Arduino can read inputs through digital input output pins and also analog input pins. The electrical signal produces by echo pin of ultrasonic sensor is given to these analog input pins. The microcontroller present in the Arduino board is microcontroller ATmega328. Required operating voltage for Arduino board is 5V. The microcontroller present in the Arduino processes the signal and calculate the distance based on the duration of echo pulse. Let the time period be T, time taken by pulse is actually for to and from travel of ultrasonic signals, while we need only half of this so therefore time is taken as T/2. Speed of the sound at sea level is 343 m/s or 34300 cm/s. Now distance is measured using the formula Distance = Speed*Time/2. Lcd display is interfaced with Arduino which can display 16 characters or numbers in column size and 2 in row size. It displays the string given in the program dumped in the Arduino board. Distance is measured from formula mentioned above, if the distance of the obstacle is below 1meter radius then the led glows and the distance between obstacle and ultrasonic sensor is displayed in the lcd display. If measured distance is above 1meter radius, then led remains in off condition and lcd displays some garbage value.

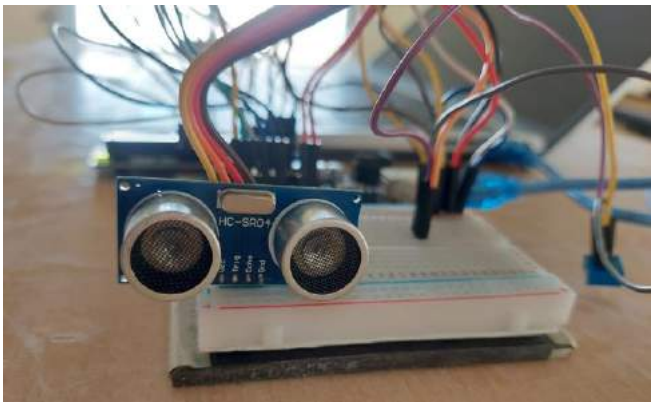

Fig. 2. Ultrasonic Sensor Used(HC-SR04)

An ultrasonic sensor is shown in Fig.2, that measures the distance to an object by emitting ultrasonic waves and converting the reflected sound into electrical signals. Ultrasound travels faster than audible sound (ultrasound is inaudible to humans). Ultrasonic sensing is one of the best ways to detect the proximity of obstacles and reliably detect levels of substances and liquids. An ultrasonic sensor module uses a transducer to send and receive ultrasonic pulses. The working principle of this module is simple. It emits a 40kHz ultrasonic pulse from the trigger pin, travels through the air, and bounces off the sensor with the echo pin if there is an obstacle or object. By calculating the time travelled by the wave and the speed of sound, the distance to the object is calculated. The ultrasonic sensor module has 4 pins: Gnd, Vcc, Echo, Trigger. Ground is considered the negative pin and is connected to system ground. Vcc powers the sensor. Typically 3.3V is required. The Trig (trigger) pin is used to trigger the ultrasonic pulse. The Echo Pen generates a pulse when it receives a reflected signal

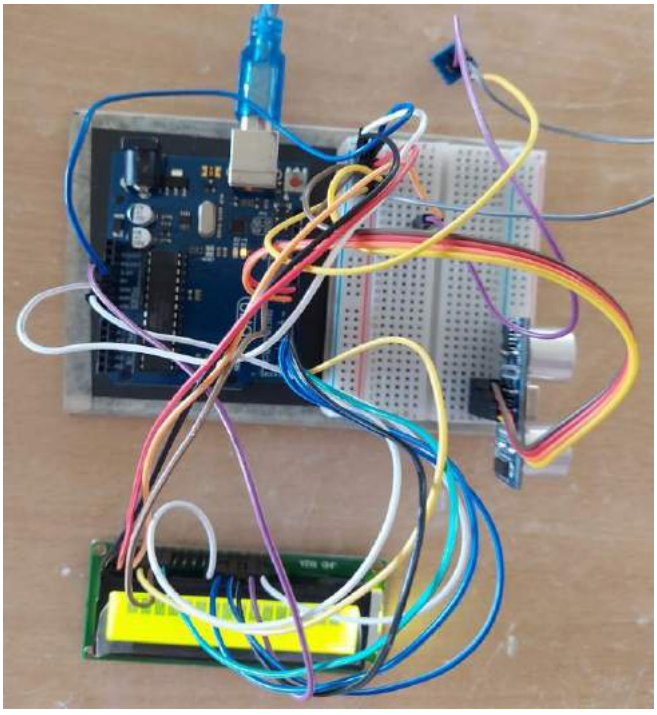

Fig. 2. The Prototype

This prototype uses an Ultrasonic sensor, Arduino, I2C LCD display, LED, Bread board and Jumper wires.Ultrasonic sensor has four pins V_{CC},Trigger,Echo and GND pins. Trigger pin is connected to 8 pin of Arduino board, Echo pin is connected to 9 pin of Arduino, GND is connected GND on breadboard, VCC is connected to source on breadboard. I2C LCD display has GND,VCC,SDA,SCL, GND is connected to GND on Arduino board, VCC is connected to 5volts on Arduino, SDA is connected to analog4 pin on Arduino pin, SCL is connected to analog5 pin on Arduino pin. Using Arduino USB power supply and code is dumped into Arduino board. The sensor will sense the signal and according to the code its gives the obstacle distance on I2C LCD display.

B. Flowchart and Code

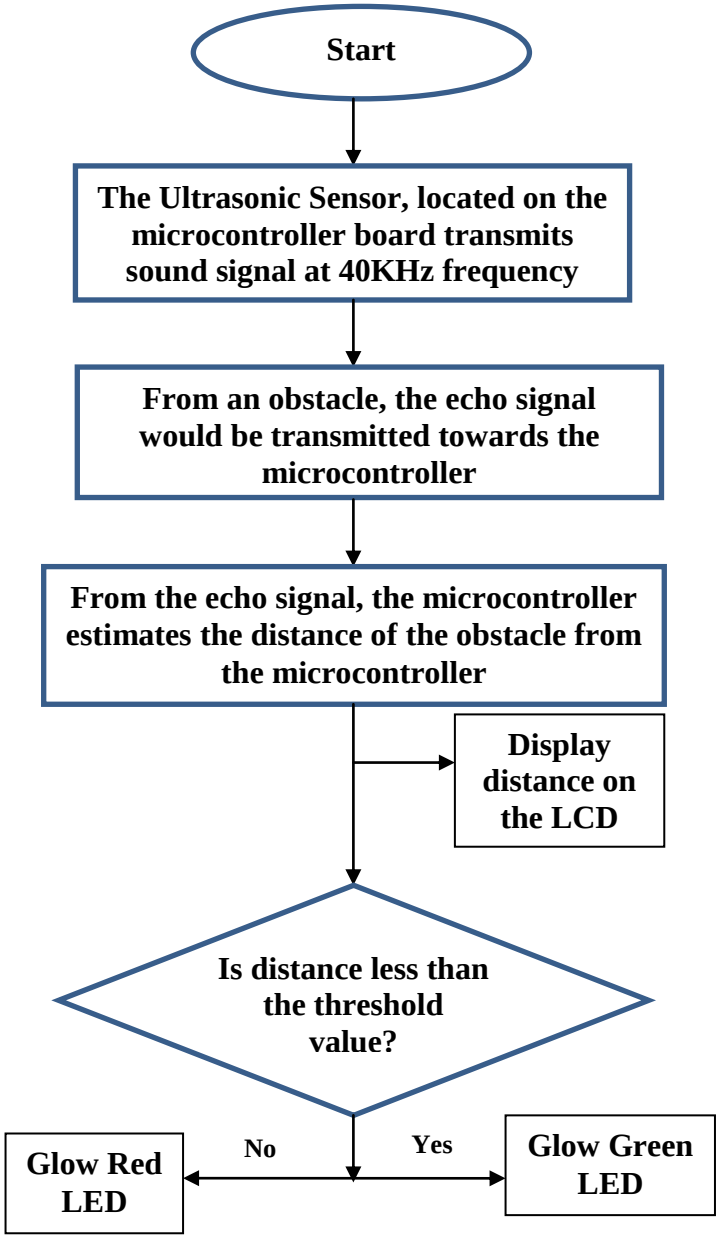

Fig. 3. Flowchart of the programming used in Ardino

Arduino would be powered using USB cable with voltage of 5V and this provides input voltage to the ultrasonic sensor. As shown in Fig.3, the sensor produces sound waves and are transmitted into air. When these waves hit the obstacle, the waves get reflected back. Reflected waves (echo signal) will be recieved by the microcontroller receiver transducer which converts sound wave into electrical signal. This electric voltage can be used to estimate the distance between obstacle and the transmitter using the microcontroller ATMEGA328 present on the arduino board. The time gap between electrical signal generation is used to measure distance and if this distance is below 1 meter, Green LED glows and the distance between ultrasonic sensor and obstacle is displayed on the LCD. If the distance is above 1 meter, the Red LED glows and the LCD displays garbage value.

CODE :

```
#include <LiquidCrystal_I2C.h>
LiquidCrystal_I2C lcd(0x27, 16, 2);
const int trigPin = 10;
const int echoPin = 11;
long duration;
int distanceCm, distanceInch;
void setup() {
lcd.backlight();
 lcd.init();
pinMode(trigPin, OUTPUT);
pinMode(echoPin, INPUT);
}
void loop() {
digitalWrite(trigPin, LOW);
delayMicroseconds(2);
digitalWrite(trigPin, HIGH);
delayMicroseconds(10);
digitalWrite(trigPin, LOW);
duration = pulseIn(echoPin, HIGH);
distanceCm= duration*0.034/2;
distanceInch = duration*0.0133/2;

lcd.setCursor(0,0);
lcd.print("Distance: "); // Prints string "Distance" on the LCD
lcd.print(distanceCm); // distanceCm is a variable which stores the value of distance
lcd.print("  cm");
delay(10);
lcd.setCursor(0,1);
lcd.print("Distance: ");
lcd.print(distanceInch);
lcd.print("inch");
delay(10);
}
```

CONCLUSION

The Prototype is designed to implement an Ultrasonic distance meter, to measure the safer distance between prototype and the obstacle. Measurement is based on sound waves reflected by the obstacle, which received by the

receiver. . It is low cost and simple design. It is able to adapt to different conditions in order to give the best results.

REFERENCES

[1] J. David and N. Cheeke, "Fundamentals of ultrasonic waves," CRC Press, Florida, USA, 2002, ISBN 0-8493-0130-0.
[2] Nils Gageik, Thilo Müller, Sergio Montenegro, "Obstacle Detection and Collision Avoidance Using Ultrasonic Distance Sensors For An Autonomous Quadrocopter" University of Würzburg, Aerospace Information Technology (Germany) Würzburg September 2012.
[3] Harish Kumar N. Deepak, G. Nagaraja J, "An IoT based Obstacle Detection and Alerting System in Vehicles using Ultrasonic Sensor", international Journal of Engineering Research & Technology (IJERT) ISSN: 2278-0181 NCETEIT – 2017
[4] A. K. Shrivastava, A. Verma, and S. P. Singh, "Distance Measurement of an Object or Obstacle by Ultrasound Sensors using P89C51RD2", International Journal of Computer Theory and Engineering, Vol. 2, No. 1 February 2010, ISSN: 1793-8201
[5] Sumit Badal, Srinivas Ravela, Bruce Draper, Allen Hanson, "A Practical Obstacle Detection and Avoidance System", Computer Vision Research Laboratory University of Massachusetts, Amherst, MA 01002.
[6] Hongjiang He, Jianyi Liu, "The Design of Ultrasonic Distance Measurement System Based on S3C2410", 2008 International Conference on Intelligent Computation Technology and Automation.
[7] D. S. Vidhya, Delicia Perlin Rebelo, Cecilia Jane D'Silva, Linford William Fernandes "Obstacle Detection using Ultrasonic Sensors", International Journal for Innovative Research in Science & Technology| Volume 2, Issue 1, PP. 316-320, April 2016.
[8] Ta-Chung Wang, Tz-Jian Lin "Unmanned Vehicle Obstacle Detection and Avoidance Using Danger Zone Approach", Transactions of the Canadian Society for Mechanical Engineering, Vol. 37, No.3, PP.529-538, 2013.
[9] D. Webster, "A pulsed ultrasonic distance measurement system based upon phase digitizing," IEEE Transaction on Instrumentation and Measurement, Vol. 43, No. 4, Aug. 1994, pp. 578-582.
[10] M. Parrilla, J. J. Anaya, and C. Fritsch, "Digital signal processing techniques for high accuracy ultrasonic range measurements," ZEEE Trans. Inst. and Meas., vol. 40, pp. 15%763, Aug. 1991.
[11] M. K. Brown, "Feature extraction techniques for recognizing solid objects with an ultrasonic range sensor," IEEE J. Robot. Aurom., vol. RA-1, pp. 191-205, Dec. 1985.
[12] N. Ancona, "A fast obstacle detection method based on optical flow" Proc. of European Conference on Computer Vision, pp. 267-271, 1992.